UNIVERSITA' DEGLI STUDI DI MILANO

FACOLTA´ DI SCIENZE MATEMATICHE FISICHE E NATURALI

Dipartimento di Chimica Organica e Industriale

Dottorato di Ricerca in Chimica Industriale

(XXIV ciclo)

TESI DI DOTTORATO DI RICERCA

Homo- and copolymerization of olefins and cyclo-olefins by homogeneous metallocene and half-metallocene catalysts

Tutor interno: Prof. Giuseppe Di Silvestro

Tutor esterno: Dott.ssa Incoronata Tritto

Coordinatore: Prof.ssa Dominique Robertò

Cornelio Massimiliano

R08358

Anno Accademico 2010-2011

INDEX

1. Introduction

1.1 Polyolefins

1.1.1 Polyolefin History and Industry

Polyolefins are the largest volume polymers in the plastic industry and mainly consist of polyethenes (PE) and polypropenes (PP) and of a smaller volume of high value polymers such as propene-butene and ethene-propene-diene (EPDM rubbers).

PE and PP are considered the best for use in any application because of their high cost/performance value; in fact, the basic units ethene and propene are very cheap materials, easily obtained from the cracking of mineral oil. Furthermore, the materials used in polyolefins can be recycled or combusted with a gain in energy, the only products being carbon dioxide and water. Hence, in a world increasingly conscious about the environment, polyolefins represent an environmentally friendly polymeric material with an effective life cycle.

World polyolefins demand was estimated around 115 million tons, with different grades for different specific end uses, and the general polyolefin demand is forecast to raise to 250 million tons by 2025.

The history of polyolefins by organometallic catalysts started about 60 years ago, in the early 1950s, this field has grown to become one of the most important ones in chemical industry. Nowadays, polyolefins cover more than the half of the entire plastic market, and a wide variety of materials, made of polyolefins, have practical application in our lives. In 1953 Ziegler discovered that high-density polyethene could be easily prepared by using a mixture of transition metal salts and a

metal salt ($TiCl_4$-$AlClEt_2$ catalyst)[1] and soon afterward in 1954, Natta demonstrated that the same catalytic system was able to perform stereospecific polymerization of propene[2]. In 1963 the Nobel Prize in Chemistry was awarded jointly to Karl Ziegler and Giulio Natta *"for their discoveries in the field of the chemistry and technology of high polymers"*. These discoveries changed polymer chemistry forever, and brought a great number of innovations promoting the rapid growth of the polyolefin industry. Since then, major development on polyolefin production and application occurred: the Ziegler-Natta catalyst activities increased enormously from 0.8 $Kg/g_{catalyst}$ up to 100 $Kg/g_{catalyst}$ and also the stereospecificity, over four generations of Ziegler-Natta catalyst systems[3, 4].

Before the discovery of Z-N catalysts, polyolefin polymers and copolymers were produced by high pressure free radical polymerization, and this process is still used to produce functional ethene copolymers, such as poly(ethene-*co*-vinyl acetate) and poly(ethene-*co*-acrylic acid), important for many industrial applications, such as sealants, food packaging, and extrusion coatings[5].

However, nowadays the industrial synthesis of polypropene is based on heterogeneous Ziegler-Natta catalysis. The active sites in heterogeneous Ziegler-Natta type catalysts are located on the dislocations and edges of transition metal salt crystal lattice[6], and the polymerization depends on electronic and steric environment of the active sites in the crystal lattice; these catalysts are able to synthesize polymers with broad molecular weight distributions and copolymers with heterogeneous compositions, reflecting the complex organometallic structure of different catalytic active sites[7]. Alternatively, polyolefins could be obtained by chromium oxide-based catalysts which polymerize ethene to give high-molecular-weight rigid polymethene-type polymers, but they are inactive towards propene. During 60 years since the discoveries of Ziegler and Natta, researchers were able to improve the characteristics of heterogeneous catalysts, that become very effective and very efficient. However, due to the presence of a high number of active sites, the problem of wide molecular weight distribution remains unresolved.

In the last 30 years, the discovery of homogeneous catalysis in chemistry has open a different horizon in polyolefin synthesis; the use of homogenous catalysts in

polymerization reaction has led to the possibility to obtain narrowest molecular weight distributions and copolymers with homogeneous distribution of the comonomer, the latter improves the processability and the mechanical properties and physical properties, such as impact, sealing, elasticity of the materials. These single-site metallocene catalysts allow to tailor the polymer structures in a way that was not possible with heterogeneous catalysts and thus allowed to expand the range of application of polyolefinic materials. The innovation of homogeneous metallocenes catalysis opened new developments in the field, and enabled to produce polyolefins by tailoring the catalyst structure and to develop and manufacture new families of polyolefin products.

PP and PE are made by a variety of processes: gas phase, slurry phase, solution or high pressure processes; each of them has its advantages depending on the final end-product. Production variables for these polymers consist of catalyst combinations, one of the four processes, comonomer selection, and polymerization post-treatments; these combinations allow for a wide range of polymers that can be used in a wide range of applications.

A better understanding of how the catalytic systems could promote the polymerization has lead to the possibility to tailor the physical properties of polypropenes obtained. Flexibility of the material obtained could be easily observed during the processability, such as extrusion and molding, that lead to well-oriented high modulus thin films and fibers for a wide range of applications.

1.1.2. Metallocene History

Metallocene based catalyst technology was expected to revolutionize the immense polyolefin industry, particularly in polyethene and polypropene markets. The discovery of metallocene catalysis has been consisedered one of the most important since the discovery of Ziegler-Natta catalysts. This optimism is reflected in the R&D efforts of the major polyolefin producers who have spent an estimated one billion dollars on metallocene research in the past years. Metallocene polyolefins were projected to penetrate a broad array of polymer markets. First with the higher

priced specialty markets, followed by the high volume and commodity markets. New markets were also expected to be created with the development of new classes of polymers that were not possible with conventional Z-N technologies. It was estimated that by the turn of the century, over 20 million tons per year of metallocene based polymers should have been produced accounting for over 10% of the global thermoplastics and elastomer market. The primary reason for the great activity in this area is that compared to conventional Ziegler-Natta technology, metallocenes offer some significant process advantages and produce polymers with very favourable properties.

The very first example of metallocene appears in 1951 when Pauson reported the reaction of cyclopentadienyl magnesium bromide and ferric chloride with the goal of oxidatively coupling the diene to prepare fulvalene. Instead, they obtained a light orange powder of "remarkable stability"[8] (Figure. 1.1). This stability was related to the aromatic character of the negative charged cyclopentadienyls, but the sandwich structure of the η^5-pentahapto compound was not recognized by them. Robert Burns Woodward and Geoffrey Wilkinson deduced the structure based on its reactivity[9]. Independently, Ernst Otto Fischer also came to the conclusion of the sandwich structure and started to synthesize other metallocenes such as nickelocene and cobaltocene[10, 11]. Ferrocene's structure was confirmed by NMR spectroscopy and X-ray crystallography[12, 13]. Its distinctive "sandwich" structure led to an explosion of interest in compounds of *d*-block metals with hydrocarbons, and invigorated the development of the flourishing study of organometallic chemistry.

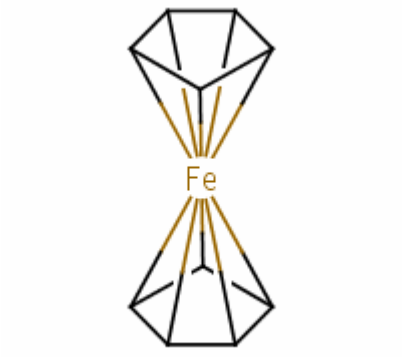

Figure 1.1 Sandwich structure of ferrocene

Starting from the discovery of the first organometallic sandwich compound, many other compounds of different transition metal atoms π-bonded to aromatic ligands were synthesized and their applications studied[14, 15, 16, 17, 18]. In 1973 Fischer of the Technische Universität München and Wilkinson of Imperial College London shared a Nobel Prize for their work on metallocenes and other aspects of organometallic chemistry[19].

After the synthesis of the first Group IV metallocenes by Wilkinson et al. in 1953[15] and the discovery of Ziegler-Natta polymerization the use of these complexes in polyolefin polymerization was tested. In 1957, Natta reported the polymerization of ethene with a mixture of titanocene Cp_2TiCl_2 and triethyl aluminium, a traditionally used cocatalyst in Z-N heterogeneous catalysis. This system was tested for the polymerization of ethene, and a very low activity was found, while no activity towards α-olefins was reported[20, 21]. The current interest in metallocene catalysts originates from the discovery at Kaminsky's laboratories in Hamburg in the mid of 1970s. While studying a homogenous $Cp_2ZrCl_2/Al(CH_3)_3$ polymerization system, water was accidentally introduced into the reactor leading to an extremely active ethene polymerization system. Subsequently, intensive studies revealed that the high activity was due to the formation of the cocatalyst methylaluminoxane (MAO), a mixture of molecules in which aluminium and oxygen atoms are alternately positioned and free valences are saturated by methyl groups[22], as a result of the hydrolysis of the trimethyl aluminium. Once the potential of metallocene catalyst has been assessed, many researchers proceeded to develop new catalytic systems.

One of the milestones in this field was the synthesis of bridged zirconocene dichloride with C_2 symmetry by Britzinger et al.[23], and the use of this class of metallocenes to produce isotactic polypropene by Kaminsky at al[24]. The prototype of this class of metallocenes is *rac*-$C_2H_4(1\text{-Ind})_2ZrCl_2$ which is the most studied one from both the synthetic and catalytic point of view; during the last 30 years, several different classes of C_2-symmetric, racemic, *ansa*-metallocenes (see Figure. 1.2) for the isospecific polymerization of 1-olefins have been developed, a high number of different ligand structures have been synthesized, and the influence of these

structures is now known at very high level. As far as the transition metal is concerned, Hf normally produces higher molecular weights than Zr and Ti, but Zr-based *ansa*-metallocenes are the most active and, practically, the only catalytic systems used. Their successes spurred efforts to find more active and stereoselective catalysts for the polymerization of a wide range of monomers.

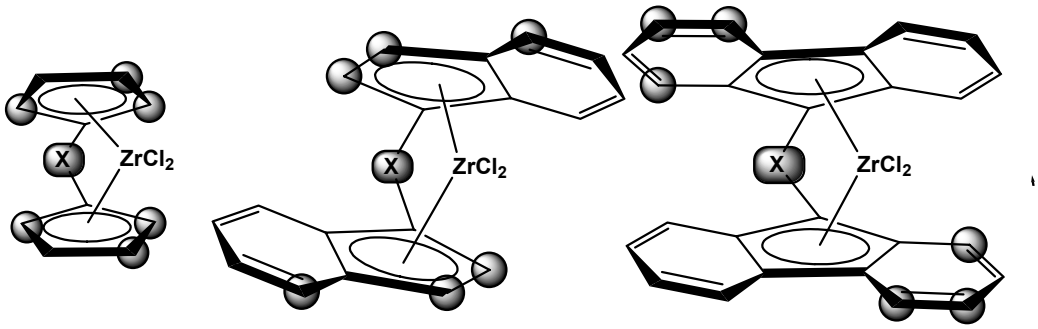

Figure 1.2. Most relevant substitution positions in C_2-symmetric biscyclopentadienyl, bisindenyl and bisfluorenyl *ansa*-C_2-symmetric isospecific metallocenes

Ewen and Razavi[25] were the first to synthesize the $Me_2C(Cp)(9\text{-}Flu)\text{-}ZrCl_2$ C_s-symmetric catalyst, able to synthesize syndiotactic polypropene (*s*-PP). The syndiospecific C_s-symmetric catalysts are those for which the two available sites are enantiotopic. Since then, the behavior[26, 27] of this new class of catalysts and the characterization[28] of *s*-PP have been extensively studied.

More recently, the research moved towards a new class of metallocene complexes belonging to C_1-symmetric class, they are complexes lacking of any symmetry element.

Mainly, there are two different classes of these kinds of metallocenes (Figure. 1.4) which are of interest, all of them bridged, hence stereorigid having two heterotopic faces: those with two cyclopentadienyl ligands one of them bearing a substituent, and those having one asymmetric cyclopentadienyl and a fluorenyl.

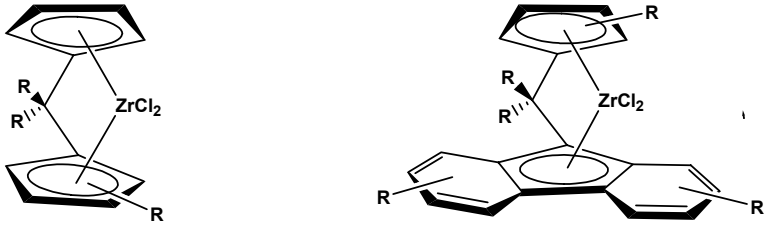

Figure 1.3 Most relevant classes of C_1-symmetric catalysts.

The first class presents a synthetic advantage with respect to the second type, since no *meso* form exists during the synthesis. However, C_1-symmetric zirconocenes with an isopropylidene bridge and substituted cyclopentadienyl or fluorenyl ligands are of large interest as catalysts for the polymerization of propene, leading to syndiotactic and hemiisotactic polymers[26]. They are stable and can be synthesized without achiral side products. For industrial use, some disadvantages have to be solved: the polymers often have low molecular mass and catalysts are not very stable at higher temperatures and deactivate rapidly; sometimes these catalysts are not active enough and give only low stereoselectivities. Therefore there is an interest to increase the activity and to make the metallocenes more stable at higher temperatures.

In the early 90s a new class of group IV metal complexes was investigated; the exchanging of a cyclopentadienyl ligand with an amido mojety leads to a new class of catalysts, referred as CGC (Constrained Geometry Catalysts), very effective in the polymerizations of ethene and higher α olefins; the efficiency of these catalysts could be attributed to the higher Lewis acidity of the metal centre, the more opened bond angle between the ring and a decrease tendency of the bulk polymer to undergo chain transfer reactions[29]. Since the first example of sandwich metal complex, and since the discovery of MAO as a much more effective activator for metallocenes than aluminium alkyls or halides, a fervent development of industrial and scientific research in the metallocene sector initiated and, until today, it has not been concluded.

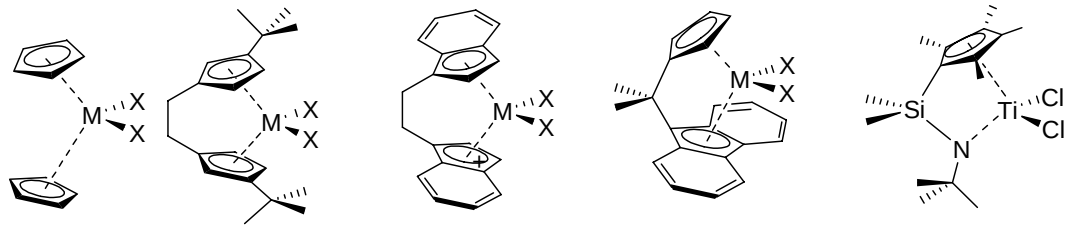

Sinn/Kaminsky 1980 | Brintzinger 1982 | Kaminsky/Brintzinger 1985 | Ewen/Razavi 1988 | Bercaw 1990

Figure 1.4. Progress in metallocene catalysis

Nowadays, the improvement in metallocene technology allows the production of polyolefin homo- and copolymers with tailored molecular structures. The metallocene catalysis allows to obtain very homogenous materials, with narrower comonomer distribution, and molecular weight distribution than the polyolefins obtained with heterogeneous Z-N catalysts. These bring many advantages on the properties of the materials; the unique rheological properties, the sharp melting peaks, the improved tensile, and elastic properties allow to commercialize the metallocenes-based polyolefins in a wide range of markets, such as packaging, automotive, wire, cable and fibers. Dow commercialised in the mid of 1990s these kind of polyolefin for packaging applications, with the trademark of AFFINITY™, for pre-packaged ready to eat salads and ELITE™ for oriented shrink films; ethene-1-octene copolymers obtained with metallocene-based catalysis are well known in a variety of wire and cable applications, from low-voltage flexible cable insulation to high voltage jacketing application[30]. The metallocene-based polyolefins have invaded also the field of termoplastics; termoplastic polyolefins (TPOs) such as ethene/octene-based co- and terpolymers have replaced the conventional thermosets and thermoplastics in automotive parts, due to their low cost, performance properties and high formulation flexibility. Many TPOs are used for multiple-gauge, large part injection molding applications[31], i.e. Dow's Trademark ENGAGE™ provide exceptional performances for multiple-gauge injection molded parts for the automotive market.

1.1.4. Olefin Polymerization Mechanism

Metallocene complexes are catalyst precursors, which need to be activated for catalysing olefin polymerizations. The MAO, the common cocatalyst used in homogeneous polyolefin catalysis, is able to activate the metallocenes complexes by replacing the chlorine atoms linked to the metal centre with two methyl groups. Moreover, MAO acts as scavenger, reacting with oxygen, water and other impurities, responsible of catalyst deactivation.

As well documented, the active species in olefin polymerization is the metallocenes cation; the formation of a 14-electron complex, $[Cp'_2ZrMe]^+$, in the presence of MAO has been detected by X-ray photoelectron spectroscopy (XPS)[32] as well as by ^{13}C nuclear magnetic resonance[33, 34] spectroscopic techniques. The presence of cationic metallocene species has also been verified by the use of weakly co-ordinating anions, such as $(C_6H_5)_4B^-$ and $(C_6F_5)_4B^-$, as counterions for alkylated metallocene cations[35]. Methylation reaction takes place before cationisation, and the methylation step has been studied by UV/VIS[36, 37]and ^1H and ^{13}C-NMR[38-42] spectroscopy. These studies have suggested the formation of a monomethylated species for a metallocene/MAO complex at low [Al]/[Zr] ratios of 10–20.

The electronically unsaturated cationic alkyl metallocenes exhibit a strong tendency to coordinate with the weak Lewis base olefin molecules. A study based on molecular orbital (**MO**) theory indicated that once an olefin coordinated to the metallocene alkyl, the insertion of the olefin into the alkyl—metal bond would proceed rapidly. The driving force for the insertion is the energy gain on converting a π bond into a σ bond, with energy release of about 20 Kcal/mol[43].

Three general mechanisms have been proposed for the coordination of the olefin to the active site of the metal centre:

1) the Cossee-Arlman mechanism[44], which involves the coordination of the monomer to the electrophilic, cationic complex, followed by monomer insertion into the metal–alkyl bond to extend the polymer chain, the insertion proceeds via polymer chain migration to the side of the olefin;

2) the metathesis model proposed by Green and Rooney[45], in which an α-hydrogen is transferred from the end of the polymer chain to the metal, leading to a metal-carbene complex, which forms a metallacyclobutane, complex with the coordinated monomer, through which the monomer inserts to the polymer chain;

3) the modified Green–Rooney model proposed by Brookhart and Green[46], in which insertion proceeds via migration of the polymer chain to the olefin ligand and is suggested to occur through a four-centre transition state, stabilised by agostic

interactions between the metal centre and an α-hydrogen of the growing chain (Scheme 1.1).

Nowadays, the latter general mechanism is the most accepted.

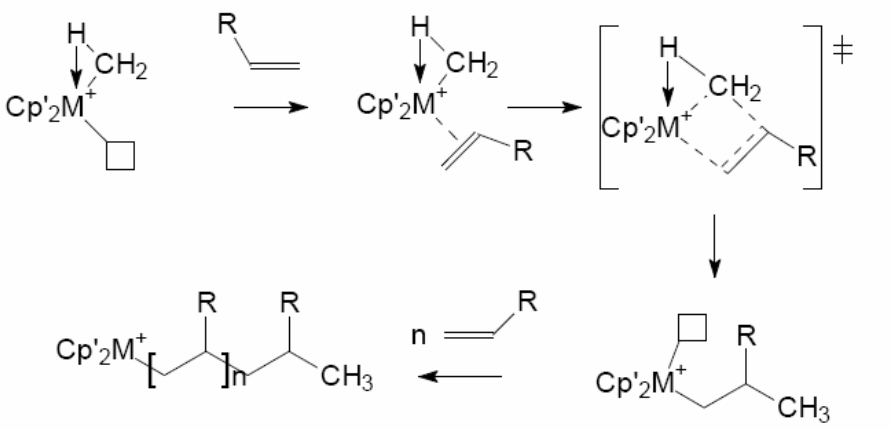

Scheme 1.1 A model for olefin co-ordination polymerisation (modified Green–Rooney) constructed by Brookhart *et al.*[46] from the Cossee–Arlman[44] and Green–Rooney[45] models. The activator is omitted for clarity, Cp'=Cp based ligand, R=H or CH_3.

The polymerization continues till a termination reaction occurs; chain terminations take place via β-H elimination to the metal or β-H elimination to a coordinate monomer, by chain transfer to aluminium or to hydrogen if it is present. (Scheme 1.2)

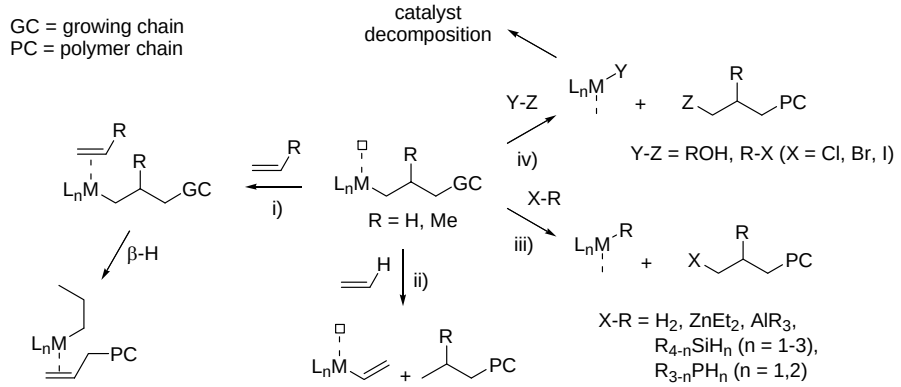

Scheme 1.2 Common intermolecular chain termination pathways in PE and PP synthesis: i) β-H transfer to monomer and chain release; ii) C-H bond activation and transfer from monomer to chain; iii) metathesis with cocatalysts or chain transfer agents; iv) poisoning and catalyst decomposition.

When the olefin being polymerized is prochiral, such as propene, a centre of asymmetry has to be considered and four different coordination modes. Thus, the steric structure of the metallocene-based catalysts can also influence the stereoselectivity of the polymerization; changing the steric structure of the ligands linked to the metal centre leads to a change in steric structure of the polymeric products and an isotactic, syndiotactic or atactic polymer could be easily obtained[47].

The four different coordination modes (A – D) possible for a prochiral 1-olefin to the complex [Zr(η^5:η^5-$C_5H_4CMe_2C_{13}H_6Me_2$) are shown in Figure 1.5.

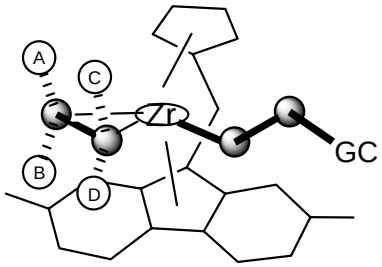

Figure 1.5 Coordination possibilities for a prochiral 1-olefin in the complex [Zr(η^5:η^5-$C_5H_4CMe_2C_{13}H_6Me_2$)(1-olefin)(growing-chain).

The steric interaction of the ligands surrounding the active centre of the catalyst with incoming monomer plays a key role in the stereoselectivity of the polymerizations. Depending on the symmetry class of the metallocene precursor it is possible to tune the microstructure of the polymer obtained.

The two-fold rotation axis in C_2-symmetric catalysts (symmetry class III) makes the two catalytic sites homotopic, enabling them to select the same propene enantiofaces allowing for the stereospecific insertion, that leads to isotactic polymer.

Differently, due to the presence of a vertical mirror plane of symmetry, the C_s-symmetric catalysts (symmetry class IV) presents two enantiotopic sites which are able to discriminate between the two prochiral enantiofaces of a propene molecule and to yield to syndiotactic polymer[48].

In contrast to C_2- and C_s-symmetric catalysts affording isotactic and syndiotactic polypropene, respectively, polymer tacticity from the C_1-symmetric systems (symmetry class V, that is no symmetry) is hard to predict (Figure. 1.6).

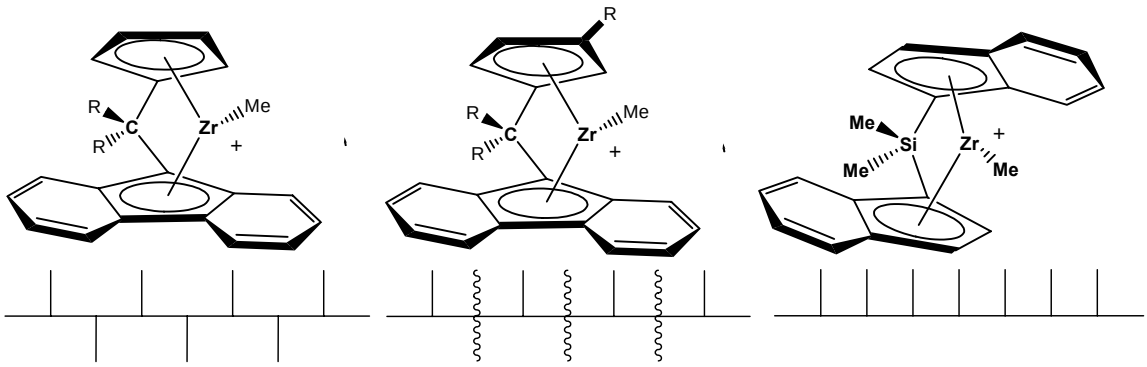

Figure 1.6 Correlation between propene architecture and syndiospecificic, hemispecific and isospecific metallocenes catalysts

^{13}C-NMR spectroscopy is a powerful method to determine the polymer microstructure, which gives a fingerprint of the events occurring during the propagation of the polymer chain. A detailed NMR analysis is a valuable tool to elucidate the polymerization mechanism, which can be utilized to tailor catalyst structure and thus to obtain polymers with tailored structures and properties.

In Figure 1.7, a total ^{13}C-NMR spectrum of polypropene produced by C_s-symmetric Me_2C-(C_5H_4)($C_{13}H_8$)$ZrCl_2$ is reported; according to the general assignment[52] the ^{13}C-NMR resonances of polypropene fall into three different groups that can be assigned to methene carbon atoms (47 - 43 ppm), to methine carbon atoms (30 – 25 ppm) and to methyl carbon atoms (20 – 16 ppm) of the propene backbone. The signals between 19.79 and 19.49 ppm (not detected because the catalyst afforded highly syndiotactic polypropene) are assigned to isotactic *mmmm* pentad, in the region between 19.24 and 19.11 ppm fall the resonances of *rmmr* pentad; in the region between 18.99 and 18.33 ppm the signals are assigned to *mmrr* pentad; the signals between 18.79 and 18.58 ppm are assigned to *rmrr* pentad, at last between 18.29 and 18.09 ppm the signals of syndiotactic *rrrr* pentad are detected.

The polymer microstructure gives a fingerprint of the event occurring during the propagation of the polymer chain, and a detailed analysis is a valuable mean to understand the polymerization mechanism, which in turn is very important to tailor catalyst structure for obtaining polymers with tailored structures and properties.

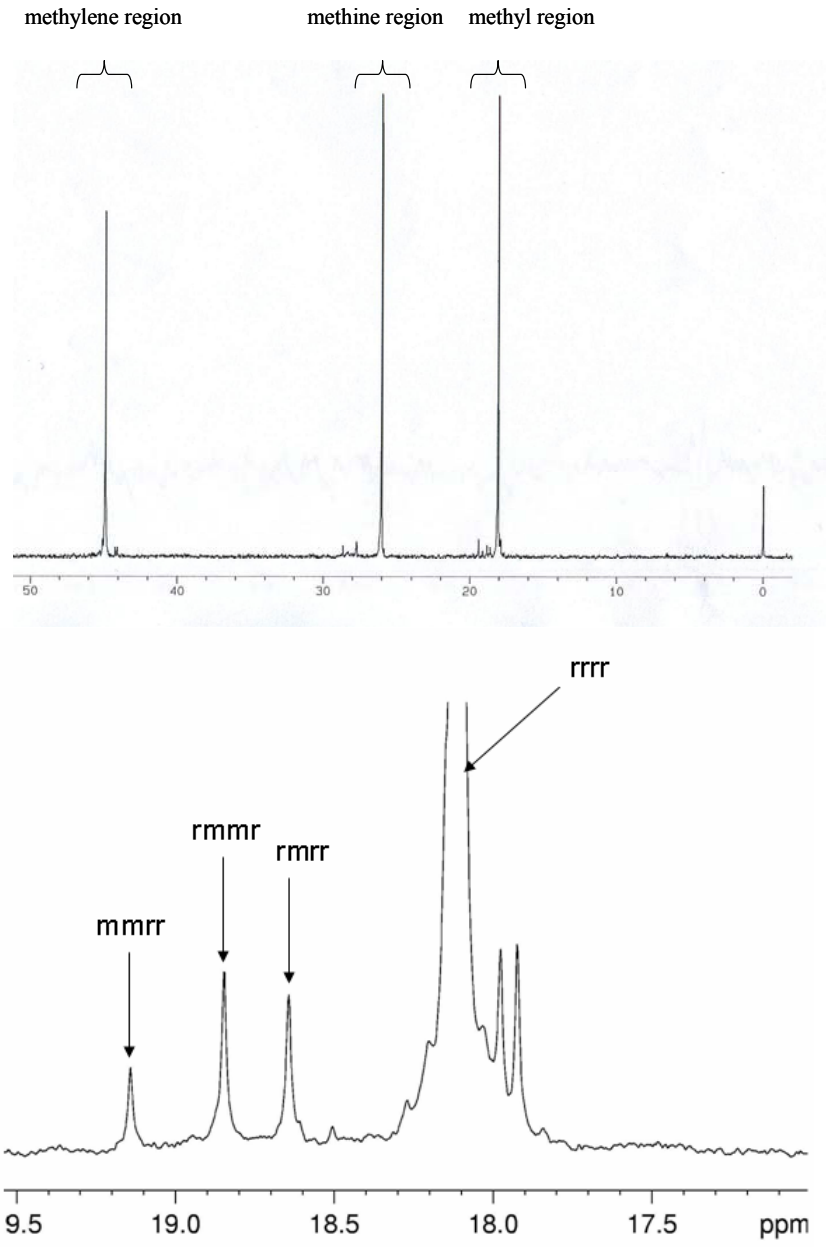

Figure 1.7 a) ^{13}C-NMR spectrum of polypropene samples obtained with C_s-symmetric catalyst Me_2C-(C_5H_4)($C_{13}H_8$)$ZrCl_2$; b) expansion of methyl region of a spectrum of polypropene sample obtained with C_s-symmetric catalyst Me_2C-(C_5H_4)($C_{13}H_8$)$ZrCl_2$.

Since the discovery of *C*$_s$-symmetric fluorenyl-containing metallocenes of the type Me_2C-(C_5H_4)($C_{13}H_8$)MCl_2 (e.g., M = Zr) by Ewen and Razavi[25-27] many

authors have debated about the origin of their syndiospecificity[49]. These systems endowed with two enantiomorphic sites are interesting as they offer the possibility of testing theories on the stereocontrol. There is unanimous consensus that the pathway for the syndiospecific propene enchainment can be explained in terms of chain migratory insertion; this is considered one of the pieces of evidence for alternation of the coordination site, which is proposed by the Cossee's[50] *alternating or migratory mechanism*. The current view is summarized as follows: i) C_s-symmetric metallocene possesses one bulky substituent (fluorenyl), which directs the growing polymer chain toward the less hindered cyclopentadienyl side; ii) the fluorenyl presents an empty space in the central region wide enough to accommodate the methyl of propene in trans with respect to the polymer chain; iii) the incoming monomer and the growing polymer chain alternate at the two enantiotopic sites, determining a migratory type of insertion (Figure 1.8). The presence of stereoerrors such as *rrrmmrrrr* is consistent with site control, the presence of a variable amount of *rrrmrrrr* indicating occasional skipped insertions.

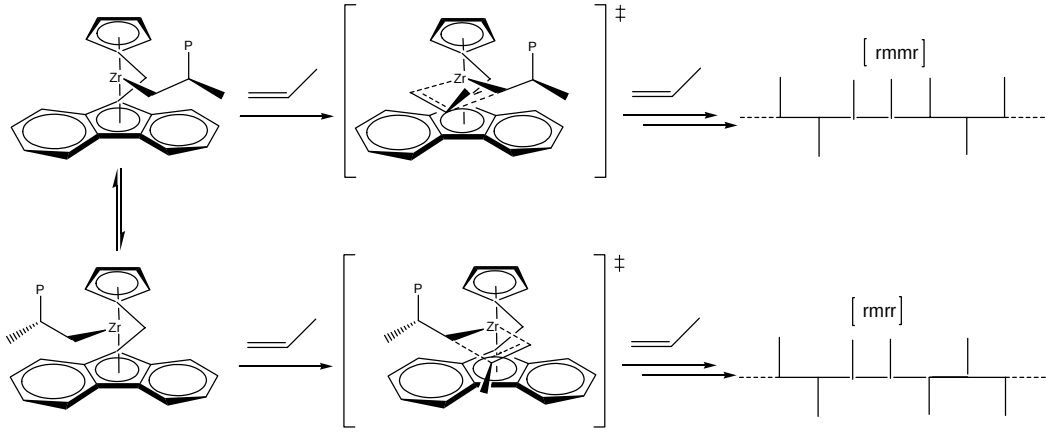

Figure 1.8 Errors in syndiotactic polypropene with C_s-symmetric metallocenes: isolated stereoerrors [rmmr] by site control and [rmrr] by site epimerization

The typical stereorrors that decrease the syndiotacticity of sPP are enantiofacial misinsertions, leading to *rrmmrr* sequences and site epimerization (back skip of the polymer chain) leading to an isolated *m* and thus to *rrrmrr* sequences.

The typical stereorrors that decrease the syndiotacticity of sPP are enantiofacial

misinsertions, leading to *rrmmrr* sequences and site epimerization (back skip of the polymer chain) leading to an isolated *m* and thus to *rrrmrr* sequences. sPP is a thermoplastic material with a high melting point and high crystallinity, which are influenced by the number of stereoerrors. After the initial reports several authors developed bridge-modified analogues, including doubly bridged metallocenes, a number of fluorenyl substituted metallocenes, as well cyclopentadienyl-substituted variants of the parent metallocene which lead to PP with different microstructures and thus with different melt transition temperatures. Incorporation of a substituent at the 3 position of the cyclopentadienyl ring induces desymmetrization of the metallocene to C_1 symmetry. As a consequence, the tacticity of propene homopolymers using C_1-symmetric catalysts is no longer syndiotactic, but polymer microstructure greatly depends on the nature and hindrance of the substituent on Cp group. When the substituent is a Me or *i*-propyl group, a hemi-isotactic or atactic polypropene is obtained; when the substituent is the bulkier *ter*-butyl substituent, isotactic polypropene is achieved. The mechanism which leads to the isotactic polypropene with C_1-symmetric Me_2C-(3-*ter*-butyl-C_5H_3)($C_{13}H_8$)MCl_2 has been a topic of debate.

1.2 Cyclic Olefins

1.2.1 History

Cyclo-olefin polymers (COP) are a family of plastic materials derived from the polymerization of strained-ring monomers which generally exhibits unique physical and mechanical properties that differ from those of polyolefins with acyclic structures.

Many different monomers such as cyclopentene (CP), cyclobutene (CB), norbornene (N), 1,4,5,8-dimethano-1,2,3,4,4a,5,8,8a-octahydronaphtalene (DMON), and 1,4,5,8,9,10-trimethano-1,2,3,4,4a,5,8,8a,9,9a,10,10a-dodecahydroanthracene could be used to obtain a wide variety of polymer for a large range of applications (Figure. 1.9).

Several routes (Figure 1.10) have been investigated to obtain COP and every route produces a polymer which is different in structure and characteristic from the others.

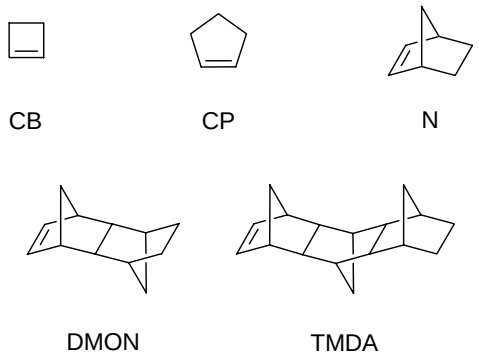

Figure 1.9 Cyclic olefin used in the synthesis of cycloolefin polymers.

The best known polymerization mechanism is the ring-opening metathesis polymerization (ROMP); the very first examples of metathesis polymer obtained through ROMP was produced in 1967 in CdF-Chemie in France, and commercialized under the name of *NORSOREX*[51].

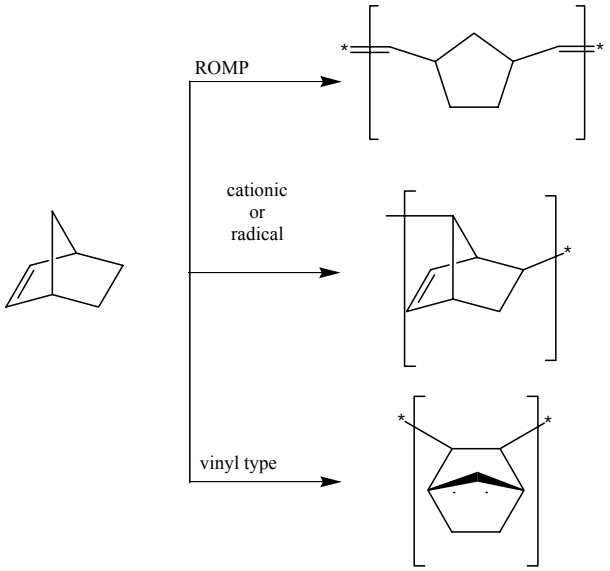

Figure 1.10 Schematic representation of the three different types of polymerization of norbornene.

The $RuCl_3$/HCl catalyzed process produces a polymer that still contains double bonds and could be crosslinked; the vulcanized polymer should operate in air and is most useful for engineeristic application, shock-proof bumper, oil spin and dumping applications.

It is also possible to catalyze the ROMP process employing tungsten, molybdenum, ruthenium catalysts or metal oxides in combination with alkylating agents, such as Et_2AlCl, and promoting agents, i.e. molecular oxygen, phenols or ethanol, or by using molecular single component complexes such as tungsten, molybdenum and ruthenium-based metal carbene complexes[52].

Not much is known about the radical polymerization of cyclic olefins; some examples appeared in literature in the 1967[53]. Very poor results were obtained: low molecular weight oligomeric materials with 2,7 connectivity of the monomers.

It is also possible to polymerize cyclic olefins through another route, usually named addition polymerization; such kind of polymerization is similar to the classical olefin polymerization and leave the cyclic structure of the monomer intact by opening only the double bond of the π-system. The first example of vinyl polymerization of cyclic olefin was reported in the early 1960 with a $TiCl_4$/Al(*iso*-Bu)$_3$[54, 55], but after the development of homogeneous single site catalysts many

review articles appeared in literature, concerning the transition metal-based, homogeneous catalysis[56, 57]; these metallocenes catalysts allow a facile polymerization of cyclic olefins without ring opening. A study by Kaminsky[58] showed that chiral metallocenes precursors activated by MAO were able to polymerize strained cyclo-olefins, such as cyclobutene and cyclopentene, that classical heterogeneous Ziegler-Natta catalysts polymerize with difficulty.

However, polycycloalkenes showed extremely high melting points which lie above their decomposition temperatures (in air). Under vacuum the melting points were found (by DSC) to be 485 °C for polycyclobutene, 395 °C for polycyclopentene, and over 600 °C for polynorbornene.[59] Therefore, such polycycloolefins are generally difficult to process, due to their high melting points and their insolubility in common organic solvents, and are of little commercial interest

The vinyl addition, catalyzed by "naked" transition metal, gives a polymer, commercialized under the trade name Avatrel[60], that possesses high glass transition and decomposition temperature, and excellent transparency as main properties, and is applied as cover layer for liquid-crystal displays and as electrooptical material.

1.2.2 Cyclic Olefin Copolymers (COCs)

To improve the processability of the polycycloolefins, the introduction of a comonomer, such as ethene or other α-olefins, allows the synthesis of cyclic olefin copolymers (COCs). Metallocene precursors activated by MAO are able to insert the linear comonomer into the polyolefin chain, and it is possible to tailor the properties by varying the comonomer content and microstructure[61, 62]. Some of the COCs show very good optical, thermal, and mechanical properties, such as excellent resistance to heat and chemicals, excellent transparency, high refractive index, high stiffness or softness[65].

Ethene(E)-*co*-Norbornene(N) copolymers are the most versatile and studied copolymers, because of their important end uses and the easily available monomers. The ethene monomers are easily obtained from the cracking of mineral oil, and

norbornene molecules derive from Diels-Alder reaction of cheap cyclopentadiene and ethene units. The norbornene–ethene copolymer features a high glass transition temperature, excellent transparency, thermal stability, and chemical resistance.

The first example of E/N copolymer was reported by Kaminsky at al. in 1989[66], when the metallocene precursor *rac*-[Et(Ind)$_2$]ZrCl$_2$ activated by MAO was investigated by addition of ethene to many cyclic monomers, such as cyclopentene, cycloheptene, cyclooctene, and norbornene; since then metallocene catalysis in cyclic olefin copolymerization has been investigated, because it is possible to easily tune the properties of the resulting copolymer by changing the metal or the ancillary ligand. Several catalysts with C_2 or C_s symmetry (Figure 1.6) have been investigated to obtain copolymers with different microstructure or N content and distribution. The glass transition temperature of poly(E-*co*-N) synthetized varied over a wide range: copolymers containing more than 50 mol-% of norbornene can have glass transition temperatures up to 220 °C [57a, 67].

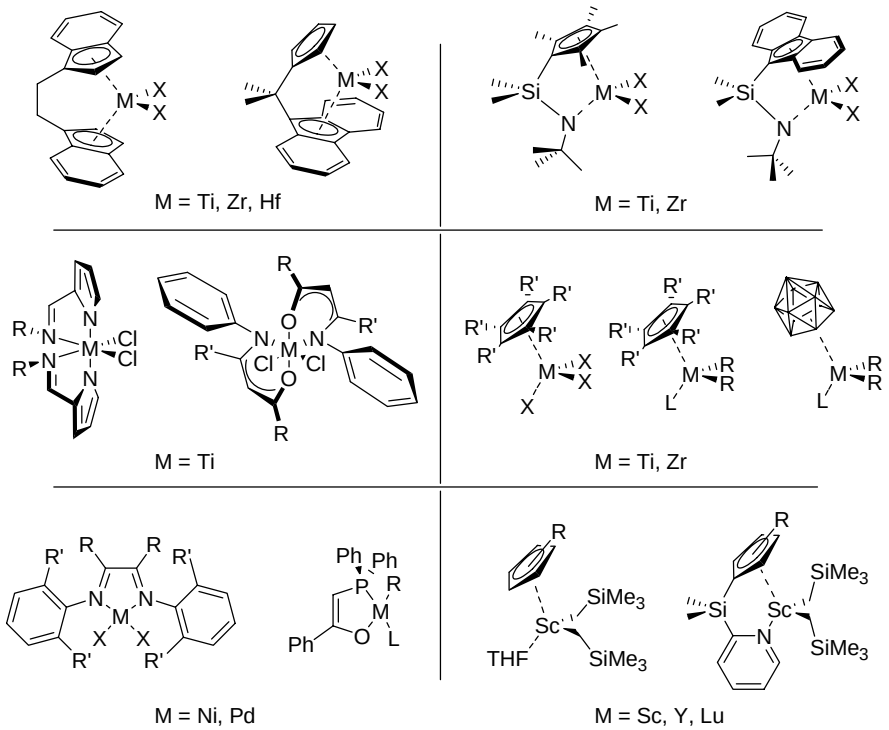

Figure 1.11 Catalysts investigated in the synthesis of ethene-co-norbornene copolymers

The investigation in the last decade of the Constrained Geometry Catalyst (CGC) allows to synthesize a perfectly alternating E/N atactic copolymer[68].

Moreover, by using cyclopentadienyl-free catalysts, a perfect control of molecular weight was achieved, and the development of late-transition metal catalysts has opened the possibility to introduce functionalized norbornene units[61, 62]. Quite recent progresses in catalysis science has lead to the possibility to syntesize cationic rare earth metal half-sandwich catalysts which show very high activity for the copolymerization of cyclic olefins; these catalysts are able to produce perfectly alternating E/N copolymers and when low amount of norbornene was used, an E/N copolymer with an ethene block poly(E-*co*-N)-*b*-PE was obtained[69].

1.2.3 Microstructure Of Poly(E-co-N)

The exploration of the polymer microstructure of poly(E-co-N) is of particular interest, since it is tightly connected to the final properties of the material. Copolymer properties are controlled by tuning the cyclic comonomer content, sequence distribution and the stereochemical placement of norbornene units, characteristics strictly connected to the structure of the catalyst employed.

Metallocene catalysts incorporate norbornene units in a *2,3-exo* fashion[70b]; one of the most relevant consequences is that norbornene cannot undergo β-H elimination, because β-H elimination is located on the endo side and trans to M-C bond, whereas the elimination of the b-hydrogen would results in an anti-Brendt olefin. (Figure. 1.12)

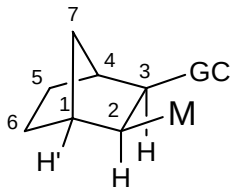

Figure 1.12 *Cis*-2,3-*exo* insertion of norbornene, which impedes β-hydrogen elimination reaction. (M = metal; GC = growing chain)

The poly(E-co-N) microstructure evaluated by ^{13}C-NMR is quite complex, and depending by the amount of norbornene incorporated and the by the catalyst structure, the copolymers display a wide number of comonomer sequences: cyclic olefin units can be arranged in alternating fashion (*ENEN*), or short norbornene

homosequences as diads (*ENNE*) or triads (*ENNN*). Moreover because the C2 and C3 carbon of norbornene units are chiral, an S/R or R/S arrangement is possible and either erythroisotactic (*meso*) and erythrosyndiotactic (*racemic*) sequences can be detected[70a]. In the following figure all the possible stereochemical environments of norbornene are illustrated.

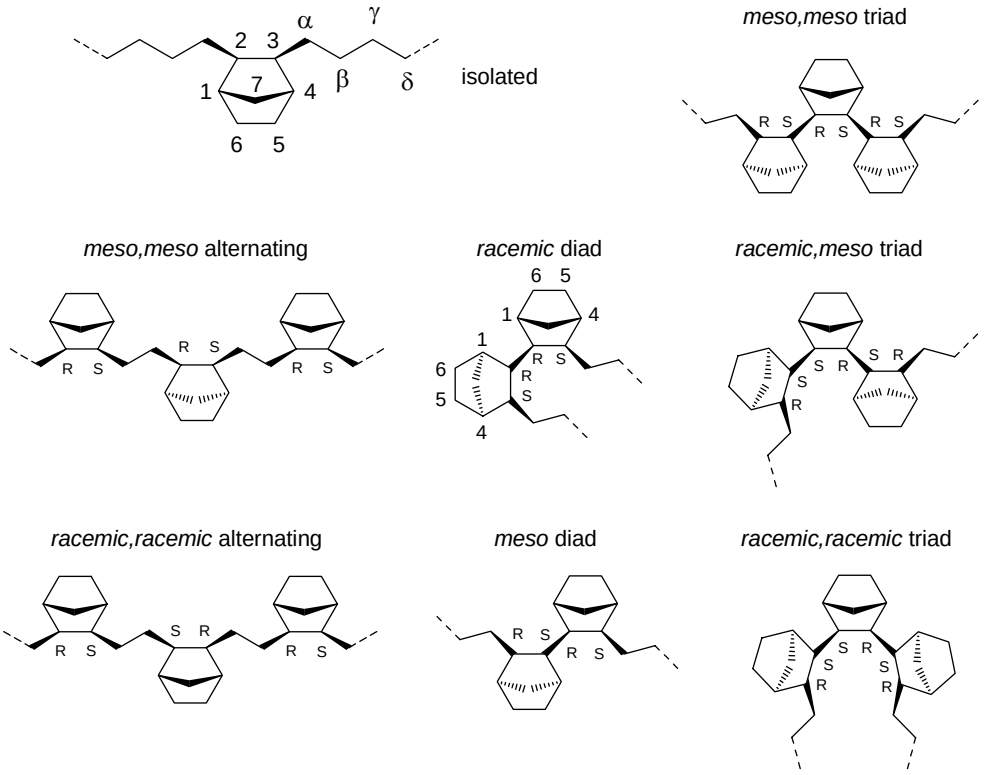

Figure 1.13 Isolated (*ENEE*), alternated (*ENEN*), dyads (*ENNE*), triads (*ENNN*) sequences along with the relative configuration of stereogenic carbon atoms.

The microstructure of copolymer obtained is linked to the structure of the metallocene symmetry. Typically, the presence of homotopic sites of C_2-symmetric catalysts generates perfectly alternating E-N units, arranged in a isotactic fashion; contrary, the copolymers obtained by using catalysts, such as the Constrained Geometry [Ti(η^5:η^1-$C_5Me_4SiMe_2N^tBu$)Cl_2], are practically atactic[69], containing both *meso* and *racemic ENEN* sequences. The presence of enantiotopic sites in C_s-symmetric catalysts, such as [Zr(η^5:η^5-$(C_6H_5)CR_2C_{13}H_8$)Cl_2] generates perfectly alternating *racemic ENEN* sequences.

Highly alternating stereoregular E-N copolymers can be obtained also by means of catalysts with two heterotopic sites, such as C_1-symmetric catalysts. In the presence of an excess of cyclic olefin, the resulting copolymers consist of highly alternating isotactic *ENEN* sequences. Interestingly, these copolymers result to be crystalline if the N content is higher than 37 mol %, showing melting points ranging between 270°C to 320°C[71].

Moreover, C_2 and C_s-symmetric catalysts could generate random E-N copolymers, containing short norbornene homosequences, allowing the synthesis of copolymers having up to 50 mol % of cyclic olefin content, and thus a material with glass transition temperature up to 220°C[72].

In general the ^{13}C-NMR resonances of poly(E-co-N) falls into four different groups[72] that can be assigned to the methene, C5/C6 and C7 carbon atoms or the methine, C1/C4 and C2/C3 resonances of norbornene. The region of C5/C6 carbon atoms of N ranges between 20.6 and 30.5 ppm and cannot be distinguished by CH_2 resonance peak of ethene molecules. The signals at 26.2 and 29.7 ppm and at 27.5 and 29.3 ppm are assigned to *meso* and *racemic ENNE* dyads, respectively. The signals of carbons C5/C6 in *ENNN* triads sequence might be overlapped with the signals of *meso* and *racemic* dyads.

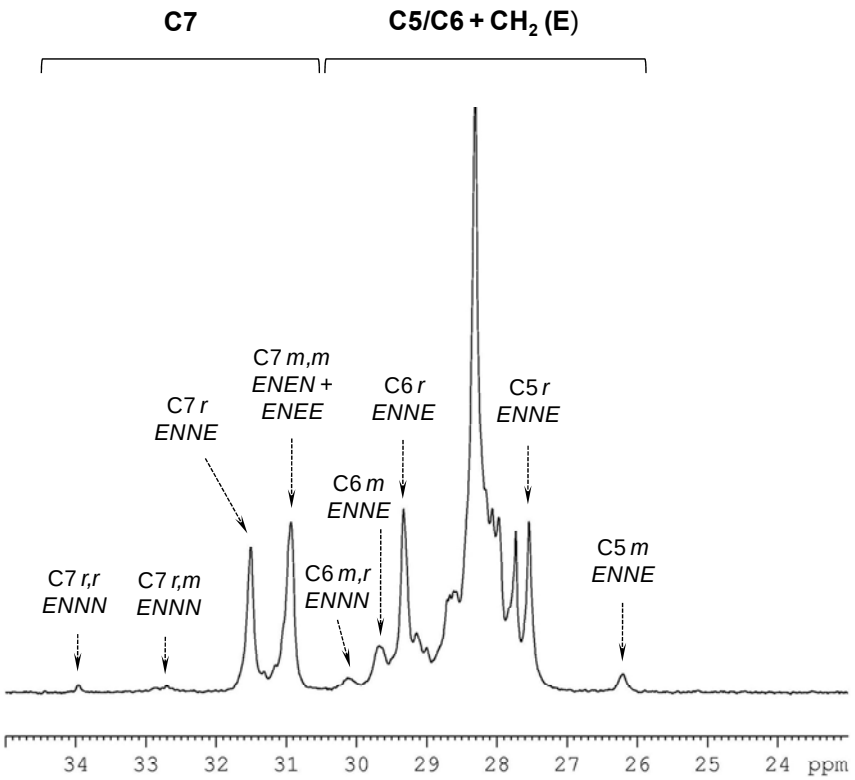

Figure 1.14 Expansion of the region between 23 and 35 ppm of the ^{13}C-NMR spectrum (108.58 MHz, $C_2D_2Cl_4$, 103 °C) of a poly(E-*co*-N) sample

The resonances of C7 (Figure 1.14) are located in the region ranging between 30.6 and 34.3 ppm; the peak at 31.5 ppm is assigned to *racemic* dyads of carbon C7 while the signals at 32.7 and 33.9 should be corresponding to the *meso,racemic* and *racemic*,*racemic ENNN* sequences, respectively.

In the region between 42.5 and 34.8 ppm (Figure 1.14), resonances attributed to C1/C4 methine carbons of N are observed. The signals located between 38.5 and 37 ppm are possible to be ascribed to *racemic*,*racemic* triads. The peaks at 39 and 39.8 ppm correspond to carbons of *racemic ENNE* sequences, while the peak at 39.5 ppm and part of the signal at 40.1 ppm are ascribed to *meso* and *racemic* alternating (*ENEN*) and isolated (*ENEE*) sequences.

At last, resonances in the region between 42.5 and 53.8 ppm (Figure 1.15) are attributed to the C2/C3 resonances of N. The peaks at 45 and 45.8 ppm are assigned to carbons C2 and C3 in isolated and *racemic* and *meso* alternating units,

respectively. The signals at 45.6 and 48 ppm correspond to *racemic* dyads, while signals ascribed to *meso* dyads are located at 46.5 and 47.1 ppm.

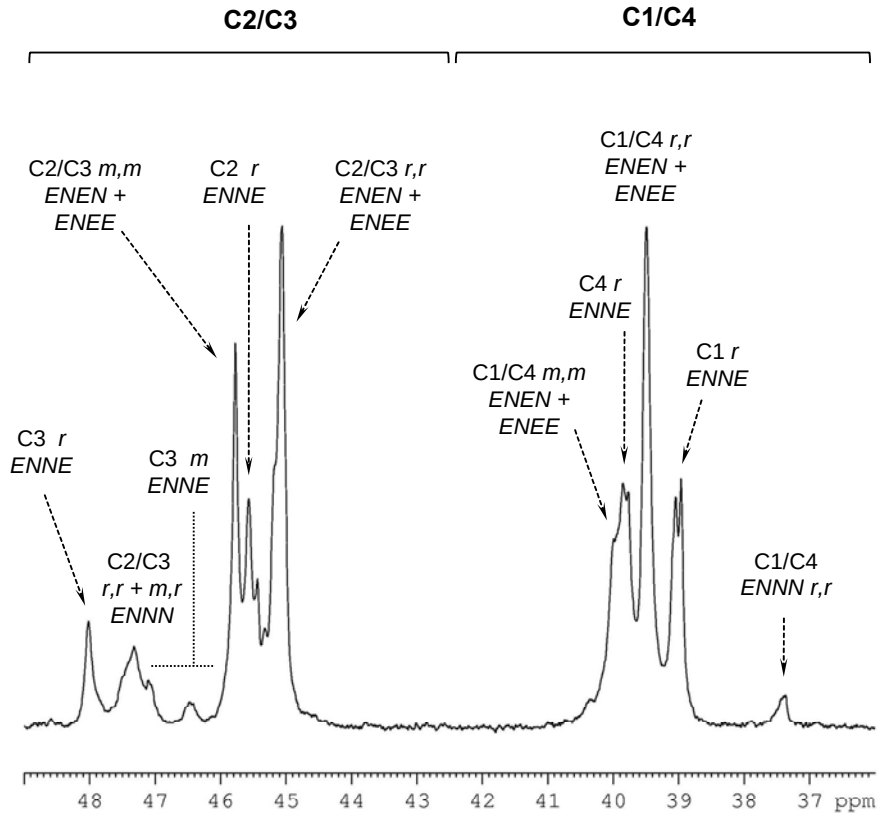

Figure 1.15 Expansion of the region between 50 and 36 ppm of ^{13}C-NMR spectrum (108.58 MHz, C2D2Cl4, 103 °C) of poly(E-*co*-N) sample.

Detailed assignments of the complex spectra of these copolymers have been achieved. Quantitative data concerning the structural characteristics of poly(E-*co*-N) from the relative intensities of the respective peaks make possible to reach a complete description of the copolymer microstructure at tetrad level or even at pentad level[62].

1.2.4 Poly(E-co-N): Properties & Applications

Ethene-*co*-norbornene copolymers (commercially TOPAS: Transparent Olefin Polymer Amorphous Structure) are suitable for the production of transparent materials for use in optical data storage, optics, e.g. lenses, sensors, and industrial

products, e.g. in the construction and lighting sectors. In Table 1.1 are reported the basic properties of poly(E-*co*-N)s compared to those of other transparent amorphous plastics, while in Table 1.2 are presented the major applications of these materials.[73]

One of the most important properties of this class of polymers is their ability to modify the glass transition temperature (T_g) simply by varying the norbornene/ethene molar ratio in the copolymer. By increasing the cyclic olefin content the stiffness of the copolymer along with the T_g and the heat deflection temperature, that is, the temperature at which a polymer or plastic sample deforms under a specified load increase. Typically, commercial grades copolymers have T_g values from 80 to 185 °C, and HDT from 75 to 170 °C. Poly(E-*co*-N) with glass transition temperature below 100 °C became more flexible and give much higher elongation at break. Notably, the flowability of the material is adjusted by controlling the molar mass (M_w) characteristics.

Table 1.1 Properties of poly(E-*co*-N) in comparison with other transparent amorphous plastics

General	**P(E-*co*-N)**	**PS**	**PC**	**PMMA**
	1.02	1.05	1.2	1.2
Flexural modulus (Msi)	0.5	0.45 - 0.5	0.34	0.45
Tensile strength (ksi)	9	6.4 - 8.2	9	10
Elongation (%)	3 - 10	2 - 4	80	5
Water absorption (%)	0,01	0.1 - 0.3	0.04	0.1
Heat deflection temperature - HDT (°C)	75 - 170	75 - 94	142	92
Glass transition temperature - T_g (°C)	80 - 185	95	150	85 - 165
Optical				
Luminous transmission (%)	92	91	88	92
Haze (%)	1	3	1	1
Index of refraction	1.53	1.59	1.59	1.5
Abbé Number	56	31	34	61
Birefringence	Low	Variable	Variable	Low

Optics – E-N copolymers are successfully applied in the production of high quality optical components. The transmittance, that extends from the visible spectrum to the UV light, is higher than that of PS and PC and equal to that of polymethyl methacrylate (PMMA), as seen in Table 1.1. Due to his aliphatic structure, poly(E-co-N) copolymers have low birefringence, witch is a critical factor in a huge range of lens and optical applications; moreover, the real advantage is the

behaviour of birefringence under the effect of an applied tensile strength, which remains rather stable, differently from maby other plastics, such as PS. These plastics also have a high Abbè number, the measure of how the refractive number change with the wavelength, that is an indication of low chromatic aberration.

Interestingly, the density of E-N copolymers is very low compared to classical transparent amorphous resins such as PC and PMMA These properties make E-N copolymers suitable for replacing glass in optical components where weight and durability are needed such as video camcorder, or hard-disk drives. On the other hand, the optical properties of poly(E-*co*-N) copolymers, combined with their very low moisture absorption, give them advantages in applications such as projection TVs and computer displays, and other applications where heat or humidity can deform acrylic or PC lenses such as higher capacity DVDs and lenses for LEDs.

Table 1.2 General applications of poly(E-*co*-N).

	Applications
Precision Optics	- Video camcorders, hard disk drives, flat panel displays, light guides for automotive - Projections and computer displays, lenses - DVDs, lenses for LEDs, printes, diffractive optics, lighting, metallized reflectors, mirrors - Toner binder in color printers
Electrical	- Thin-film capacitors
Medical and Diagnostic	- Syringe, serum vials, blood containers, petri dishes, test tubes, diagnostic and biomedical container - Cuvettes (spectrophotometer readings) - Microtiter plates, contact lens tooling, inhaler and dialysis parts
Packaging	- Flexible films for food, drugs, cosmetics, personal care - Bags and pouches for drinks and food. - Blister packaging, shrink films.

Electrical applications – E/N copolymers are good electrical insulators, with constant electrical properties over a wide range of temperatures and frequencies. Low electron mobility and non-polarity could generate high resistivity and low dissipation factor that makes the copolymer particularly useful in thin-film capacitors. Poly(E-*co*-N)-based capacitors can be smaller and more energy efficient

than those of polypropene (PP) in applications as AC motor starter and high-frequency semiconductor circuits.

Medical and diagnostic applications – These copolymers also possess a high transparency, excellent moisture barrier and chemical resistance to hydrolysis, both in acidic and basic environment, as well as to polar organic chemicals. These properties enable E-N copolymers to be suitable for medical and diagnostic applications. Pharmaceutical and biomedical containers made of poly(E-*co*-N) can withstand all common sterilization regimes and displays excellent shatter resistance. Consequently, they can replace glass in several application (Table 1.2).

Packaging applications –. Poly(E-co-N) copolymers are suitable for direct food contact applications and are largely used in flexible packaging for food, drugs, cosmetics, and consumer products; combining these materials with polyethene (PE) in blend films enhances the stiffness and sealability of the material, by keeping moisture out or preventing moisture loss during storage. They can be combined with PE in monolayer blend films or used in multilayer structures with layers of other resins. Typical uses for these blends include blister packaging, shrink films, and further packaging applications where improved moisture barrier and sealability are needed.

Finally, poly(E-*co*-N) are processible by all commonly used methods for thermoplastics including injection molding, cast and blown film extrusion and coextrusion, injection blow-molding, and injection-stretch blow molding.

Recycling – The recyclability of these copolymers depends on the polymers which are combined with; in fact, most of the poly(E-*co*-N) packaging applications involve mixed structures with other polymers. Although many blends and multilayered structures should be coded with the recycling number “7” under the SPI system (Society of the Plastics Industry), certain PE combinations may use the code of the majority PE component. For instance, a LDPE structure having a minor amount of poly(E-*co*-N) may retain a SPI recycle code of “4”.

1.3. Scope of the Work

Propene-based Homo- and Copolymers. The introduction of metallocenes in copolymerization reactions has created new opportunities for the synthesis of olefin copolymers with uniform compositions and random sequence distributions and with tailored microstructures and properties. Propene copolymers by homogeneous metallocenes form a new class of thermoplastic elastomers with lower melting points, lower glass transition temperatures and higher impact strength than stereoregular PP homopolymers. The copolymerization of propene with ethene is a common way of tailoring the density and crystallinity of ethene polymers. It is known that by adding low amount, ranging between 1 and 5 mol %, of ethene it is possible to obtain a material that is more elastic than iPP or sPP homopolymer, and simultaneously allows the control of the crystallization process.

The molecular weight control is an important issue for accessing the practical production of polymeric materials. Indeed, both for C_s-symmetric and C_2-symmetric catalysts it was found that the M_w of ethene-propene copolymers are in general lower than those of propene homopolymers. Thus, much efforts have been dedicated to synthesize C_2-symmetric catalysts, which give high molar masses, being copolymers based on iPP the most interesting one for industrial applications.

Incorporation of a substituent at the 3 position of the cyclopentadienyl ring of bridged $(C_5H_4)(C_{13}H_8)MCl_2$ with C_s symmetry induces desymmetrization of the metallocene to C_1 symmetry. The microstructure of propene homopolymers using C_1 symmetric metallocenes greatly depends on the nature and hindrance of the substituent on Cp group. When the substituent is a Me or *i*-propyl group, a hemi-isotactic or atactic polypropene is obtained; when the substituent is the bulkier *ter*-butyl substituent, isotactic polypropene is achieved. These systems are amenable to study fine details of the polymerization mechanism. Moreover, they have the potential of being used for producing iPP, indeed if the group used to introduce C_1 symmetry is large enough isotactic PP is obtained, which is of great interest from a practical point of view since the isotactic polymers synthesized by C_2-symmetric

indenyl based catalysts often produce small undesirable fractions of atactic polymers[74].

The mechanism which leads to the isotactic polypropene with C_1-symmetric Me_2C-(3-*ter*-butyl-C_5H_3)($C_{13}H_8$)MCl_2 has been a topic of debate. For this reason a number of complex C_1-symmetric metallocenes have been synthesized and studied recently[75].

The aim of this part of the project on propene polymerization catalysis with C_1-symmetric fluorenyl-containing metallocenes bearing one or two *ter*-butyl substituents at the 3 position of Cp or at 3 position of the fluorenyl groups. The main objective of this investigation was: to assess the impact of these changes on the polymerization mechanism and on catalytic performances for obtaining isotactic polypropene with high molar masses; to identify among the C_1 symmetric catalysts those most promising for obtaining copolymers with high molar masses, as well as to give a rationale to such possibility. In particular the effect of one or two *ter*-butyl substitutions on the catalytic activity, on the stereoerrors, and on molar masses in conditions which tend to approach those used in industrial processes was evaluated. Thus, C_1-symmetric metallocenes were subjected to MAO-cocatalyzed propene homopolymerizations at different temperatures and monomer concentrations. Stereoerrors were investigated by ^{13}C-NMR analysis. A comparison of the polymer microstructures on the basis of statistical analysis was performed and mechanisms which lead to the observed microstructures were tested. An analysis of chain end groups by ^{1}H-NMR analysis in order to understand the role of substituents on polymer molar masses.

Finally, the industrial synthesis of homo- and copolymers by homogeneous catalysts has to be achieved by supported systems in liquid propene because homogeneous processes present serious drawbacks such as reactor fouling as well as morphological issues. Thus, we have made efforts to study the variables that need to be controlled in order to produce in the laboratory reproducible copolymers with highly active supported catalysts.

Norbornene-based Co- and Terpolymers. A promising approach to further expand the properties of COCs is the introduction of a third monomer like a linear α–olefin such as 1-octene or the substitution of the bicyclic norbornane unit with a cyclopentane unit by 1-5 hexadiene cyclopolymerization.

The possibility of 1,5-hexadiene to cyclize by 1,2-addition of a double bond of diene, followed by intramolecular cyclization to form cyclopentane structures is an interesting feature which can lead to polymers with interesting properties; in fact, due to steric reasons, the polymerization of five member ring cycloolefins is poor active. Metallocene-mediated cyclopolymerization of 1,5-hexadiene may represent an alternative synthetic route to cycloolefin copolymers.

The presence of a long linear α-olefin into E-N copolymer backbone could increase the flexibility of the copolymer chain and improve the commercial applicability of the material, while maintaining a high transparency and the other characteristic properties of E-N copolymers.

Recently, a PhD study has been performed by Roberto Marconi on ethene, norbornene, 1,5-hexadiene or 1-octene terpolymerizations by two different representative group IV metal-based catalysts [$Zr(\eta^5:\eta^5\text{-}C_5H_4CPh_2C_{13}H_8)Cl_2$] (**I**) and [$Ti(\eta^3:\eta^1\text{-}C_{13}H_8SiMe_2NCMe_3)Cl_2$] (**II**), and by the family of catalysts [$M(L_1L_2AB)$] bearing different substituents on the ancillary ligand, activated by methylaluminoxane (MAO)

The main drawback of the catalytic systems used was the difficulty to obtain high molecular weight terpolymers with high cyclopentane units content and with vinylic and crosslinking degree as low as possible. The addition of 1-octene termonomer remarkably decreased the activity for all the catalytic systems investigated, compared to E/N copolymerizations, and terpolymer molar masses.

Nonbridged half-metallocene-type group IV transition metal complexes of the type Cp'M(L)X_2 (Cp' = cyclopentadienyl group; M = Ti, Zr, Hf; L = anionic ligand such as OAr, NR_2, $N{=}CR_2$, etc.; X = halogen or alkyl) in combination with appropriate activators such as MAO are efficient catalysts for copolymerization of ethene with α-olefins containing bulky substituents such as vinylcyclohexane and 3-

methyl-1-pentene, and with cyclic olefins, yielding polymers with high molecular weight and in high activities[76-78].

The aim of this work was to explore these catalysts in ethene, norbornene, 1,5-hexadiene or 1-octene terpolymerizations since in principle, their coordinatively open structure offers the opportunity to readily accommodate 1,5-hexadiene or 1-octene monomers and to lead to terpolymers with novel properties.

References

1. (a) K. Ziegler, E. Holzkamp, H. Breil, H. Martin, *Angew. Che*m., **1955**, *67*, 541; (b) K. Ziegler, *Angew. Chem*., **1964**, *76*, 545.

2. (a) G. Natta, *Angew. Chem*., **1956**, *68*, 393; (b) G. Natta, *Angew. Chem*., **1964**, *76*, 533.

3. J. C. Chadwick, Ziegler-Natta catalysts. *Encyclopedia of polymer science and technology*. **2002**.

4. J. C. Salamone. *Polymeric materials encylopedia*. CRC press, Boca Raton (USA), **1996**.

5. M. W. Perrin *Polymerization of ethene. Research*, **1953**, *6*, 111.

6. J. Boor, *Ziegler-Natta Catalyst and Polymerization*, Academic Press: New York 1979, 92, 103.

7. G. W. Coates, *Chem. Rev*. **2000**, *100*, 1223; (b) W. Kamisky, M. Arndt-Rossenau, in: J. Scheirs, W. Kamisky (Eds.), *Metallocene-based Polyolefins*, Wiley&Sons, Chichester, **2000**, .89.

8. T. J. Kealy, P. Pauson, *Nature*, **1951**, *168*, 1039.

9. G. Wilkinson, M. Rosenblum, M. C. Whiting, R. B. Woodward *J. Am. Chem. Soc.,* **1952,** *7,* 2125.

10. E. O. Fischer, W. Pfab *Zeitschrift für Naturforschung B* **1952,** *7,* 377.

11. (a) P. F. Eiland and R. Pepinsky *J. Am. Chem. Soc.,* **1952**, *74,* 4971.

12. J. Dunitz, L. Orgel, A. Rich *Acta Crystal.* **1956,** *9,*: 373.

13. P. Laszlo, R. Hoffmann *Angew. Chem. (Int. Ed.)*, **2000**, *39*, 123.

14. (a) G. Wilkinson, *J. Am. Chem. Soc.*, **1952**, *71*, 6146; (b) G. Wilkinson, *J. Am. Chem. Soc.*, **1952**, *71*, 6148; (c) G. Wilkinson, *J. Am. Chem. Soc.*, **1954**, *76*, 209; (d) G. Wilkinson, F. A. Cotton, *Chem. Ind. (London)*, **1954**, *11*, 307.

15. G. Wilkinson, P. L. Pauson, J. M. Birmingham, F. A. Cotton, *J. Am. Chem. Soc.*, **1953**, *75*, 1011.

16. P. L. Pauson, G. Wilkinson, *J. Am. Chem. Soc.*, **1954**, *7*6, 2024.

17. G. Wilkinson, J. M. Birmingham, D. Seyferth, *J. Am. Chem. Soc.*, **1954**, *76*, 4179.

18. (a) T. S. Piper, G. Wilkinson, *Chem. Ind. (London)*, **1955**, 1296; (b) T.S. Piper, G. Wilkinson, *Naturwiss.*, **1955**, *42*, 625; (c) T. S. Piper, G. Wilkinson, *Naturwiss.*, **1956**, 43, 15; (d) T. S. piper, G. Wilkinson, *J. Inorg. Nucl. Chem.*, **1956**, *3*, 104.

19. "Press Release: The Nobel Prize in Chemistry 1973". The Royal Swedish Academy of Sciences. **1973**.

20. (a) G. Natta, P. Pino, G. Mazzanti, U. Giannini, E. Mantica, M. Peraldo, *Chim. Ind. (Paris)*, **1957**, *39*, 19; (b) G. Natta, P. Pino, G. Mazzanti and U. Giannini, *J. Am. Chem. Soc*., **1957,** *79,* 2975.

21. (a) D. S. Breslow, *US Pat., 537039*, **1955**; (b) D. S. Breslow, N. R. Newburg, *J. Am. Chem. Soc*., **1957,** *79,* 5072.

22. (a) H. Sinn, W. Kaminsky, H. J. Wollmer, R. Woldt, *Angew. Chem*., **1980**, *92*, 396; (b) H. Sinn, W. Kaminsky, *Adv. Organomet. Chem*., **1980,** *18,* 99.

23. Ferdinand R. W. P. Wild; M. Wasiucionek, G. Huttner, H. H. Brintzinger, *J. Organomet. Chem.* **1985**, *288*, 63.

24. (a) W. Kaminsky, K. Külper, H. H. Brintzinger, Ferdinannd R. W. P. Wild, *Angew. Chem.,* **1985**, *97,* 507. (b)W. Kaminsky, M. Arndt, *Adv. Polym. Sci.,* **1997**, *127,* 143.

25. J.A. Ewen, R.L. Jonas, A. Razavi. *J. Am. Chem. Soc*, **1988**, *110*, 6255.

26. J. A. Ewen, M. J. Elder, R. L. Jones, L. Haspeslagh, J. L. Atwood, S. G. Bott, K. Robinson, *Makroml. Chem. Macomol. Symp*., **1991**, *48/49*, 253.

27. J. A. Ewen, M. J. Elder, R. L. Jones, S.Curtis, H. N. Cheng. *Catalytic Olefin Polymerization Studies in Surface Science and Catalysis*; Keii, T., Soga, ., Eds., Elsevier: New York, **1990.**

28. .(a) G. Balbontin, D. Dainelli, M. Galimberti, G. Paganetto; *Makroml Chem*, **1992**, *193*, 693; (b) A. Galambos, M. Wolkowicz, R. Zeigler, *Catalysis in Polymer Synthesis*; ACS Symp. Ser. *496*; Vandemberg, E. J., Salamone; (c) A. J. Lovinger, B. Lotz, D. D. Davis, F. J. Padden; *Macromolecules*, **1993**, *26*, 3494; (d) P. Sozzani, R. Simonutti, M. Galimberti; *Macromolecules*, **1993**, *26*, 5782; (e) J. Rodriguez-Arnold, A. Zhang, S. D. Z. Cheng, A. Lovinger; E. T. Hsieh, P. Chu, T. W. Jhonson, K. G.

Honnell, R. G, Geerts; S. J. Palackal, G. R. Hawley, M. B. Welch; *Polymer*, **1994**, *35*, 1884.

29. H. Braunschweig, F. M Breitling, *Coord. Chem. Rew.*, **2006**, *250*, 2691 P. G. Gassmann, M. R. Callstrom,. *J. Am. Chem. Soc.,* **1987**, *109*, 7875.

30. S. Betso, L. Kale and J. Hemphill, Constrained geometry catalyzed polyolefins in durable and wire and cable applications, J. Scheirs, W. Kaminsky, Editors *Metallocene-based polyolefins*,**.** Wiley **2000**, *2*, 517.

31. K. Sehanobish, S. Wu, J. Dibbern and N. Laughner, Constrained geometry single-site catalyst technology elastomers and plastomers for impact modifications and automotive applications, J. Scheirs, W. Kaminsky, Editors *Metallocene-based polyolefins*, Wiley. **2000,** *2,* 161.

32. (a) J. J. Eisch, S. I. Pombrick, G. X. Zheng, *Organomet* **1993**, *12*, 3856. (b) C. Sishta, R. M. Halthorn, T. J. Marks, *J. Am. Chem. Soc.,* **1992**, *114*, 1112.

33. (a) A. R. Siedle. R. A. Gleason, W. B. Lamanna, *Organomet*, **1990**, *9*, 1290; (b) M. Bühl, G. Hopp, W. von Philipsborn, S. Beck, M. H. Prosenc, U. Rief, *Organomet*, **1996**, *15*, 778.

34. M. J. Bochmann, *J. Chem. Soc., Dalton Trans*., **1996**, *255*.

35. J. A. M. van Beek, P. J. J. Pieters, M. F. H. van Tol., *Proceedings of symposium Metallocenes '95*, Brussels, April 26-27 (**1995**).

36. (a) D. Coevoet, H. Cramail, A. Deffieux, *Macromol. Chem. Phys*., **1998**, *199*, 1451; (b) D. Coeveoet, H. Cramail, A. Deffieux, *Macromol. Chem. Phys*., **1998**, *199*, 1459.

37. I. Tritto, S. Li, M. C. Sacchi, G. Zannoni, *Macromol. Chem. Phys*., **1993**, *26*, 7112.

38. D. Cam, U. Giannini, *Macromol. Chem*., **1992**, *193*, 1049.

39. (a) I. Tritto, S. Li, M. C. Sacchi, P. Locatelli, G. Zannoni, *Macromol*, **1995**, *28*, 558; (b) I . Tritto, M. C. Sacchi, S. X. Li, *Macromol. Symp*., **1995**, *89*, 289; (c) I. Tritto, M. C. Sacchi, S. X. Li, *Macromol. Symp*., **1995**, *97*, 101.

40. I. Tritto, R. Donetti, M. C. Sacchi, P. Locatelli, G. Zannoni, *Macromol*, **1997**, *30*, 1247.

41. M. Bochman, S. J. Lancaster, *Angew. Chem. Int. Ed. Engl*., **1994**, *33* 1634.

42. J. W. Lauher, R. Hoffmann, *J. Am. Chem. Soc.* **1976**, *98*, 1729.

43. (a) R. H. Grubbs, G. W. Coates. *Acc. Chem. Res*., **1996**, *29*, 86; (b) H. Kraykedat, G. G. Brintinger, *Angew. Chem. Int. Ed. Engl*., **1990**, *29*, 1412; (c) W. E. Piers, J. E. Bercaw, *J. Am. Chem. Soc.*, **1990**, *112*, 9406.

44. (a) P. Cossee, *J. Catal*., **1964**, *3*, 80; (b) E. Arlman, P. Cossee, *J. Catal*., **1964**, *3*, 99.

45. (a) K. J. Ivin, J. J. Rooney, C. D. Stewart, M. L. H. Green, R. Mahtab, *J. Chem. Soc. Chem. Commun.*, **1978**, *604*; (b) M. L. H. Green, *Pure Appl. Chem*., **1978**, *50*, 27; (c) D. T. Lavery, J. J. Rooney, *J. Chem. Soc. Faraday Trans*., **1983**, *79*, 869.

46. M. Brookhart, M. L. H. Green, *J. Organomet. Chem*., **1983**, *250*, 395.

47. L. Resconi, L. Cavallo, A. Fait, F. Piemontesi, *Chem. Rev.* **2000**, *100*, 1253.

48. M. Farina,' G. Di Silvestro, P. Sozzani *Macromol.,* **1993**, *26*, 946.

49. (a) Ewen, J. A.; Elder, M. J.; Jones, R. L.; Curtis, S.; Cheng, H. N. In Catalytic Olefin Polimerization, Studies in Surface Science and Catalysis; Keii, T. Soga, K., Eds.; Elsewier: New York, 1990; p. 439. (b) Farina, M.; Terragni, A. Makromol. Chem. Rapid. Commun. 1993, 14, 791. (c) Razavi, A.; Peters, L.; Nafpliotis, L.; Vereecke, D.; Den Dauw, K. Macromol. Symp. 1995, 89, 345. (d) Busico, V.; Cipullo, R.; Talarico, G.; Segre, A. L.; Caporaso, L. Macromolecules, 1998, 31, 8720-8724. (e) Veghini, D., Henling, L. M.; Burkhardt, T. J.; Bercaw, J. E. J. Am. Chem. Soc. 1999, 121, 564-573. (f) Marks, T. J.; Chen, M. C.; Roberts, J. A. S. J. Am. Chem. Soc. 2004, 126, 4605-4625.

50. (a) Cossee, P., Tetrahedron Lett. 1960, 12. (b) Cossee, P. Tetrahedron Lett. 1960, 17.

51. A. Marbach, R. Hupp, *Rubber World*, **1989**, p. 30.

52. K. J. Ivin, J. C. Mol, "Olefin Metathesis and Metathesis Polymerization", Academic Press, San Diego, CA 1997, p. 407.

53. P. Kennedy, H. S. Makowsky; *J. Macromol. Sci., Chem.* **1967**, *A1*, 345.

54. G. Sartori, F. C. Ciampelli, N. Cameli, *Chim. Ind (Milano)*, **1963**, *45*, 1478.

55. Ger. 2421838 (1975), VEB Leuna-Werke (GDR),: J. P. Koinzer, U. Langbein, E. Taeger, *Chem. Abstr.*, **1976**, *84*, 60227y.

56. (a) G. G. Hlatky, *Coord. Chem. Rev.*, **1999**, *181*, 243; (b) A. L. McKnight, R. M. Waymouth, *Chem. Rev.*, **1998**, *98*, 2587; (c) H. H. Brintzinger, D. Fischer, R. Mulhaupt, B. Rieger, R. M. Waymouth, *Angew. Chem. Int. Ed. Engl.*, **1995**, *34*, 1143.

57. (a) H. G. Alt, A. Koppl, *Chem. Rev.*, **2000**, *100*, 1205; (b) G. Fink, B. Steunmertz, J. Zechlin, C. Przybyla, B. Tesche, *Chem, Rev.*, **2000**, *100*, 1377; (c) L. Resconi, L. Cavallo, A. Fait, F. Piemontesi, *Chem. Rev.*, **2000**, *100*, 1253; (d) K. Angermund, G. Fink, V. R. Jensen, R. Kleinshmidt, *Chem. Rev.*, **2000**, *100*, 1457; (e) H. G. Alt, *J. Chem. Soc. Dalton Trans.*, **1999**, 1703; (f) N. Kashiwa, J. I. Imuta; *Catalysis Surveys Japan*, **1997**, *1*, 125; (g) M. Bochman, *J. Chem- Soc., Dalton Trans.*, **1996**, 255. M. Aulbach, F. Kuber, *Chem. Unserer Zeit*, **1994**, *28*, 197.

58. W. Kaminsky, A. Bark, M. Arndt, *Makromol. Chem., Macromol. Symp.*, **1991**. *47,* 83.

59. W. Kaminsky, A. Bark, I. Dake, in: T. Keii, K. Soga (Eds.), *Catalytic Olefin Polymerization*, Kodansha–Elsevier, Tokyo–Amsterdam, **1990**, p. 425.

60. N.R. Grove, P.A. Kohl, S.A.B. Allen, S. Jayaraman, R. Shick, *J. Polym. Sci., Part B: Polym. Phys.* **1999**, *37*, 3003.

61. X. Li, Z. Hou, *Coord Chem Rev.*, **2008**, *252*, 1842.

62. (a) I. Tritto, L. Boggioni, D. R. Ferro, *Coord. Chem. Rev.* **2006**, *250*, 212; (b) I. Tritto, L. Boggioni, C. Zampa, M. C. Sacchi, D. R. Ferro, *Topics in Catalysis*, **2006**, *40*, 151.

63. (a) *Modern Plastics* **1995**, *72* (9), 137; (b) G. Khanarian, *Opt. Engin.* **2001**, *40*, 1024; (c) J. Y. Shin, J. Y. Park, C. Liu, J. He, S. C. Kim, *Pure Appl. Chem* **2005**, *77*, 801.

64. W. Kaminsky, R. Spiehl, *Macromol. Chem. Phys.*, **1989**, *190*, 515.

65. W. Kaminsky, A. Laban, *Applied Catalysis A: General*, **2001**, *222*, 47.

66. W. Kaminsky, R. Spiehl, *Macromol. Chem. Phys.*, **1989**, *190*, 515.

67. (a) A.L. McKnight, R.M. Waymouth, *Macromol,* **1999**, *32*, 2816; (b) D. Ruchatz, G. Fink, *Macromol,* **1999**, 31, 4674.

68. (a) Z. Hou, Y. Luo, X. Li, J. Organomet. Chem., 2006, 691, 2734; (b) A. Ravasio, C. Zampa, L. Boggioni, I. Tritto, J. Hitzbleck, J. Okuda, *Macromolecules*, **2008**, *41*, 9565.

69. (a) Z. Hou, Y. Luo, X. Li, *J. Organomet. Chem.*, **2006**, *691*, 2734; (b) A. Ravasio, C. Zampa, L. Boggioni, I. Tritto, J. Hitzbleck, J. Okuda, Macromolecules, **2008**, *41*, 9565.

70. (a) *Modern Plastics* **1995**, *72* (9), 137; (b) G. Khanarian, *Opt. Engin.* **2001**, *40*, 1024; (c) J. Y. Shin, J. Y. Park, C. Liu, J. He, S. C. Kim, *Pure Appl. Chem.* **2005**, *77*, 801.

71. (a) M. Arndt, I. Beulich, *Macromol. Chem. Phys*. **1998**,*199*, 1221; (b) N. Herfert, P. Montag, G. Fink, *Makromol. Chem.* **2001**, 94, 3167.

72. I. Tritto, C. Marestin, L. Boggioni, L. Zetta, A. Provasoli, D. R. Ferro, *Macromol*., **2000**, *33*, 8931.

73. see http://www.topas.com/.

74. E. Kirillov, T. Roisnel, A. Razavi, J. F. Carpentier, *Organometallics*, **2009**, 28, 5036

75. Miller, S. A.; Bercaw, J. E.. *Organometallics*, **2006**, *25*, 3576-359

76. K. Nomura, *Dalton Trans.* **2009**, 8811, and references therein

77. K. Nomura, W. Wang, M. Fujiki, J. Liu, *Chem. Commun.* **2006**, *25*, 2659

78. K. Nomura, N. Naga, M. Miki, K. Yanagi and A. Imai, *Organometallics* **1998**, *17*, 2152.

2. Experimental Part

2.1 General Remarks

All the reagents were manipulated under nitrogen inert atmosphere with rigorous absence of oxygen and moisture. Manipulations were carried in flamed or oven-stored Schlenk-type glassware using high vacuum lines (10^{-6} Torr), standard Schlenk-line and glove-box techniques (O_2 < 2 ppm).

2.2 Reagents

Gases – Nitrogen, ethene and propene were supplied by Air-Liquide, and purified by fluxing through columns filled with BTS-catalysts, $CaCl_2$ and finally molecular sieves 4 A 4-8 mesh. Ethene concentration in toluene was calculated according to Henry's law:

$$C_E = P_E H_0 e^{\frac{\Delta H_L}{RT}} \qquad \text{(Eq. 2.1)}$$

Where $C_E, P_E, H_0, \Delta H_L, R$, and T are: ethene concentration (M), ethene pressure (atm), Henry coefficient (0.00175 mol L^{-1} atm^{-1}), ethene solvation enthalpy in toluene (2596 cal mol^{-1}), universal gas constant (1.989 col mol^{-1} K^{-1}) and temperature (K), respectively.

Toluene - was purchased from Sigma Aldrich, dried with anhydrous $CaCl_2$ for two days and then freshly distilled on sodium under nitrogen atmosphere in a special apparatus specifically planned for distillations.

Norbornene (N) - (Bicyclo[2,2,1]hept-2-ene) was purchased from Sigma-Aldrich and dried before use. A flamed three-necked 0.5 L round bottom flask equipped with a Allihn condenser, a stopcock, and a recovery bend was charged with N (MW 94.16, Mp 44-46 °C, Bp 96 °C), previously melted in a hot-water bath. Then, little pieces of sodium were added under a counterflow of N_2. Next, the solution was stirred under reflux overnight. Finally, N was distilled in a round bottom Schlenk previously calibrated (W_1) containing accurately dried molecular sieves. After weighing the Schlenk containing the norbornene (W_2), some distilled toluene was added, and the Schlenk (W_3) was weighed once more. Finally, the density of N/toluene solutions was calculated by means of the equation reported below, empirically determined in our group, linear in the range 30-80 wt % of N.

$$\rho = (9 \cdot 10^{-5} \cdot \text{wt N\%}) + 0.8652 \qquad \text{(Eq. 2.2)}$$

Where ρ and wt N% are the density of N/toluene solution (g mL^{-1}) and the weight percent of norbornene, respectively.

1-octene (O) - (98%, Sigma-Aldrich) was dried by refluxing on $LiAlH_4$ overnight, distilled under nitrogen atmosphere in a Schlenk containing dried molecular sieves, and stored at 4 °C.

1,5-Hexadiene (HED) - (97%, Sigma-Aldrich) was dried by refluxing over CaH_2 for 12h, distilled under nitrogen atmosphere in a Schlenk containing dried molecular sieves, and stored at 4 °C.

Methylaluminoxane (MAO) - purchased from Crompton as a toluene solution (10 wt-% Al), was dried in vacuum (50 °C, 4 h, 0,1 mm Hg) increasing the temperature till 60 °C to remove solvent and unreacted trimethylaluminum (TMA), and used as white powder.

1,2-Dideutero-1,1,2,2-tetrachloroethane - ($C_2D_2Cl_4$) was purchased from Cambridge Isotope Laboratories and used without further purification.

Catalysts - C_s-symmetric catalyst [$Zr(\eta^5:\eta^5\text{-}C_5H_4C(i\text{-}Pr)_2C_{13}H_8)Cl_2$] (**7**), C_1-symmetric catalyst [$Zr(\eta^5:\eta^5\text{-}C_5H_4CPh_2(3\text{-}t\text{-but})C_{13}H_8)Cl_2$] (**1**), C_1-symmetric catalyst [$Zr(\eta^5:\eta^5\text{-}$ (3-Met)$C_5H_4C(i\text{-}Pr)_2(3\text{-}t\text{-but})C_{13}H_8)Cl_2$] (**2**), C_1-symmetric

catalyst [Zr(η^5:η^5- (3-*t*-but)C_5H_4C(*i*-Pr)$_2$(3-*t*-but)$C_{13}H_8$)Cl_2] (**3**), C_1-symmetric catalyst [Zr(η^5:η^5-C_5H_4C(*i*-Pr)$_2$(3-*t*-but)$C_{13}H_8$)Cl_2] (**4**), C_1-symetric catalyst [Hf(η^5:η^5-C_5H_4C(*i*-Pr)$_2$(3-*t*-but)$C_{13}H_8$)Cl_2] (**5**), C_1-symmetric catalyst [Hf(η^5:η^5-(3-*t*-but)C_5H_4C(*i*-Pr)$_2$(3-*t*-but)$C_{13}H_8$)Cl_2] (**6**) were kindly supplied by Dr. Razavi (Total Petrolchemicals, Belgium).

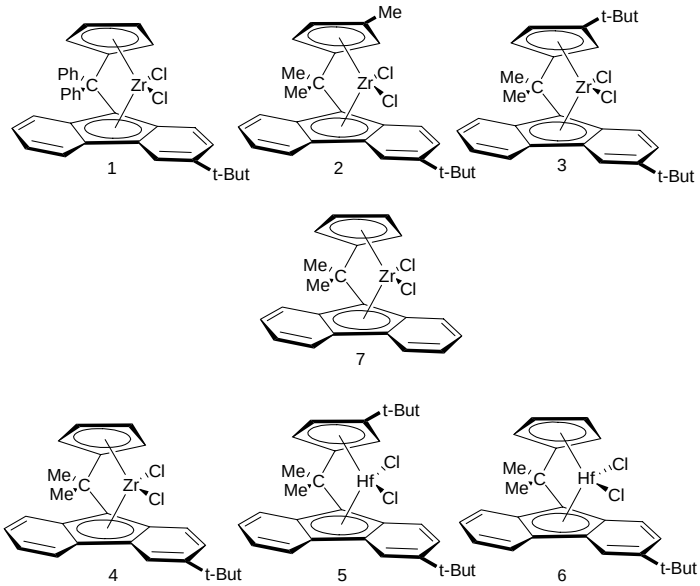

Figure 2.1 Group IV metal-based precursors investigated in the synthesis of propene homopolymerizations, and propene ethene copolymerizations.

Half sandwich titanocenes: [Ti(η^5-C_5H_5(N=C(*t*-But)$_2$)Cl_2], [Ti(η^5-(*t*-but)C_5H_5(N=C(*t*-But)$_2$)Cl_2] and [Ti(η^5-(*t*-but)C_5H_5(O-(2,6-*i*-Pr)$_2C_6H_3Cl_2$] were kindly supplied by Dr. Nomura (Tokyo Metropolitan University, Japan).

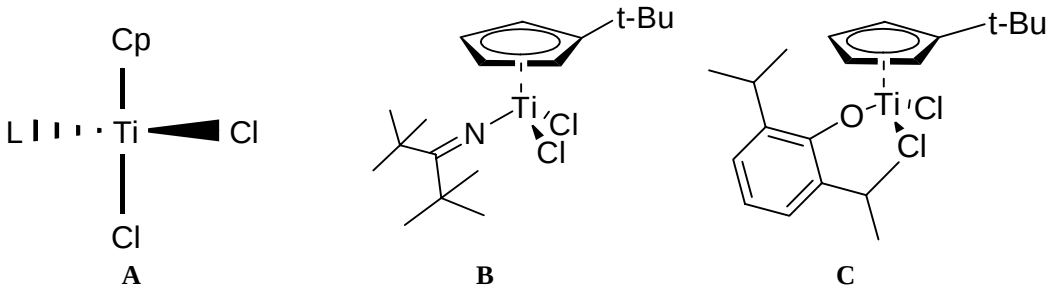

Figure 2.2 Half sandwich titanocene precursors investigated in the synthesis of norbornene-ethene copolymerizations and norbornene-ethene-1,5-hexadiene, and norbornene-ethene-1-octene terpolymerizations

2.3 General Procedures

All the homo and copolymerizations were carried out in a 0.5-L Büchi® BEP280 laboratory autoclave equipped with a Metal Type 3 vessel and a cyclone 250 magnetic stirrer, or in a smaller scale 250 ml laboratory stainless steel autoclave. The manipulation of air sensitive catalysts and co-catalysts was carried out in a flame or oven-stored Schlenk type glassware, using high vacuum line and glove-box techniques. The solvent was freshly distilled from Na and stored on molecular sieves before every use.

2.3.1. Polymerization Procedure with homogeneous catalysts

a) Propene-based homopolymerizations:

0.5 Stainless steel autoclave. Before starting the polymerization reactions, the reactor was evacuated for 60 min at 90 °C and conditioned three times with nitrogen. After cooling down to reaction temperature, the reactor was filled with the right amount of toluene and with the solution of MAO in toluene, previously prepared. In batch propene homopolymerizations after thermal equilibration, the reactor system was saturated with propene at the desired pressure. In slurry homopolymerizations, a weighted amount of propene (ranging from 25 to 30 g) had to be transferred into the reactor. This operation resulted to be one of the main drawbacks that limited the reproducibility of our experiments. A flamed evacuated bomb (Figure 2.3), equipped with a needle valve, was linked to the source of gaseous propene through a metal line, cooled down in liquid nitrogen for 30 seconds and, opening the valve for 30 seconds, filled with propene; the monomer was transferred into the autoclave connecting the bomb to the reactor, through a *Swagelok* tube, immersing the bomb into a hot water bath (~ 70 °C) for 60'', rotating the bomb and opening the valve for 10''. After equilibration, the reaction was initiated by injection of the metallocene precursors dissolved in toluene. The polymerizations were quenched by addition of 2 mL of ethanol, and precipitated in ethanol. The products were filtered, redissolved in

boiling toluene and reprecipitated in ethanol under stirring. The products were filtered and dried under vacuum at 70 °C for several hours until constant weight.

b) Propene-based copolymerizations:

0.5 Stainless steel autoclave. Before starting the polymerization reactions, the reactor was evacuated for 60 min at 90 °C and conditioned three times with nitrogen. After cooling down to reaction temperature, the reactor was filled with the right amount of toluene and with the solution of MAO in toluene, previously prepared. In the meanwhile, A flamed evacuated bomb (Figure 2.3), equipped with a needle valve, was linked to the source of gaseous propene through a metal line, cooled down in liquid nitrogen for 30 seconds and, opening the valve for 30 seconds, filled with propene; the monomer transferred into the autoclave connecting the bomb to the reactor, through a *Swagelok* tube, immersing the bomb into a hot water bath (~ 70 °C) for 60'', rotating the bomb and opening the valve for 10''. After thermal equilibration, the reactor system was saturated with ethene at the desired pressure. The reaction was initiated by injection of the metallocene precursors dissolved in toluene. The ethene pressure was kept constant during the polymerization reaction through an automatic mass flow valve and a mass flow controller (Figure 2.4 b) and c)).The polymerizations were quenched by addition of 2 mL of ethanol, and precipitated in ethanol. The products were filtered, redissolved in boiling toluene and reprecipitated in ethanol under stirring. The products were filtered and dried under vacuum at 70 °C for several hours until constant weight..

c) Norbornene-based co- and terpolymerizations:

0.25 Stainless steel autoclave. Before starting the polymerization reactions, the reactor was evacuated for 60 min at 90 °C and conditioned three times with nitrogen. After cooling down to reaction temperature, the reactor was filled with the right amount of toluene, with the solution of MAO in toluene, previously prepared, with the correct amount of norbornene (toluene solution) and the appropriate amount of third monomer 1-octene, or 1,5-hexadiene (pure). After thermal equilibration, the reactor system was saturated with ethene at the desired pressure. The reaction was

initiated by injection of the metallocene precursors dissolved in toluene. The ethene pressure was kept constant during the polymerization reaction through an automatic mass flow valve and a mass flow controller (Figure 2.4 b) and c)). The polymerizations were quenched by addition of 2 mL of ethanol, and precipitated in ethanol or acetone. The products were filtered, redissolved in boiling toluene and precipitated in acetone under high-speed stirring (10000 rpm) by means of Ultra Turrax T50 basic dispersing instrument. The products were filtered and dried under vacuum at 70 °C for several hours until constant weight..

a) Propene-based homopolymerizations:

0.25 Stainless steel autoclave. Before starting the polymerization reactions, the reactor was evacuated for 60 min at 90 °C and conditioned three times with nitrogen. After that the reactor was cooled down to room temperature. In the meantime, a proper volume (50 or 100 mL) round-botton Shlenk previously evacuated was filled wit h hydrogen and linked to the autoclave through a Tygon tube. In the meanwhile a flamed evacuated bomb (Figure 2.3), equipped with a needle valve, was linked to the source of gaseous propene through a metal line, cooled down in liquid nitrogen for 30 seconds and, opening the valve for 60 seconds, filled with propene (~ 60 g); the monomer was transferred into the autoclave connecting the bomb to the reactor, through a *Swagelok* tube, immersing the bomb into a hot water bath (~ 70 °C) for 60'', rotating the bomb and opening the valve for 10''. After thermal equilibration, the temperature was raised to 40 °C for the prepolymerization step. In the meantime, the catalyst was prepared in glove box: the right volume (ranging between 150 to 300 μl) of catalyst solution was collected under stirring with a pipette, transferred into a polypropene 5 ml syringe and handly-mixed with the right volume of cocatalyst solution collected with the same syringe. The prepolymerization steps started when the solution of catalyst was injected and continued for 10 minutes till the temperature was raised to 70 °C. The polymerizations were quenched by addition of 1 ml of ethanol, the polymer powders were collected and dried under vacuum at 70 °C for a couple of hours until constant weight.

b) Propene-based copolymerizations:

0.25 Stainless steel autoclave. Before starting the polymerization reactions, the reactor was evacuated for 60 min at 90 °C and conditioned three times with nitrogen. After that, reactor was cooled down to room temperature. In the meantime, a proper volume (50 or 100 mL) round-botton Shlenk previously evacuated was filled with hydrogen and linked to the autoclave through a Tygon tube. In the meanwhile A flamed evacuated bomb (Figure 2.3), equipped with a needle valve, was linked to the source of gaseous propene through a metal line, cooled down in liquid nitrogen for 30 seconds and, opening the valve for 30 seconds, filled with propene; the monomer was transferred into the autoclave connecting the bomb to the reactor, through a *Swagelok* tube, immersing the bomb into a hot water bath (~ 70 °C) for 60'', rotating the bomb and opening the valve for 10''. After thermal equilibration, the system was saturated with the right overpressure (calculated by Eq 2.1) of ethene. In the meantime, the catalyst was prepared in glove box: the right volume (ranging between 150 to 300 μl) of catalyst solution was collected under stirring with a pipette, transferred into a polypropene 5 ml syringe and handly-mixed with the right volume of cocatalyst solution collected with the same syringe. The copolymerizations started when the solution of catalyst was injected and the ethene pressure was kept constant by the means of a mass flow valve and a mass flow controller (Figure 2.4 b) and c)). The reactions were quenched by addition of 1 ml of ethanol, the polymer powders were collected and dried under vacuum at 70 °C for a couple of hours until constant weight..

2.3.1.1 High pressure autoclave reactor

All the experiments were carried out in a Buchi® BEP280 laboratory autoclave equipped with a 0.5 L Type 3 Metal pressure vessel with a maximum operating pressure of 60 bar, or in a smallest scale 0.250 L stainless steel laboratory autoclave, with a maximum operating pressure of 80 bar. The principal components of the 0.5 L reactor systems are displayed in Figure 2.4. The reactor vessel was supplied with a heat jacket (**1**) connected to a thermostat circulation bath for temperature regulation,

associated to a Temperature Control Unit (Polystat, cc2 model, Huber) (Figure 2.4b). The internal reactor temperature was monitored with a thermocouple (Pt100 model, Achelit) inserted into the reactor vessel and connected to the Temperature Control Unit. The reactor was equipped with a cyclone 250 magnetic stirrer (Figure 2.4c), and was connected to high-pressure gases and high vacuum system throughout standard *Swagelok'*s instrumentation, including compression fittings, valves, tubing, and gauges

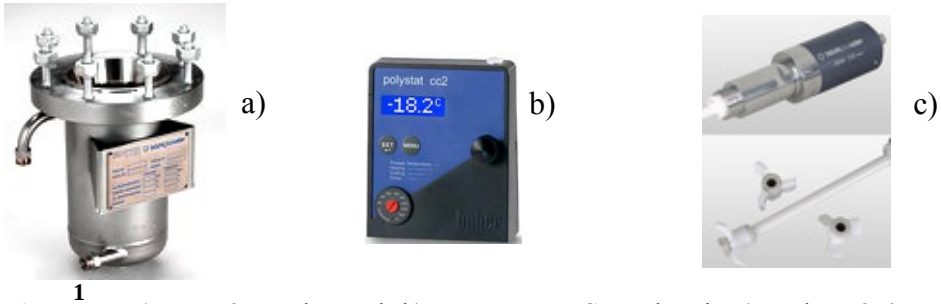

Figure 2.4 a) Type 3 metal vessel; b) Temperature Control Unit; c) cyclone 250 magnetic stirrer.

Pressure measurements were performed by a MKS Baratron and the reactor pressure was regulated by a mass flow controller connected to a MKS *Multi Gas Pressure Controller* (MGC) Type 647C (Figure. 2.5). The pressure control menu displays the ethene consumption (in terms of flow of ethene) and the actual pressure with its unit

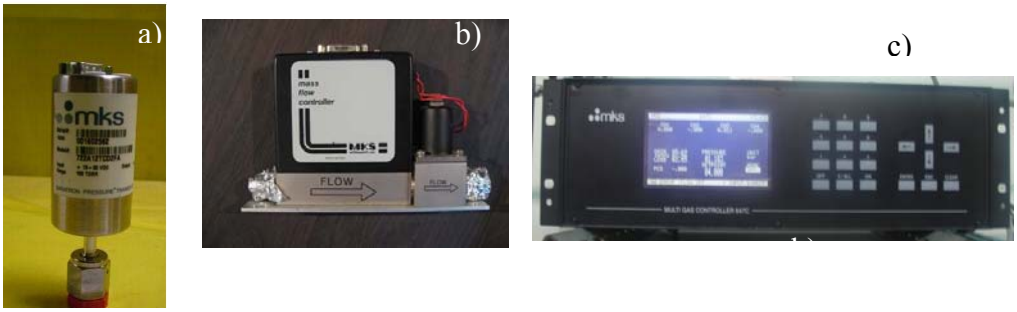

Figure 2.5 a) MKS Baratron; b) mass flow controller; c) Multi Gas Pressure Controller Type 647C.

The smaller scale reactor was equipped with an external thermostatic bath (Figure 2.6), for temperature regulation, associated to a Temperature Control Unit

(Polystat, cc2 model, Huber) (Figure 2.4b). The internal reactor temperature was monitored with a thermocouple (Pt100 model, Achelit) inserted into the reactor vessel and connected to the Temperature Control Unit. The reactor was equipped with an helicoidal stirrer, and was connected to high-pressure gases and high vacuum system throughout standard *Swagelok'*s instrumentation, including compression fittings, valves, tubing, and gauges

The autoclave cap (Figure. 2.6) presents three inlets: an injection point for the reaction mixture (**1**), the injection system for the catalyst solution (**2**) connected to N_2 line and high pressure N_2 line, an inlet for ethene monomer gas supply or for liquid propene injection(**3**) and a rupture disc (**4**) to provide protection against over-pressure (safely limit the maximum pressure to 55 bar).

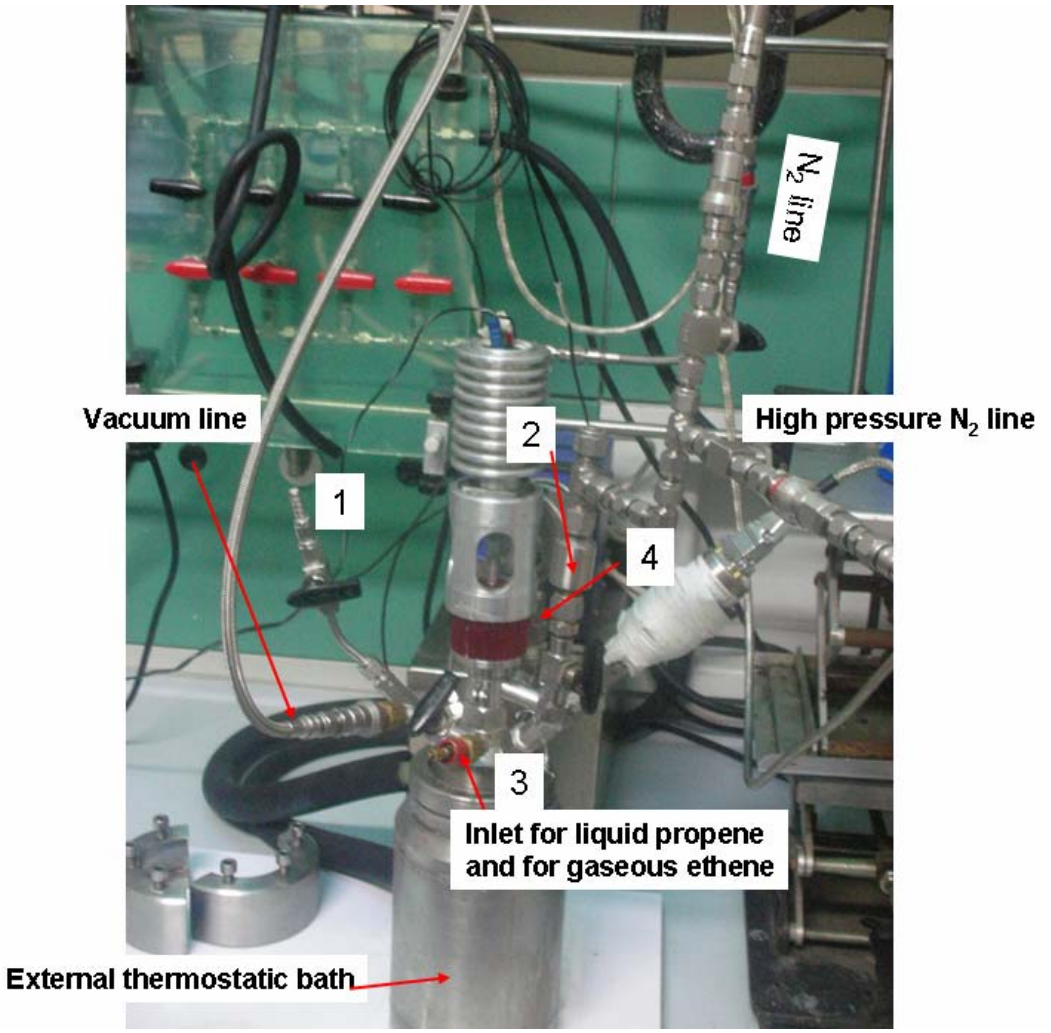

Figure 2.6 Autoclave cap

2.4 Physical And Analytical Measurements

The resulting polymers were characterized by ^{13}C-NMR to evaluate the monomer content and the polymer microstructure, and by ^{1}H-NMR spectroscopy to determine the chain-end groups. Glass transition temperatures ($\boldsymbol{T_g}$) molar masses ($\boldsymbol{M_w}$), and molar masse distributions ($\boldsymbol{D}$) were examined by DSC and SEC measurements, respectively.

2.4.1 Differential scanning calorimetry (DSC)

Measurements were performed on a Pyris 1 Perkin-Elmer instrument. The samples (around 8-9 mg) were heated from -20 to 200 °C at 20 °C/min, with a nitrogen flow (30 mL/min), using heating and cooling rates of 20 °C/min. A first scan was realized to erase the thermal history of each polymer. T_gs were recorded during a second thermal cycle.

2.4.2 Size Exclusion Chromatography (SEC)

SEC measurements were performed on about 15-20 mg of product dissolved in *o*-dichlorobenzene at 105 °C by a GPCV2000 high temperature size exclusion chromatography (SEC) system from Waters (Millford, MA, USA) equipped with two online detectors: a viscometer (DV) and a differential refractometer (DRI). The column set was composed of three mixed TSK-Gel GMHXL-XT columns from Tosohaas. The universal calibration was constructed from 18 narrow **D** polystyrene standards, with the molar mass ranging from 162 to 5.48•10^6 g/mol.

2.4.3 Nuclear Magnetic Resonance (NMR)

The spectra were recorded on Bruker NMR Advance 400 Spectrometer (100.58 MHz, ^{13}C; 400 MHz, ^{1}H) operating in the PFT mode at 103 °C. Chemical shifts for ^{1}H were referred to internal solvent resonances and chemical shifts for ^{13}C were referred to hexamethyldisiloxane (HMDS). For NMR analysis about 100 mg of

polymeric sample was dissolved in $C_2D_2Cl_4$ in a 10 mm NMR tube and transferred to the spectrometer with the probehead preequilibrated at 103 °C.

The applied settings were the following: 10 mm probe, 90° pulse angle (12.50 μs); 64 K data points; acquisition time 0.93 s; relaxation delay 16 s; 3-4 K transient.

Some ^{13}C-DEPT NMR experiments were performed. In this case, the spectra were measured with composite pulse decoupling using the sequence τ_1-90°-τ_2-180°, 90°-τ_2-135°, 180°-τ_2-CPD-acquire, with delays τ_1 of 5s, and τ_2 of 3.8 ms and 90° pulse widths of 14.3 ms.

2.4.3.1 Polypropene Microstructure

The quantitative determination of the isotacticity or syndiotacticity percentage of polypropene samples obtained with the different metallocenes precursors depicted in Figure 2.1 was calculated on the basis of observed integrals (*I*) in ^{13}C-NMR spectra of propene pentads. An expansion of methyl region (20- 17 ppm) of a ^{13}C-NMR spectrum of polyPP samples with a polymer general structure and the relative label of pentads is depicted in the next figure[1].

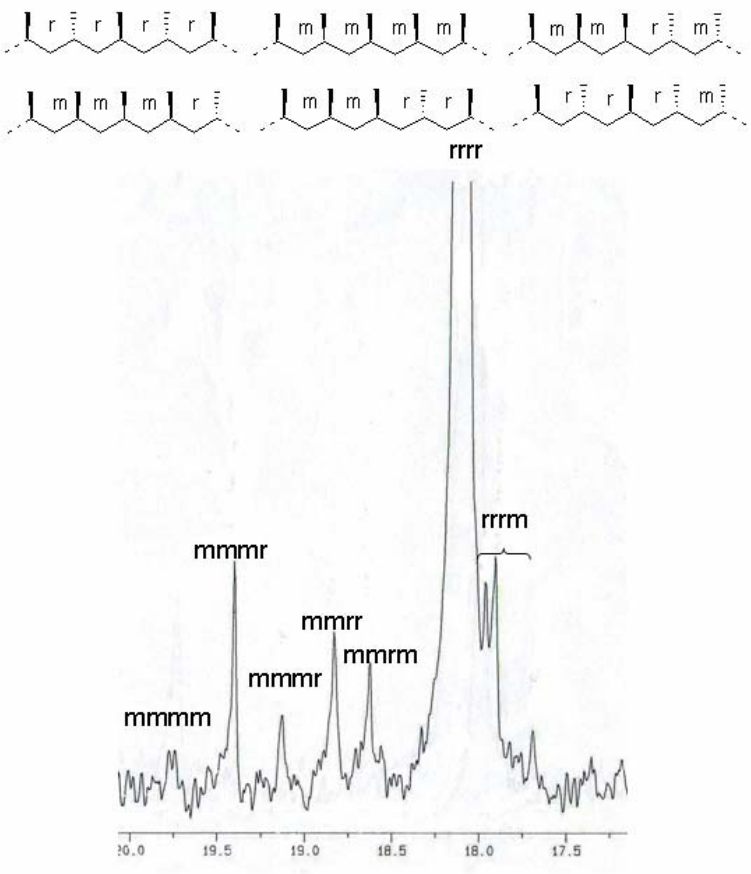

Figure 2.7 Methyl region expansion of a ^{13}C-NMR spectrum of PolyPP, structure and relative pentad assignments.

2.4.3.2 Ethene (E) content in the copolymers

The quantitative determination of ethene (E) and propene (P) content in poly(E-*co*-P)s was calculated on the basis of observed integrals (*I*) in ^{13}C-NMR spectra of ethene and propene carbons. A general spectrum of poly(P-*co*-E) with a copolymer general structure and the relative label of carbon atoms is depicted in the next figure.

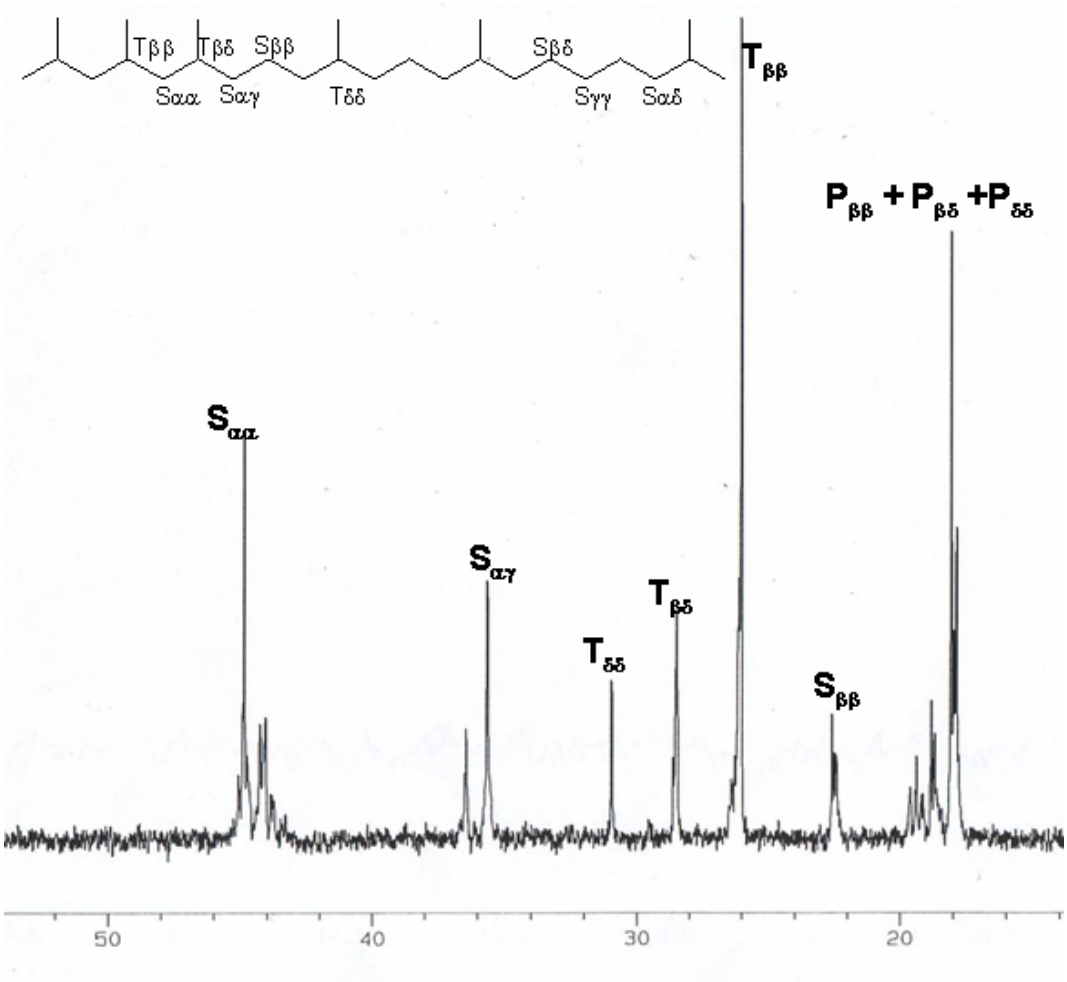

Figure 2.8 Poly(E-*co*-P) general spectrum, structure and relative assignment of carbon atoms.

The compositions were calculated from the following equations:

$$E(mol\%) = \frac{[E]}{[E]+[P]} \bullet 100 = \frac{I_E}{I_E + I_P} \bullet 100 \qquad \text{(Eq. 2.3)}$$

$$I_E = I_{EE} + \frac{1}{2} I_{PE} \qquad \text{(Eq. 2.4)}$$

$$I_P = I_{PP} + \frac{1}{2} I_{PE} \qquad \text{(Eq. 2.5)}$$

$$I_{EE} = \frac{1}{2}(I_{S_{\beta\delta}} + I_{S_{\alpha\delta}}) + \frac{1}{4} I_{S_{\gamma\delta}} \qquad \text{(Eq. 2.6)}$$

$$I_{PP}=I_{S_{\alpha\alpha}} \quad \text{(Eq. 2.7)}$$

$$I_{PE}=I_{S_{\alpha\gamma}}+I_{S_{\alpha\delta}} \quad \text{(Eq. 2.8)}$$

Where $I_{S_{\beta\delta}}$ and $I_{S_{\alpha\delta}}$ are the intensities of methylene carbons of two adjacent ethene units; $I_{S_{\gamma\delta}}$ is the intensity of methylene carbons between an ethene and propene units, $I_{S\alpha\alpha}$ is the intensity of the methylene carbon between two tertiary carbons and $I_{S_{\alpha\gamma}}$ is the intensity of the methylene carbon of an ethene units inserted between two propene units.

2.4.3.3. Chain end analysis in propene based homopolymers

The quantitative determination of the four chain end groups was calculated from the observed integrals (*I*) in ^{1}H-NMR of vinylidene, allyl, 2-butenyl and 4-butenyl protons. A schematic representation of the four chain end groups with the relative label of the proton atoms and the NMR assignment is depicted in Scheme 2.1.

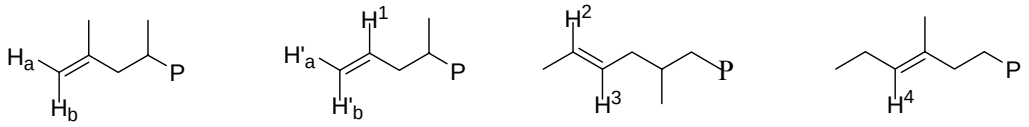

vynilidene allyl 2-butenyl 4-butenyl

H_a	Singlet 4.59
Hb	Singlet 4.66
H'$_a$	Broad Singlet 4.88 ppm
H'$_b$	Doublet 4.94 ppm (J = 6.2 Hz)
H^1	Complex Multiplet 5.72 ppm
H^2	Complex Multiplet 5.38 ppm
H^3	Complex Multiplet 5.38 ppm
H^4	Triplet of Multiplets: 5.11 ppm (J = 7.0 Hz)

Scheme 2.1 Chain end groups and relative label of proton with ^{1}H-NMR assignment.

2.4.3.4. Norbornene (N) content in the copolymers

The quantitative determination of norbornene (N) content in poly(E-*co*-N)s was calculated from the observed integrals (*I*) in ^{13}C-NMR spectra of ethene and propene carbons. A general spectrum of poly(E-*co*-N) with a copolymer general structure and the relative label of carbon atoms is depicted in the next figure.

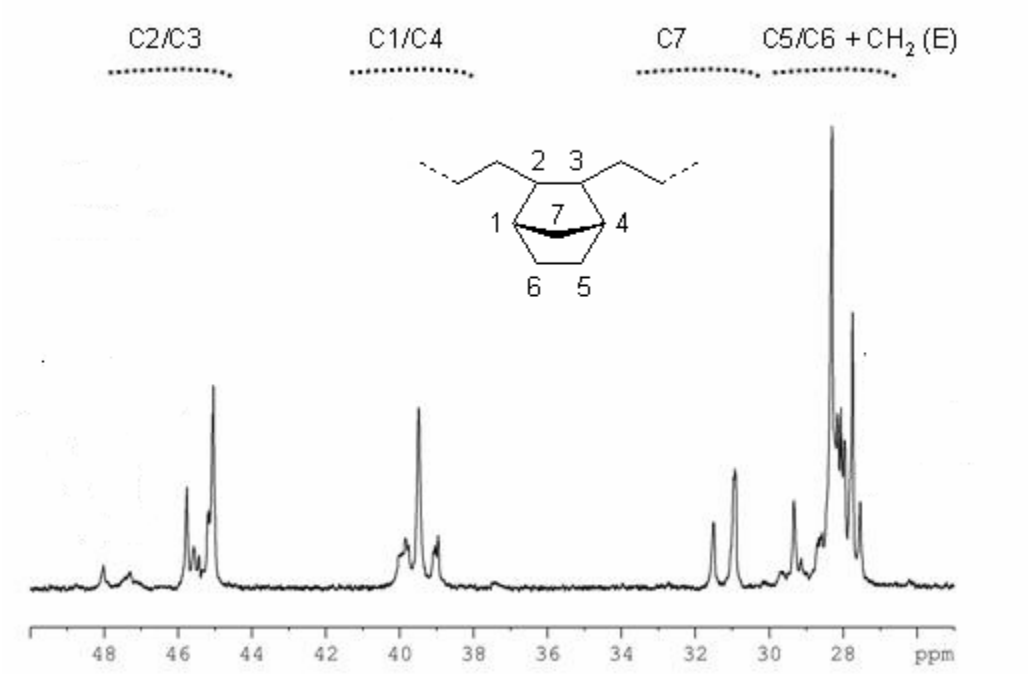

Figure 2.9 Poly(E-*co*-N) general spectrum, structure and relative assignment of carbon atoms.

The composition was calculated on the basis of the following equation[2]:

$$N(mol\,\%) = \frac{[N]}{[N]+[E]} \bullet 100 = \frac{\frac{1}{3}(I_{C2/3} + I_{C1/4} + 2I_{C7})}{I_{CH_2}} \bullet 100 \qquad \text{(Eq. 2.9)}$$

where $I_{C2/3}$, $I_{C1/4}$, and I_{C7} are the peak intensities of C2/C3, C1/C4, and C7 carbons in norbornene units, and I_{CH_2} indicates the total area of peaks from 26.2 to 34.3 ppm. From the relative peak intensities of the carbons C5/C6, it was possible to estimate the content of *racemic* and *meso NN* dyads sequences.

2.4.3.5 1-Octene (O) content in the terpolymers

On the basis of the peak intensity (*I*) of carbons in the ^{13}C-NMR spectra it was possible to estimate the content of norbornene (N), ethene (E), and 1-octene (O) in poly (E-*ter*-N-*ter*-O) polymers. A general spectrum of poly(E-*ter*-N-*ter*-O) with a terpolymer general structure and the relative label of carbon atoms is depicted in

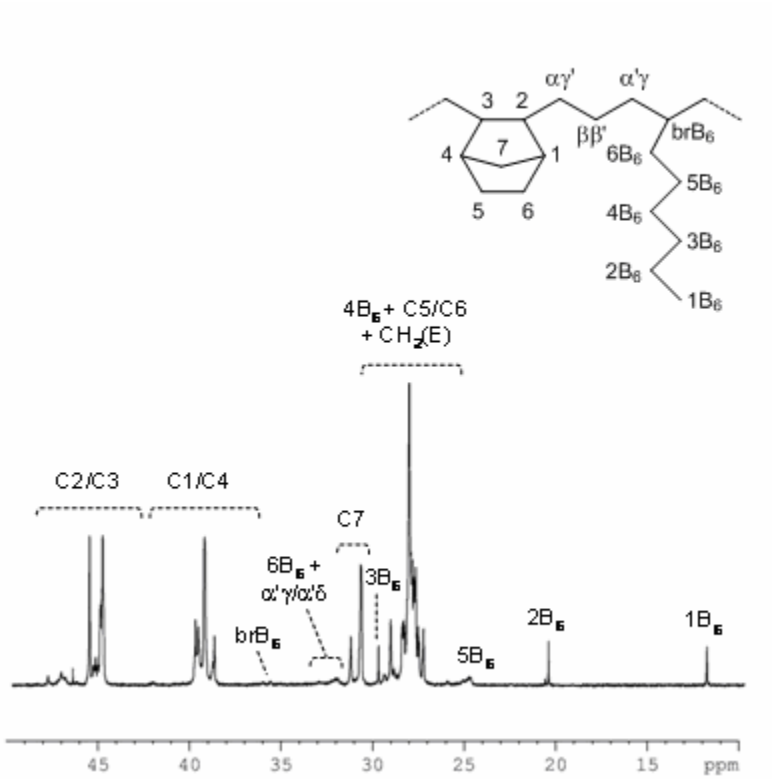

Figure 2.10. Poly(E-*ter*-N-*ter*-O) general spectrum, structure and relative assignment of carbon atoms.

The composition was calculated according to the following equations[2]:

$$N(mol\%) = \frac{[N]}{[N]+[E]+[O]} \bullet 100 = \frac{\bar{I}_N}{\bar{I}_N + \bar{I}_E + \bar{I}_O} \bullet 100 \qquad \text{(Eq. 2.10)}$$

$$O(mol\%) = \frac{[O]}{[N]+[E]+[O]} \bullet 100 = \frac{\bar{I}_O}{\bar{I}_N + \bar{I}_E + \bar{I}_O} \bullet 100 \qquad \text{(Eq. 2.11)}$$

$$\bar{I}_N = \frac{1}{2} I_{2/3} \qquad \text{(Eq. 2.12)}$$

$$\bar{I}_E = \frac{1}{2}\left(I_{CH_2} - 2\bar{I}_N - 3\bar{I}_O\right) \quad \text{(Eq. 2.13)}$$

$$\bar{I}_O = \bar{I}_{1B6} \quad \text{(Eq.2.14)}$$

where $I_{2/3}$ is the peak intensity of the methyne carbons C2/C3 in the norbornene units, I_{CH_2} is the total area of peaks from 30.6 to 24.3 ppm, and I_{1B_6} indicates the peak intensity of the methyl carbon $1B_6$ in the 1-octene unit (Scheme 2.2).

2.4.3.6 1,5-Hexadiene (HED) content in the terpolymers

The compositional analysis of poly(E-*ter*-N-*ter*-HED) was calculated on the basis of the peak intensity (*I*) of carbons in the ^{13}C-NMR spectra. 1,5-Hexadiene could be inserted into the polymeric chain as 1-butenyl branches (Vy) or as cyclopentane units (CP) connected at C_1 and C_3 positions to the polymer backbone. The 1,3-cyclopentane units can assume both *cis*- and *trans*- conformations of the ring. Figure 2.12 shows the general spectrum of poly(E-*ter*-N-*ter*-HED) with a terpolymer general structure and the relative label of carbon atoms

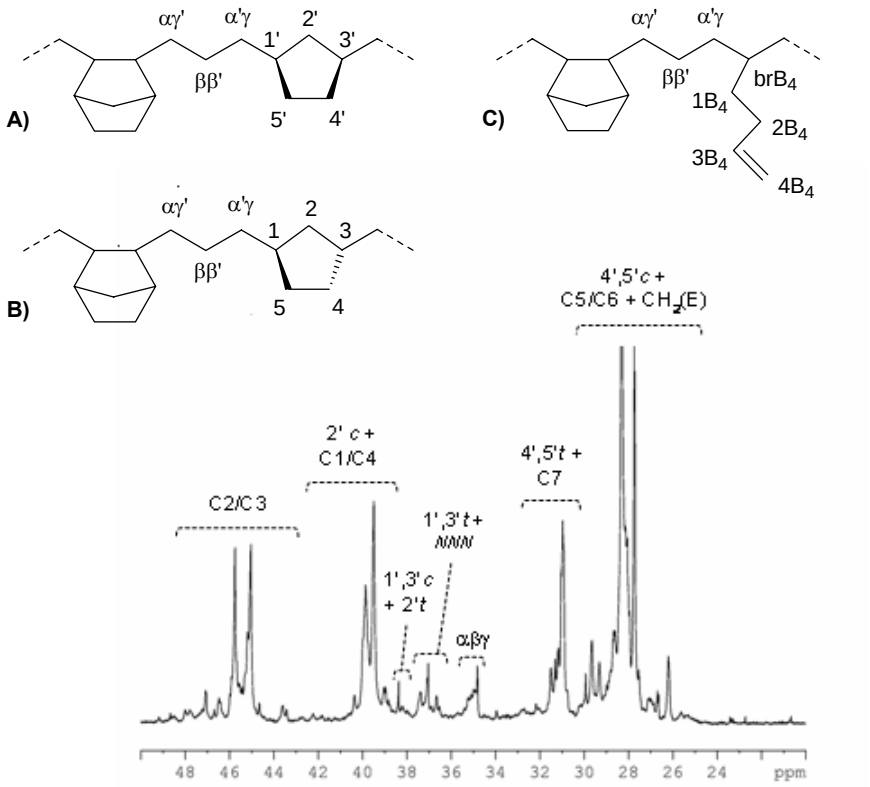

Figure 2.11 General poly(E-*ter*-N-*ter*-HED) spectrum, molecular structures and relative assignment of carbon atoms. A) *cis*-1,3-cyclopentane unit; B) *trans*-1,3-cyclopentane unit; C) 1-butenyl branch.

The composition was calculated according to the following equations[2]:

$$N(mol\%) = \frac{[N]}{[N]+[E]+[CP]+[Vy]} \bullet 100 = \frac{\bar{I}_N}{\bar{I}_N + \bar{I}_E + \bar{I}_{CP} + \bar{I}_{Vy}} \bullet 100 \qquad \text{(Eq. 2.15)}$$

$$CP(mol\%) = \frac{[CP]}{[N]+[E]+[CP]+[Vy]} \bullet 100 = \frac{\bar{I}_{CP}}{\bar{I}_N + \bar{I}_E + \bar{I}_{CP} + \bar{I}_{Vy}} \qquad \text{(Eq. 2.16)}$$

$$Vy(mol\%) = \frac{[Vy]}{[N]+[E]+[CP]+[Vy]} \bullet 100 = \frac{\bar{I}_{Vy}}{\bar{I}_N + \bar{I}_E + \bar{I}_{CP} + \bar{I}_{Vy}} \bullet 100 \qquad \text{(Eq. 2.17)}$$

$$\bar{I}_N = \frac{1}{2} I_{2/3} \qquad \text{(Eq. 2.18)}$$

$$\bar{I}_{\mathrm{E}} = \frac{1}{2}\left(I_{CH_2} - 2\bar{I}_{\mathrm{N}} - I_{4,5c}\right) \qquad \text{(Eq. 2.19)}$$

$$\bar{I}_{\mathrm{CP}} = \frac{1}{2} I_{1,3c} + I_{2t} \qquad \text{(Eq. 2.20)}$$

$$\bar{I}_{\mathrm{Vy}} = \frac{1}{2}\left(I_{4\mathrm{B}_4} + I_{3\mathrm{B}_4}\right) \qquad \text{(Eq. 2.21)}$$

where $I_{2/3}$ is the peak intensity of the methyne carbons C2/C3 in the norbornene units, I_{CH_2} is the total area of peaks from 30.6 to 26.2 ppm, $I_{4,5c}$ is the peak intensity of the 4,5-*cis* carbon atoms evaluated by the integral of the methyne carbons 1,3-*cis*. $I_{1,3c}$ and I_{2t} indicate the peak intensity of methyne carbons 1,3-*cis* and the methylene carbon 2-*trans* of the cyclopentane unit, respectively; I_{4B_4} and I_{3B_4} indicate the peak intensity of the unsaturated carbon atoms $4B_4$ and $3B_4$ of pendant double bonds (Scheme 2.4).

The quantitative determination of the cyclopentane (CP) units content in poly(E-*ter*-N-*ter*-HED) was calculated using a supplementary method. The composition calculations allowed to estimated a maximum amount $CP_{\max}$ incorporated in the terpolymers. The CP content was calculated as follows:

$$\mathrm{CP_{MAX}\ (mol-\%)} = \frac{[\mathrm{CP}]_{\max}}{[\mathrm{N}]+[\mathrm{E}]+[\mathrm{Vy}]+[\mathrm{CP}]_{\max}} \times 100 = \frac{\bar{I}_{CP_{MAX}}}{\bar{I}_N + \bar{I}_E + \bar{I}_{CP_{MAX}} + \bar{I}_{Vy}} \times 100 \qquad \text{(Eq. 2.22)}$$

$$\bar{I}_{\mathrm{CPmax}} = \frac{1}{2}\left(I_{\alpha\beta\gamma} - I_{\mathrm{C1/C4}}\right) \qquad \text{(Eq. 2.23)}$$

where $I_{\alpha\beta\gamma}$ is the total area of peaks between 34.8 and 35.4 ppm related to methylene carbon atoms immediately adjacent to CP units, while $I_{C1/C4}$ is the peak intensity of the *NNN* triad of carbons C1/C4 *m,m* of norbornene[2].

References

1. V. Busico; R. Cipullo; *Prog in Polym Sci*., **2001** *26* 443.

2. R. Marconi **PhD Thesis**: *Terpolymerization of α-Olefins and Non-Conjugated Dienes with Norb rnene and Ethylene by Group IV Metal Based Catalysts* **2010.**

3. Results and Discussion of Propene-based Homo- and Copolymers

3.1 Propene homopolymerization by C_1 homogenous metallocene based catalysts

The metallocene catalysis allows to tailor the microstructure and the molecular weight of polymers by tuning the structure of the catalyst. The introduction of metallocenes has also created new opportunities for the synthesis of olefin copolymers with uniform compositions and random sequence distributions, with tailored microstructures and properties. Molecular weight and microstructure are two of the most important polymer characteristics which influence the final properties of the material and their end use.

The development of a C_s-symmetric class of catalysts with two enantiomorphic sites, by Ewen and Razavi[1], has opened the possibility to synthesize syndiotactic polypropene: the two enantiomorphic sites of these catalysts enable an alternating orientation of propene insertion, thus forming syndiotactic polypropene (sPP) chain. sPP is a thermoplastic material with high melting point and high crystallinity.

Incorporation of a substituent at the 3 position of the cyclopentadienyl ring of Me_2C-$(C_5H_4)(C_{13}H_8)MCl_2$ (M = Ti, Zr, Hf) induces desymmetrization of the metallocene to C_1 symmetry[2]. As a consequence, the tacticity of propene homopolymers using C_1-symmetric catalysts is no longer syndiotactic, but polymer microstructure greatly depends on the nature and hindrance of the substituent on Cp group. When the substituent is a Me or *i*-propyl group, a hemi-isotactic or atactic

polypropene is obtained; when the substituent is the bulkier *ter*-butyl substituent, isotactic polypropene is achieved. These systems are amenable to study fine details of the polymerization mechanism. However, if the group used to introduce C_1 symmetry is large enough isotactic PP is obtained, which is of great interest from a practical point of view since the isotactic polymers synthesized by C_2-symmetric indenyl based catalysts often produce small undesirable fractions of atactic polymers[3].

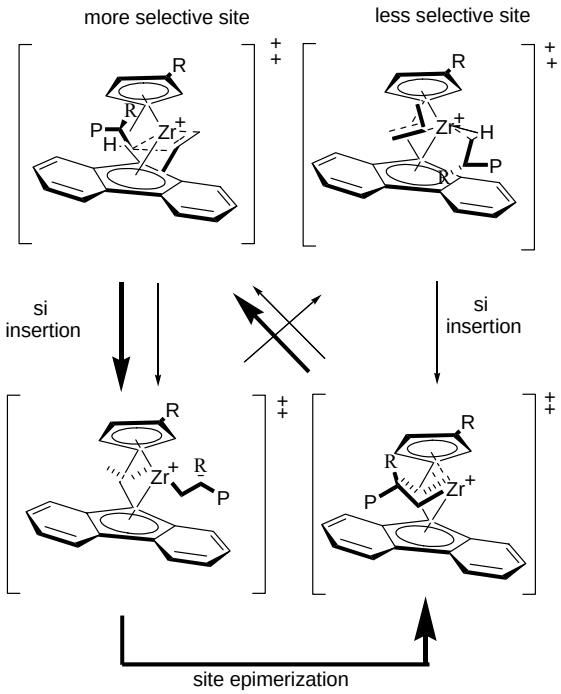

Scheme 3. 1. Enantiomorphic site control with epimerization (bold line); alternating mechanism (plain line): alternation between a perfectly stereoselective site and a variably stereoselective site (left side), alternation between two sites of various stereoselectivity (right side)

The mechanism which leads to the isotactic polypropene with C_1-symmetric Me_2C-(3-*ter*-butyl-C_5H_3)($C_{13}H_8$)MCl_2 has been a topic of debate. According to the site epimerisation mechanism the *t*-Bu side of Cp group is too sterically hindered to accommodate the growing polymer chain, that needs a site epimerisation before every monomer insertion, according the alternating mechanism there are two sites of different stereoselectivity (Scheme 3.1).

For this reason a number of complex C_1-symmetric metallocenes have been synthesized and studied recently[4].

The aim of this part of the project on propene polymerization catalysis with C_1-symmetric fluorenyl-containing metallocenes bearing one or two *ter*-butyl substituents at the 3 position of Cp or at 3 position of the fluorenyl groups. The main objective of this investigation was to assess the impact of these changes on the catalytic performances for obtaining isotactic polypropene with high molar masses.

Thus, propene homopolymerizations by C_1-symmetric metallocenes were studied at different temperatures and monomer concentrations to evaluate the catalytic performance in terms of activities, microstructures, and molecular weights.

Stereoerrors were investigated by ^{13}C-NMR analysis. A comparison of the polymer microstructures on the basis of statistical analysis was performed and mechanisms which lead to the observed microstructures were tested.

At last but not least, in order to identify among the C_1 symmetric catalysts those most promising for obtaining copolymers with high molar masses, an analysis of chain end groups by ^{1}H-NMR analysis was performed in order to understand the role of substituents on the mechanism of the processes that lead to chain terminations as well as to give a rationale to such possibility.

3.1.1 Screening of C_1 homogenous metallocene based catalysts for Propene homopolymerization

In order to investigate all the factors explained above a set of propene homopolymerizations by using different C_1-symmetric catalysts sketched in Figure. 3.1. provided us by Total was performed.

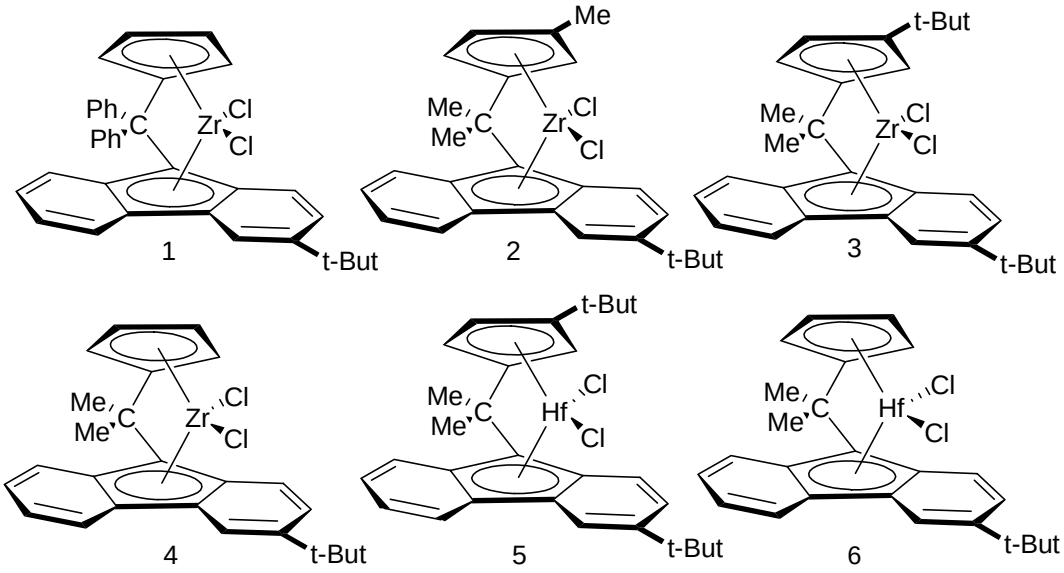

Figure 3.1 The six C_1-symmetric catalysts used in propene homopolymerizations

Initially, a preliminary screening of all the catalysts under propene atmospheric pressure and with Al/M m.r. equal to 3000, 3 μmol of catalysts loaded, temperature of 50 °C, total volume equal to 50 ml of toluene has been done. In Table 3.1 the homopolymerization activities are reported only for catalysts **1** and **3**, showing very low activities, while all the other catalysts are practically inactive under these conditions.

Table 3.1 In batch homopolymerization activity

Catalyst	Activity [ç]
CAT 1	91.5
CAT 3	25

Temperature = 50° C; Solvent = 50 ml Toluene; [Al]/[Zr] = 3000; Propene Pressure = 1 bar; Catalysts = 3 μmol;

[ç] $Kg_{PP} \bullet mol_{Zr}^{-1} \bullet h^{-1}$

Then, the catalysts have been tested in autoclave under the experimental conditions, listed in the following table, in order to get close to industrial conditions; the results obtained are reported in Table 3.3.

Table 3.2 Autoclave experimental conditions

	IN AUTOCLAVE
Total volume	500 ml
Temperature	50° C
Solvent	150 ml of Toluene
Pressure	5 bar
Al-Zr ratio	3000
Catalysts	10 μmol

All the catalysts are active under these experimental conditions except catalyst **5**; To test the purity of the catalyst **5**, a single test in ethene polymerization has been ran at 7 bar, but the catalyst resulted to be inactive also under these conditions; this could be probably due to low degree of purity of the catalyst sample.

Table 3.3 Homopolymerization activity for the six catalysts used under autoclave conditions listed in Table 3.2

Catalyst	**Activity** [c]
CAT 1	612
CAT 2	68
CAT 3	72
CAT 4	334
CAT 5	n/a
CAT 6	112

The best catalyst performance has been obtained by the diphenyl bridged zirconocenes **1**. Among the isopropyl bridged metallocenes, metallocene **4,** which has no substituent on the Cp resulted the most active, while the Cp *t*-butyl substituted metallocenes give the lower activities. The Hf-based metallocene shows lower activity with respect to the homologous zirconocene one. This is in agreement with theoretical studies concerning the interaction between the metal and the carbon of inserting monomer; as consequence of the α-hydride interaction, the polarity of Hf-C bond decreases, thus the speed of the insertion and the propagation rate is lowered[1]. Moreover, the cationic transition state with Zr is more stable than the one with Hf metal.

All the homopolymers have been characterized by size exclusion chromatography to determine the molar masses and molar mass distributions. The molecular weight of a polyolefin, defined as the average degree of polymerization, made with single-centre metallocene catalysts is given by Eq. 3.1,

$$\bar{P}_n = \frac{\sum R_p}{\sum R_r} \qquad \text{Eq. 3.1}$$

that is, in terms of reaction rates, the molecular weight of polyolefins is given by the ratio between the overall rate of propagation (R_p) and the sum of all rates of chain release reactions (R_r): this means that the molecular weight is dependent on the type of catalyst and the kinetics of the process. The SEC results are reported in the table below.

Table 3.4 Polypropene molecular weights and molecular weight distributions

Catalyst	M_w	**D**
Type	**Kg/mol**	M_w/M_n
1	321	2,57
2	94	3,06
3	30	2,32
4	108	2,14
5	n/a	n/a
6	495	4,93

The Hf-based catalyst produce polymers with the highest molar masses. In perfect agreement with the trend reported in literature, the atomic radius of Hf metal is large enough to decrease the rate of chain termination reactions. The catalyst **1** produces very high M_w polypropene; this can be assessed to presence of diphenyl-bridge; in fact, the electromagnetic fields induced by ring currents of the phenyl groups of the bridge causes a deformation of the electron clouds of the aromatic π-system of the fluorenyl six membered rings and a redistribution of the electron densities concentrated on different atoms. These non-bonded interactions are at the origin of the slight structural modifications of the molecule, of the displacement of the transition metal further out of the mouth of the ligand and of the greater exposure of its frontier orbitals that are more diffuse and their orientation in space is affected by the new electronic requirement of the ligand. It has been proposed[5-9] that this electronically and sterically unsaturated reactive species is stabilized by agostic interactions with α-hydride anions; this interaction would maintain the active centre intact in the absence of the monomer, keep it receptive to coordination of another incoming monomer molecule for successive insertion, and is crucial for the formation of polymers with high molecular weights.

For the homopolymers obtained using **2** and **3** catalysts we note a decrease of M_w due to the absence of diphenyl-bridge and probably to the presence of Me and *t*-Bu group on the Cp side of catalysts, which slow down the propagation rate. Concerning the polydispersity, all the homopolymers showed a typical Gaussian profile, except the polymer obtained by using the Hf-based metallocene, that showed a quite high value.

On the basis of this preliminary screening in autoclave, we chose to investigate deeply the catalytic performance and the properties of the polymers obtained with the three most promising catalysts in various experimental conditions. So propene homopolymerizations were conducted under slurry experimental conditions at three different temperatures (30, 50, and 70 °C) by using the zirconocene precursors **1**, **3**, and **4**.

Homopolymerizations have been performed in a 250 ml autoclave under three different temperatures in order to evaluate the effect of temperature on the activities and on the polymer properties (e.g. microstructure and molar masses), under slurry conditions, as close as possible to those used in industrial production (e.g. temperature 70 °C, liquid propene).

Detailed experimental conditions are reported in Table 3.5.

Table 3.5 Autoclave experimental conditions

	AUTOCLAVE
Total volume	250 ml
Temperature	30°, 50°, 70°C
Solvent	Toluene: 50 ml
Propene	~ 25 g
Co-Catalyst	MAO
Al/Zr m.r.	3000
Catalysts	5 μmol

In Table 3.6 the homopolymerization activities are reported.

Due to the presence of diphenyl bridge the catalyst **1** is the most active, whereas the bulkier *t*-Bu group on Cp side of the catalyst **3** leads to the lowest activity. Moreover, the polymerization temperature influences the activities; for all the catalysts the higher the temperature the lower the activity. This should be due to the combined effect of increase of the activation energy ($\Delta E^{\ddagger}$) of the propagation step

with the temperature and the deactivation of the catalyst with the increase of the polymerization temperature.[10]

Table 3.6 Homopolymerization activity results for the three best catalysts chosen

Catalyst	T	[Propene]	Pressure	Activity
type	°C	mol_P/V	bar	$Kg_{PP}/mol_{Zr}•h•P$
1	30	5.3	4.7	2780
1	50	12.0	10.5	1510
1	70	3.8	6.9	1026
4	30	12.5	7.7	1043
4	50	13.3	12.9	695
4	70	12.9	15.4	238
3	30	14.5	8.2	337
3	50	14.9	12.0	187
3	70	16.2	16.9	152

The polymers have been characterized by SEC to determine the molar masses and the molar mass distribution; in the following table the SEC results are showed.

Table 3.7 Homopolymer molecular weight and molecular weight distribution

Catalyst	T	[Propene]	Pressure	M_w	D
type	°C	mol_P/V	bar	kg/mol	M_w/M_n
1	30	5.3	4.7	247	2.92
1	50	12.0	10.5	125	5.79
1	70	3.8	6.9	129	2.07
4	30	12.5	7.7	141	1.67
4	50	13.3	12.9	106	1.87
4	70	12.9	15.4	73	1.88
3	30	14.5	8.2	224	2.14
3	50	14.9	12.0	228	1.63
3	70	16.2	16.9	100	3.90

Catalyst structure influences molecular weight too. Indeed, similar to the previous results (see Table 3.4) diphenyl-bridged system yields higher M_w than isopropyl-bridged catalyst (**4**). In addition, M_w linearly depends on temperature and the higher the temperature the lower the M_w. At higher temperatures, indeed, the energy barrier of chain release processes is lower, and the rate of chain transfer becomes faster, leading to a polymer with low molecular weight.

Anyway, because the propene concentration in the polymerization medium is quite the same for all the reactions, an increase of temperature leads to an increase of pressure, and the pressure behaves oppositely to the temperature.

3.1.2 Polypropene microstructure

All the homopolymers obtained were characterized by ^{13}C-NMR. The percentage of syndiotactic (***rrrr***), isotactic (***mmmm***) and two of the most common stereo errors pentads (***rmrr*** and ***rmmr***) for the homopolymers obtained with the five active catalysts are listed in Table 3.8.

An expansion of the methyl region of some of the polypropene samples has been depicted in Figure 3.2.

Catalyst **1**, even being a C_1-symmetric catalyst, produces mainly syndiotactic polypropene. This should be due to the presence of a *t*-Bu substituent on the Flu rather than on the Cp: *t*-Bu substituent on the Flu does not lead to the steric hindrance as when it is located on Cp, thus inducing isotactic polymerization. Catalyst **3**, which has one *t*-Bu on Cp and one on Flu gives a highly isotactic polypropene and behaves like the 3-*t*-Bu Cp substituted C_1-catalysts. catalyst **2**, with one methyl group on Cp side of the molecule produces practically atactic polypropene, while catalyst **4**, the *iso*-propyl bridged analogous of **1**, surprisingly, produces very low syndiotactic polypropene.

Table 3.8 Pentad distributions for polypropene obtained by using all the active C_1-symmetric catalysts under the experimental conditions listed in Tab. 3.1

Catalyst	*rrrr*	*mmmm*	*rmrr*	*rmmr*
type	**mol %**	**mol %**	**mol %**	**mol %**
1	78.04	0	3.96	1.51
2	43.85	12.37	15.17	2.46
3	n/a	95.35	0	0
4	33.30	0	5,5	0

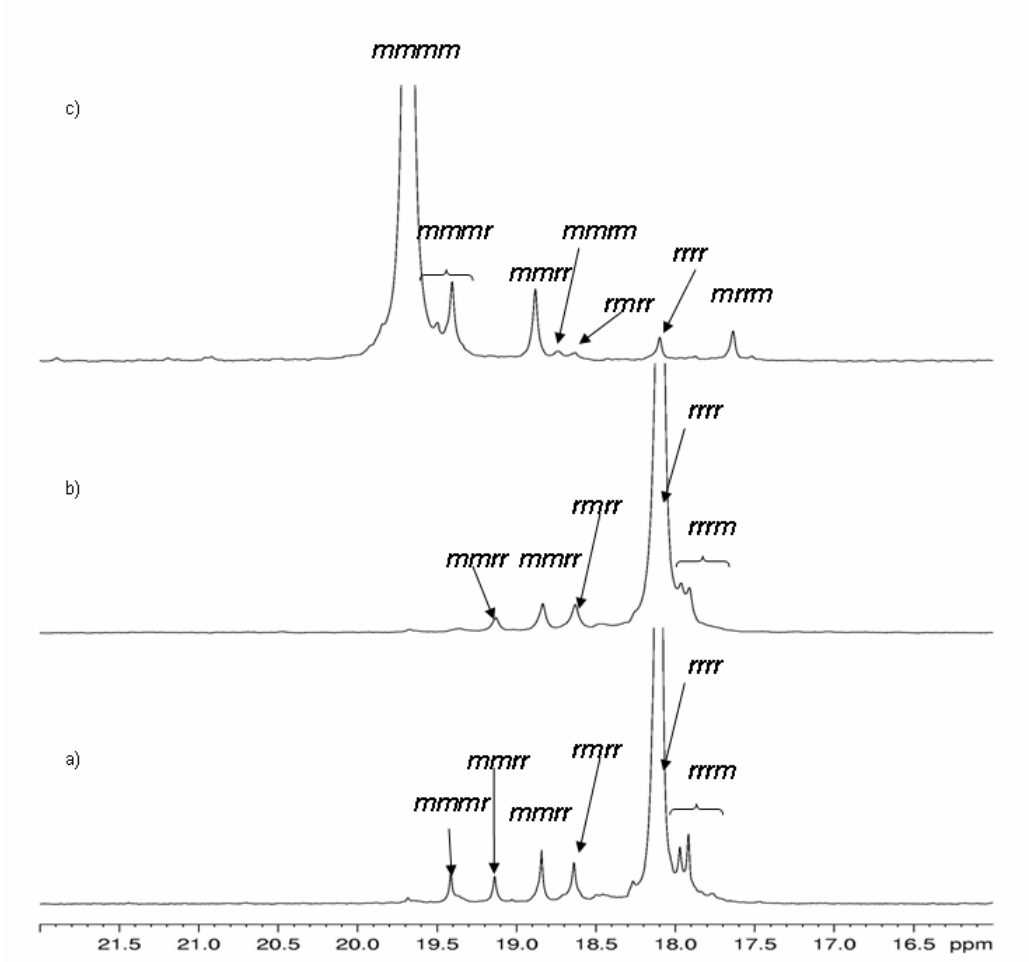

Figure 3.2 Methyl region of ^{13}C-NMR spectra (108.58 MHz, $C_2D_2Cl_4$, 103 °C) of polyPP samples prepared at 50 °C by: a) catalyst **1**; b) catalyst **4**; c) catalyst **3**.

To have a better evaluation of the polymerization mechanism that influences the polymer microstructure, a statistical analysis has been performed on the basis of the ^{13}C-NMR data acquired for the polymers obtained under slurry conditions reported in Table 3.5 by using the three most promising zirconocene precursors.

Observed polymer tacticity has been compared to that predicted by three statistical models (Scheme 3.2). The first is enantiomorphic site control, which is predicted by the site epimerization mechanism, since it employs a single site with enantioselectivity α.

Table 3.9 Pentad distributions for polypropene obtained by using the three most relevant C_1-symmetric catalysts chosen, under the experimental conditions listed in Tab. 3.5

Catalyst	Pressure	$[C_3]$	*T*	*rrrr*	*mmmm*	*rmrr*	*rmmr*
type	**bar**	**mol_P/V**	**°C**	**mol %**	**mol %**	**mol %**	**mol %**
1	4.7	5.3	30	69.8	0.7	7.9	2.1
1	10.5	12.0	50	54.1	1.2	12.5	2.9
1	6.9	3.8	70	58.9	0.8	12.2	2.6
4	8.8	12.5	30	77.3	0.8	3.6	2.1
4	12.6	17.7	50	69.4	1.9	5.7	2.4
4	11.6	13.9	50	77.6	0.7	4.2	2.0
4	17.6	12.9	70	68.0	1.2	6.5	2.6
3	8.2	14.5	30	0.6	86.9	0.7	1.7
3	12.0	14.9	50	1.3	88.8	1.2	1.7
3	16.9	16.2	70	0.8	84.0	1.9	2.1

Observed polymer tacticity has been compared to that predicted by three statistical models (Scheme 3.2). The first is enantiomorphic site control, which is predicted by the site epimerization mechanism, since it employs a single site with enantioselectivity α.

The second is an alternating model that is generally applicable to a catalyst that regularly alternates insertions between a perfectly stereoselective site ($\alpha = 1$) and a variably stereo selective site having a stereoselectivity equal to β. This model employs a single independent parameter.

The third is an alternating model that is applicable to a catalyst that regularly alternates insertions between two variably stereoselective sites. The stereoselectivity of one site is α, and the stereoselectivity of the other site is β. This model employs two independent parameters. Both alternating models assume that no site epimerization is occurring.

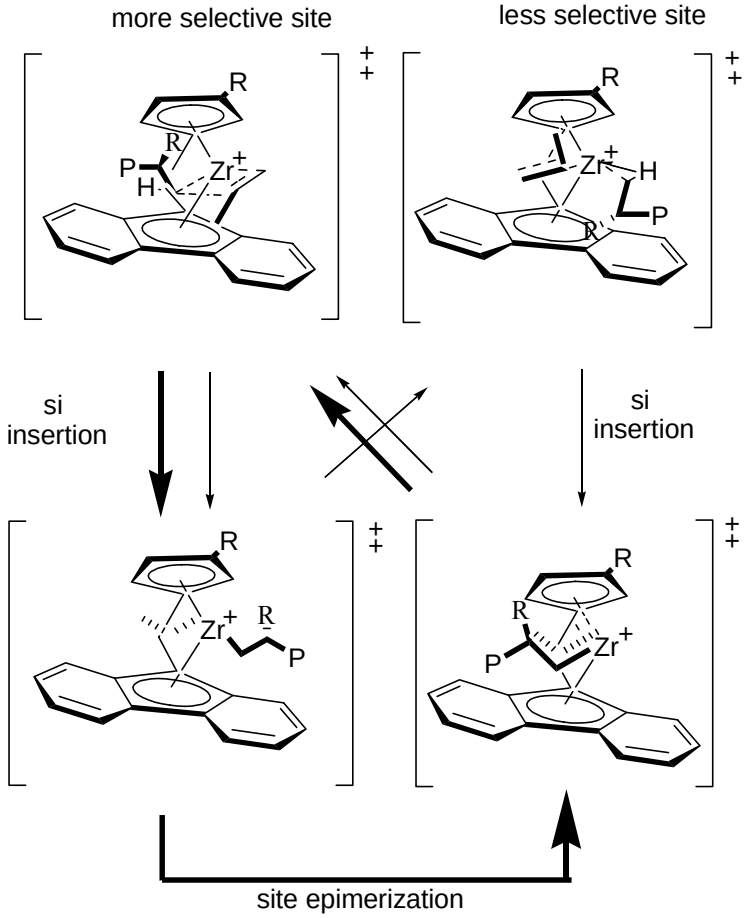

Scheme 3.2 Predicted statistical model: enantiomorphic site control (bold line); alternating mechanism (plain line): alternation between a perfectly stereoselective site and a variably stereoselective site (left side), alternation between two sites of various stereoselectivity (right side)

We compare the polymer tacticity predicted for the polypropene obtained by C_1-catalyst having the *ter*-butyl substituent on the Cp (**8**)[11], on the Fluorenyl ligand (**1, 4**) or both (**3**) to those obtained with the C_s–symmetric catalyst Me_2C-$(C_5H_4)(C_{13}H_8)ZrCl_2$ (**7**).

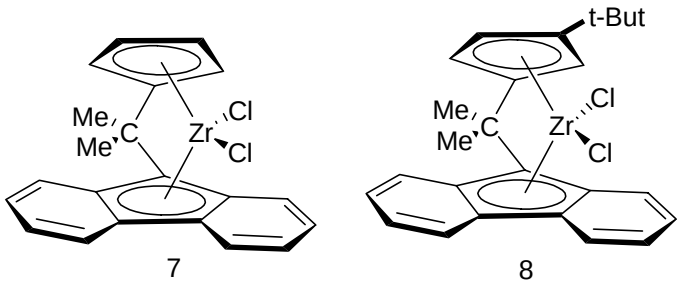

Figure 3.3 Structure of the reference catalysts 7 and 8 used for the statistical treatment of the polypropene microstructure.

For C_s-symmetric catalyst**,** the r.m.s. errors (Figure 3.4, Table 3.10) provided by the fits from the site epimerization mechanism and the alternating one are very different, indicating that the alternating two site mechanism better predicts the microstructure of polypropene produced by this catalyst

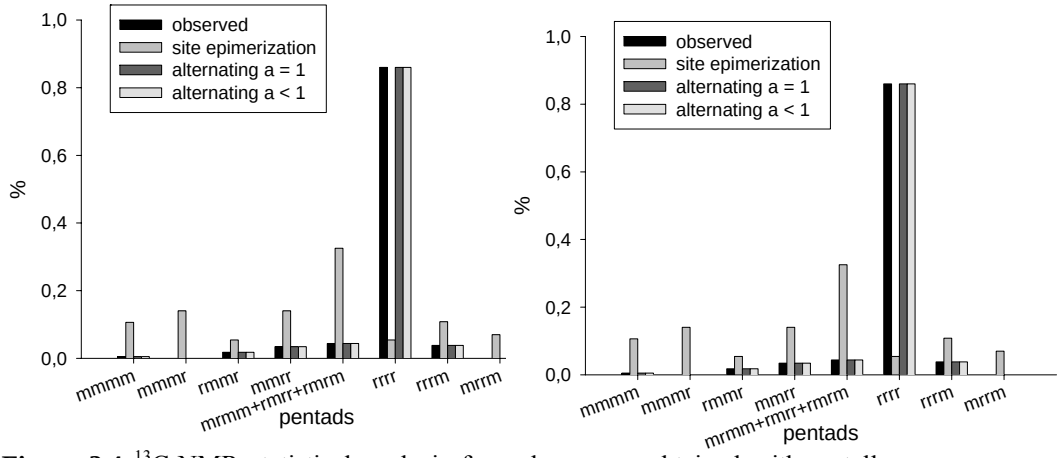

Figure 3.4 ^{13}C-NMR statistical analysis for polypropene obtained with metallocenes precursors **7** (left) and **8** (right)

Table 3.10 r.m.s error fit for microstructural analysis of PP obtained with cat (**7**) and catalyst (**8**)

CAT 7 T 30°C	**α**	**β**	**r.m.s. (%)**	**CAT 8 T = 40°C**	**α**	**β**	**r.m.s. (%)**
site epimerization	0.631		29.45	site epimerization	0.952	/	0.687
alternating $\alpha = 1$	1	0.054	1.66	alternating $\alpha = 1$	1	0.906	0.886
alternating $\alpha < 1$	0.972	0.028	1.52	alternating $\alpha < 1$	0.953	0.952	0.687

On the contrary, for catalyst **8**, bearing one *tert*-butyl group on Cp ligand, the r.m.s. errors (Figure 3.4, Table 3.10) provided for the three predictive mechanisms are very similar. Such similarity was considered by Bercaw et al[11] too similar to

draw definitive conclusions if concerning whichever mechanism, site epimerization or alternating, predicts the microstructure of the polypropene produced. Here, we would like to point out that the lowest r.m.s. errors are found for the epimerization and for the alternating mechanism with two sites of variable stereoselectivity. In addition, the site epimerization model gives an α value of 0.952, exactly the same α and β values are found for the alternating mechanism with variable stereoselectivity.

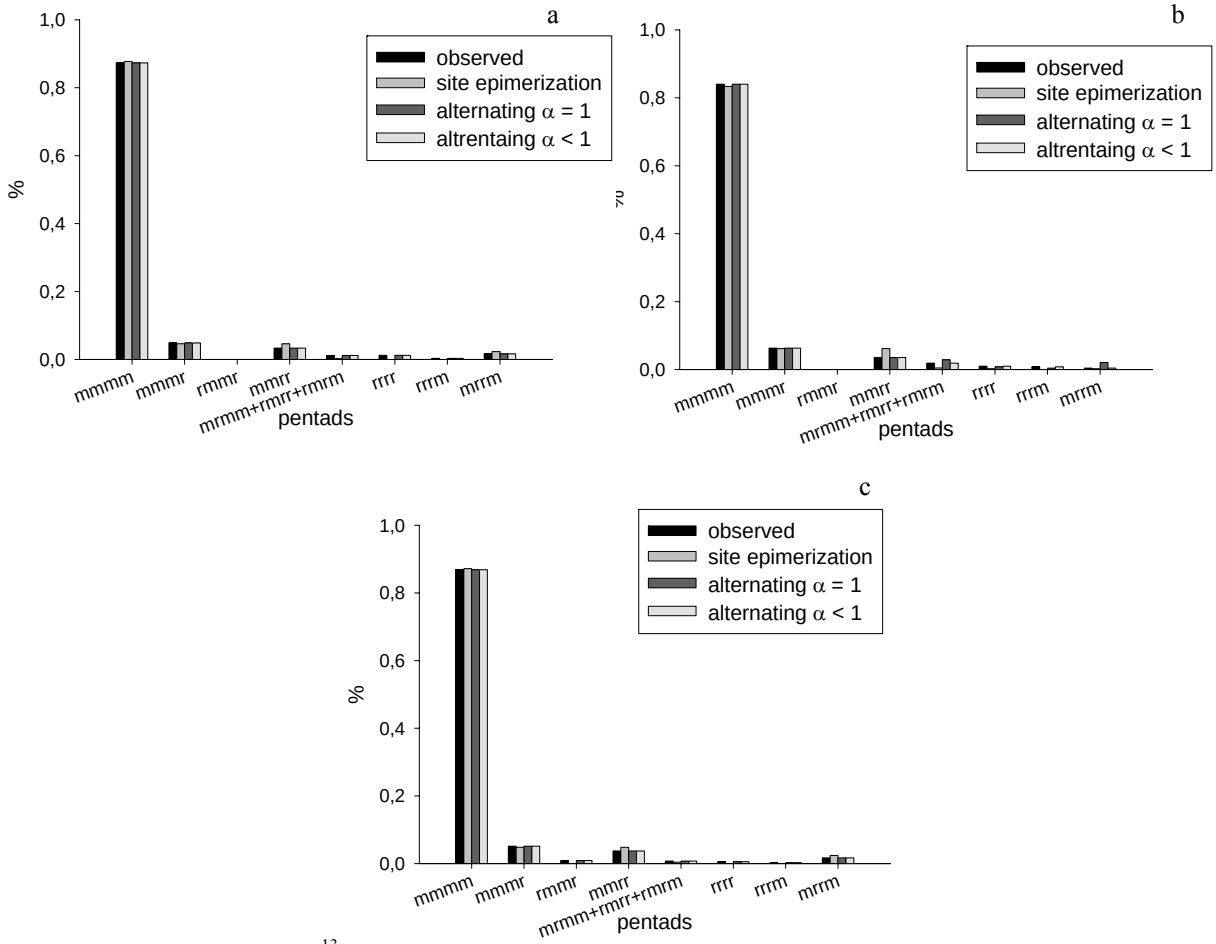

Figure 3.5 Statistical ^{13}C-NMR analysis of polypropene samples obtained by using C_1-symmetric catalyst **(3)** at (ac) 70 °C

The r.m.s. errors provided for catalyst **3** (Figure 3.5, Table 3.11) are low and very similar, as to indicate that all mechanisms are possible, that is as for catalyst **7** the mechanism should be alternating, but the presence of the second *ter*-butyl on the

same half-space makes the epimerization necessary. This is confirmed from the slight changes in the microstructure with temperature or monomer concentration. Indeed, as described by Bercaw[11], when the alternating mechanism is operating and the site epimerization mechanism is accessible, it is possible to detect an increased isotacticity with the polymerization temperature, at the same propene concentration, and a decreasing in isotacticity by increasing the propene concentration (see Tab. 3.9).

Table 3.11 r.m.s error fit for microstructural analysis of polyPP obtained with cat (**3**)

T = 30 °C [P] = 14.5	α	β	**r.m.s. (%)**
site epimerization	0.973	/	0.578
alternating $\alpha = 1$	1	0.947	0.646
alternating $\alpha < 1$	0.973	0.973	0.578
T = 50 °C [P] = 14.9	α	β	**r.m.s (%)**
site epimerization	0.974	/	0.719
alternating $\alpha = 1$	1	0.949	0.784
alternating $\alpha < 1$	0.974	0.974	0.719
T = 70 °C [P] = 16.2	α	β	**r.m.s (%)**
site epimerization	0.967	/	1.272
alternating $\alpha = 1$	1	0.936	1.155
alternating $\alpha < 1$	0.967	0.967	1.352

Regarding catalyst **4**, with one *ter*-butyl on the fluorenyl, results are rather similar to those of catalyst **8** with one substituent on the Cp even though **8** gives an isotactic polypropene and **4** a mainly syndiotactic one (Figure 3.6, Table 3.12). Indeed, for all the three polymerization temperatures, the epimerization mechanism could not predict the pentad distribution, while both the alternating mechanisms well describe the observed microstructure. It is worth noting that also when the alternating mechanism is preferred, an increase in polymerization temperature slightly reduces the stereospecificity.

Table 3.12 r.m.s error fit for microstructural analysis of polyPP obtained with cat (**4**)

Catalyst 4	T (°C)	α	β	r.m. (%)
site epimerization	30	0.377	/	26.50
	50	0.379	/	26.57
	70	0.379	/	24.55
alternating $\alpha = 1$	30	1	0.091	2.72
	50	1	0.090	2.71
	70	1	0.131	3.88
alternating $\alpha < 1$	30	0.952	0.048	2.33
	50	0.952	0.048	2.32
	70	0.952	0.073	3.11

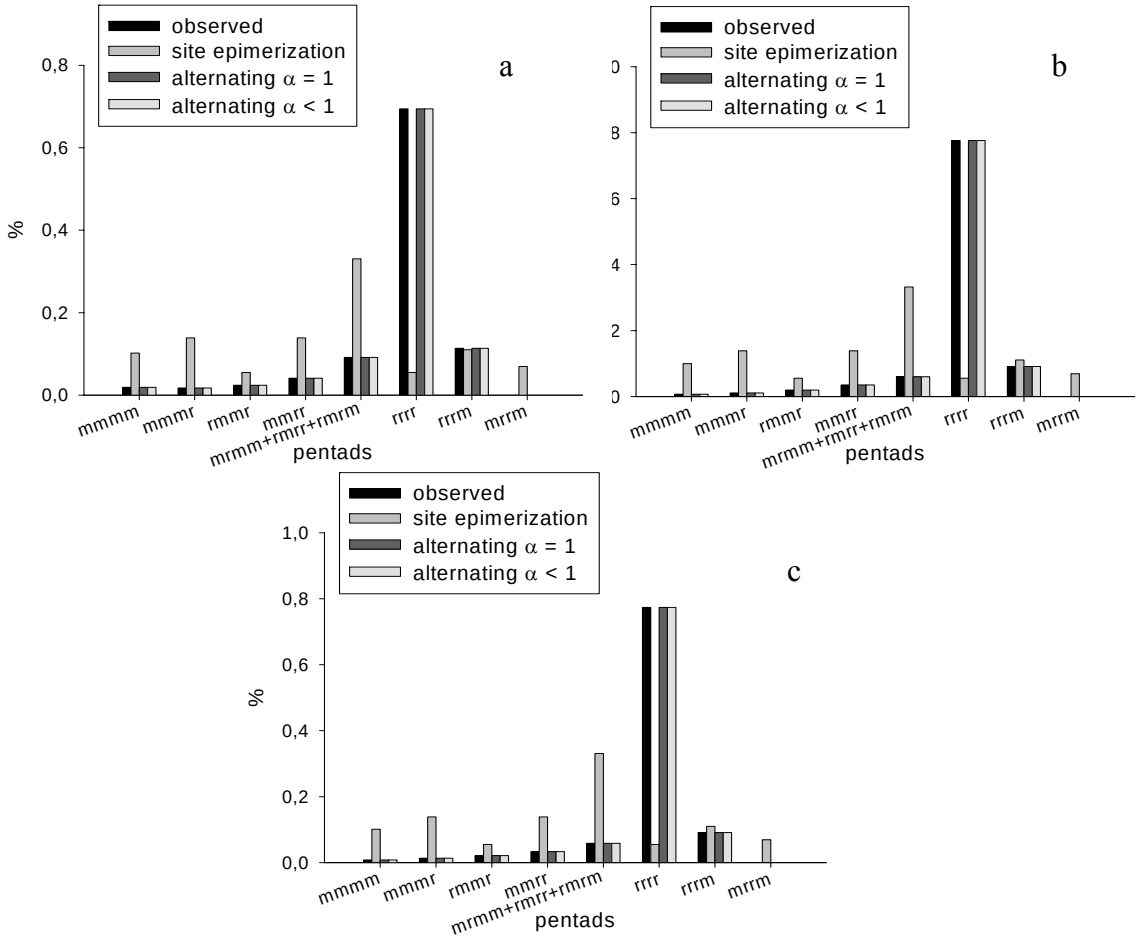

Figure 3.6 Statistical ^{13}C-NMR analysis of polypropylene samples obtained by using C_1-symmetric catalyst (4): a) 30 °C, b) 50 °C, c) 70 °C.

Statistical analysis of polypropene by catalyst **1** (Figure 3.7, Table 3.13) reveals results similar to those from **4**.

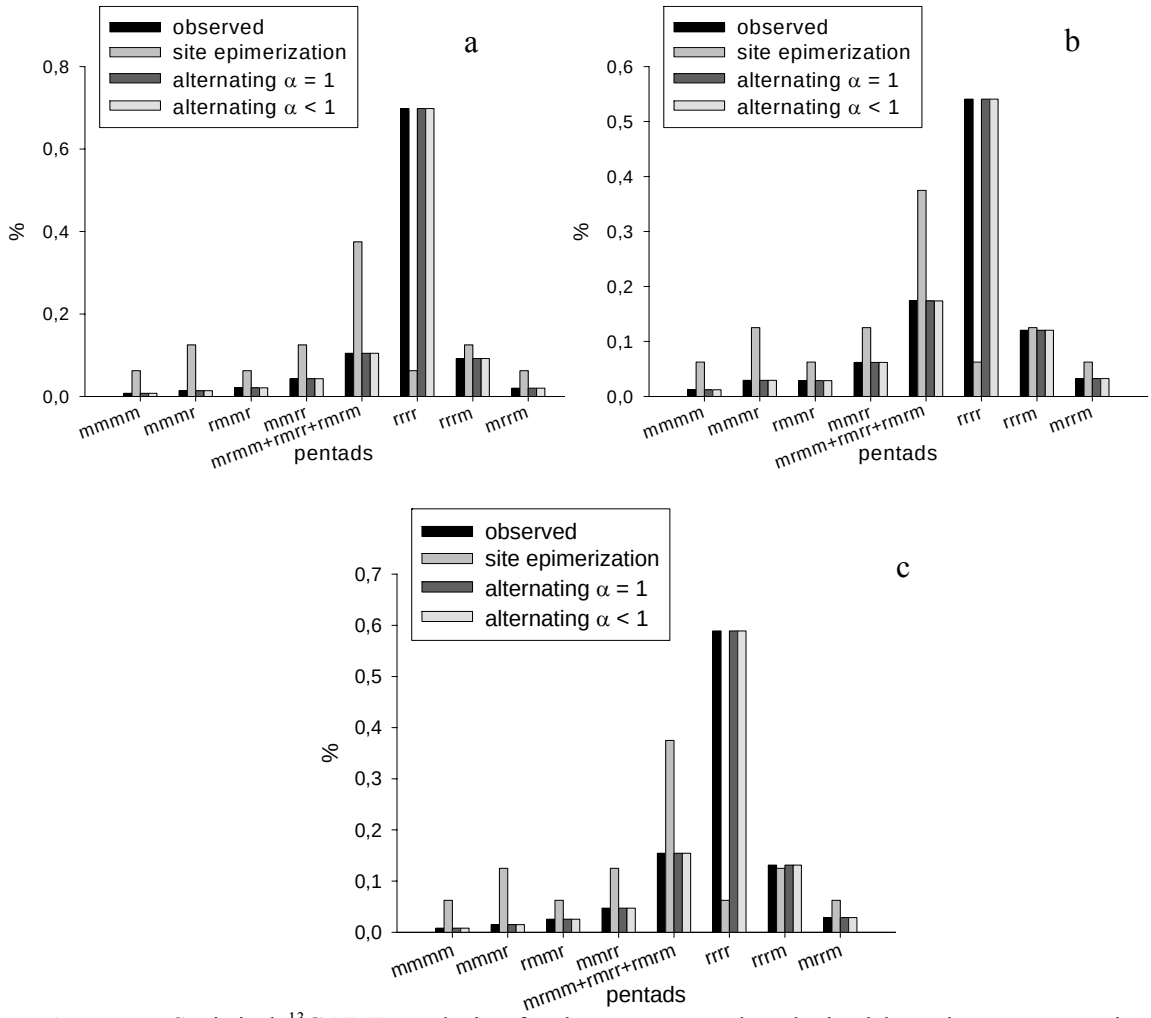

Figure 3.7 Statistical ^{13}C-NMR analysis of polypropene samples obtained by using $_{CI}$-symmetric catalyst **1**: a) 30 °C, b) 50 °C, c) 70 °C.

Table 3.13 r.m.s error fit for microstructural analysis of polyPP obtained with cat (**1**)

Catalyst 1	**T (°C)**	α	β	**r.m.s. (%)**
site epimerization	30	0.500	/	23.65
	50	0.500	/	17.86
	70	0.500	/	20.890
alternating $\alpha = 1$	30	1	0.121	4.30
	50	1	0.198	6.88
	70	1	0.173	6.33
alternating $\alpha < 1$	30	0.933	0.067	3.57
	50	0.121	0.881	4.87
	70	0.102	0.898	4.75

Thus, the statistical analysis of propene microstructure confirms that the stereospecificity can increase with decreasing the monomer concentration for both

catalysts **1** and **4** and due to the absence of hindered substituents on Cp side the alternating mechanism is preferred with respect to the site epimerization one. For the catalyst **3**, the data collected by the analysis indicate that the alternating mechanism is possible, but the site epimerization becomes necessary due to the presence of the two substituents: one on the Cp and on the Flu groups.

In conclusion even though recent DFT computational studies indicate that it is difficult to assess whether a site epimerization-controlled mechanism takes place in these polymerizations[12], the statistical analysis of polypropene microstructures made at different temperatures and propene concentration from metallocenes with gradual changes on the substitution and thus gradual desymmetrization of the C_s symmetry allowed us to obtain experimental evidences that support the following conclusion: the alternating mechanism, that is the chain migratory insertion, occurs, but the presence of tert-butyl on the Cp renders the site epimerization mechanism competitive, especially when a second *ter*-butyl is present on the same half-space, that makes the epimerization necessary. This is confirmed by the slight changes in the microstructure with temperature or monomer concentration. Indeed, it is possible to detect an increased isotacticity with the rise of polymerization temperature, at the same propene concentration, which favors unimolecular site epimerization over bimolecular propagation and a decrease in isotacticity by increasing the propene concentration.

The lower activity of catalyst **3** with respect to catalyst **2** is also in line with the need for the polymer chain to back skip (or epimerize) to the original position before the subsequent insertion, that is, almost all the insertions occur on the same site.

3.1.3 Chain end analysis

Molar masses strongly depend on the structure of the cyclopentadienyl ligands, since the number, the size, and the position of different substituents induce different non-bonded interactions in the intermediates and transition states leading to chain transfer reactions. Thus, all the homopolymers have been characterized by ^{1}H-NMR to determine the chain end groups.

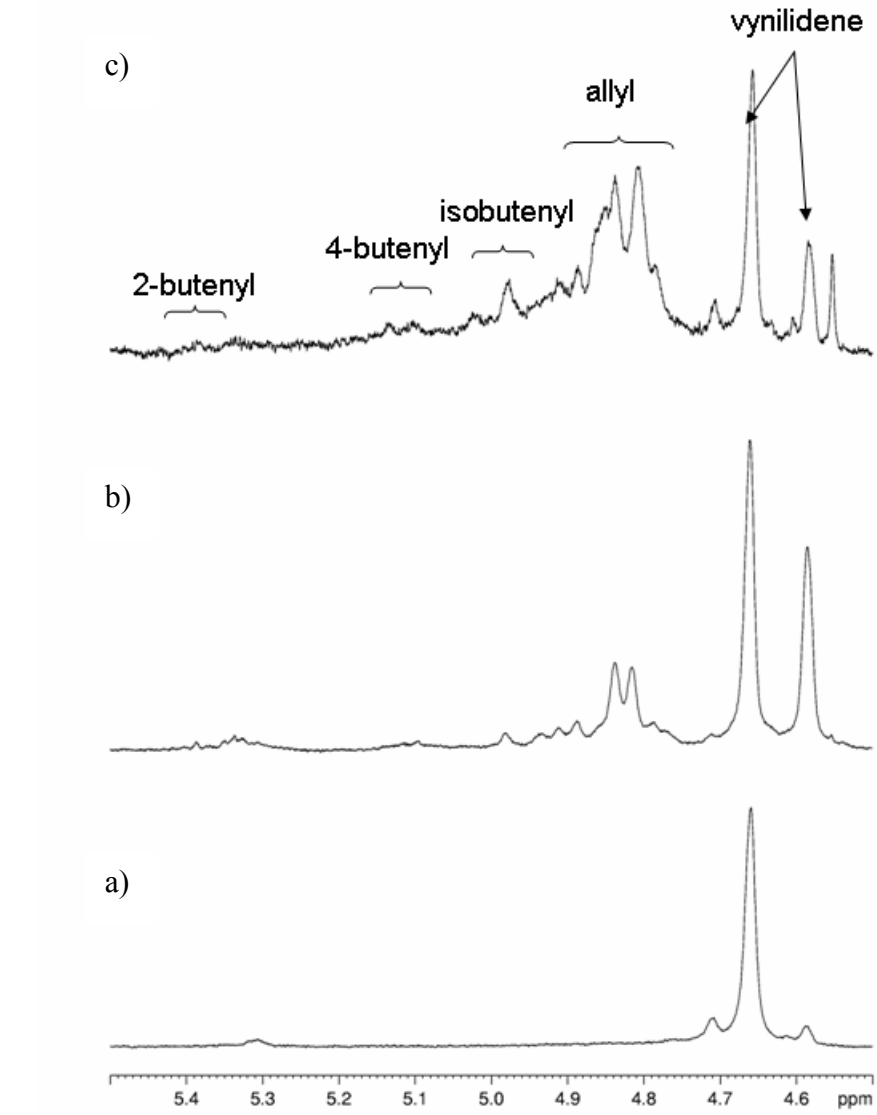

a)

Figure 3.8 Olefinic region expansion of ^{1}H-NMR spectra (108.58 MHx, $C_2D_2Cl_4$. 103 °C) of polyPP samples obtained with: a) Catalyst **3** 50 °C; b) catalyst **4** 50 °C; c) catalyst **1** 50 °C.

The expansion of the olefinic region of ^{1}H-NMR spectra of polypropene obtained with precatalysts **1**, **4**, and **3** are displayed in Figure 3.8.

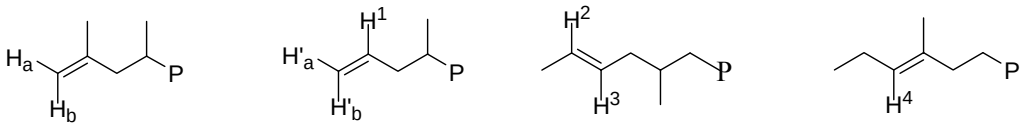

vynilidene allyl 2-butenyl 4-butenyl

Figure 3.9 Main unsaturated chain end groups forming during the propene polymerizations

The main unsaturated chain end groups, that form during the propene polymerization, were detected and identified in polypropene: vinylidene, allyl, 2-butenyl and 4-butenyl[13]. $\mathbf{H_a}$ Singlet 4.59 , $\mathbf{H_b}$ Singlet 4.66 ,$\mathbf{H'_a}$: Broad Singlet 4.88 ppm, $\mathbf{H'_b}$: Doublet 4.94 ppm (J = 6.2 Hz), $\mathbf{H^1}$: Complex Multiplet 5.72 ppm, $\mathbf{H^2}$: Complex Multiplet 5.38 ppm, $\mathbf{H^3}$: Complex Multiplet 5.38 ppm, $\mathbf{H^4}$: Triplet of Multiplets: 5.11 ppm (J = 7.0 Hz)[13].

In the following scheme the most common chain termination mechanisms are reported.

Scheme 3.2 Chain termination mechanism: (a) *β*-hydrid transfer to monomer; (b) *β*-methyl abstraction to metal; (c) *β*-hydride transfer to monomer after a 1,2 insertion

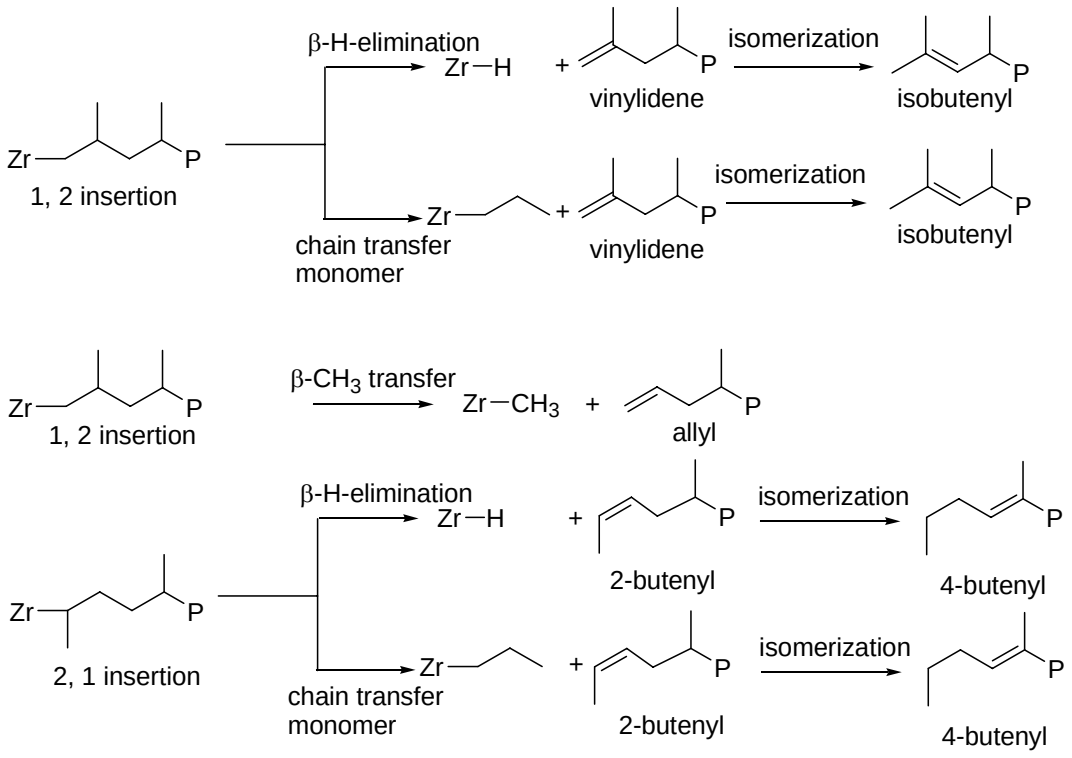

Vinylidene end groups are produced via β-hydrogen transfer to the metal or to the monomer after a primary insertion, isobutenyl groups derive from isomerization of the vinylidenes. Allyl end groups are formed via β-methyl abstraction. 2-Butenyl end groups are produced via β-hydride transfer after a secondary insertion of propene. 4-Butenyl unsaturated chain end groups are formed during the polymerization by isomerization of the 2-butenyl groups.

The two protons of vinylidene groups should have to have the same intensity, the area of the peaks at 4.59 and 4.66 ppm is not the same. This has been reported by several authors such as Resconi[14] and Kawahara et al.[15] to the different chemical environment of the internal vinylidene resonance is 4.68 ppm close to the low field resonance of H_b proton. The internal vinylidenes arise from allylic activation (Scheme 3.3), which involves development of H_2, which can act as chain transfer and thus to each internal vinylidenes could correspond a saturated chain end groups.

Scheme 3.3 Formation of internal vinylidenes by propene insertion at the η^3-allyl intermediate

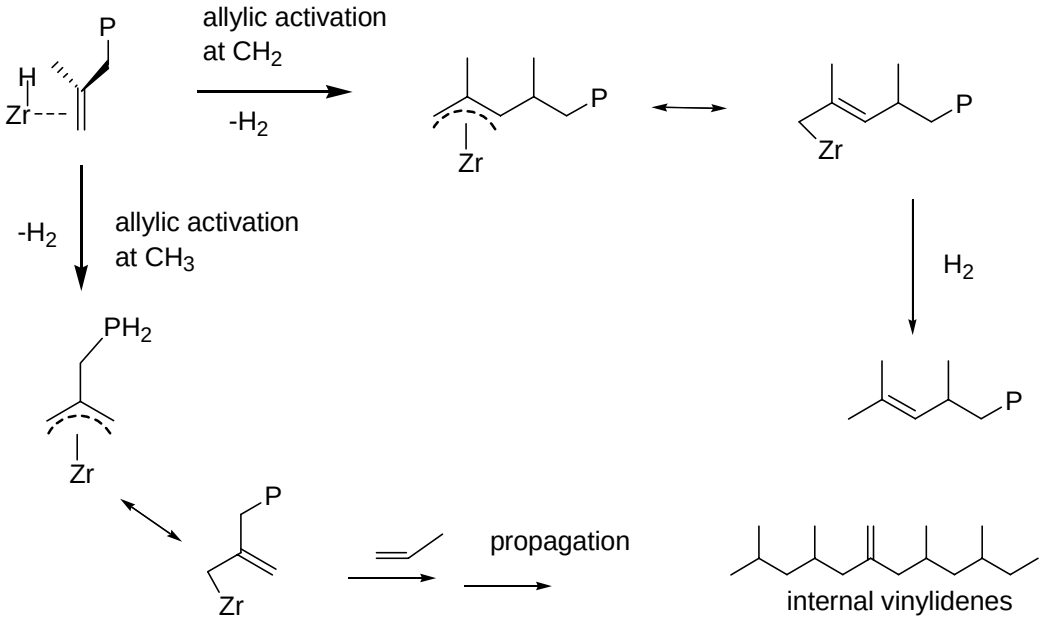

Results are tabulated in Table 3.10. Previous studies on mechanisms in propene polymerization by chain end group analysis[15, 16] report that the β-hydride transfer strongly depends on temperature and pressure, that is, the higher the temperature and

the lower the pressure, the higher is the percentage of vinylidene groups with respect to the allyl group percentage.

Table 3.10 Chain end group percentage calculated from ^{1}H-NMR spectra

Cat	T	Vinylidene	Int. Vinylidene	Isobutenyl	Allyl	2-butenyl	4-butenyl
	°C	mol %	mol %	mol %	mol %	mol %	mol %
1	30	18	3	26	13	21	19
1	50	40	8	17	8	12	15
1	70	16	9	35	11	16	13
4	30	15	9	53	18	5	0
4	50	38	13	32	9	3	5
4	70	50	12	26	5	3	4
3	30	65[a]	0	0	8	5	0
3	50	12	70	6	6	3	3
3	70	24	68	3	3	3	0

In Figure 3.10 the relative changes of unsaturated left end groups observed in PP obtained with **1**, **4**, and **3** catalysts of Table 3.10 at different temperatures are displayed. In the figure vinylidenes is the sum of vinylidenes, internal vinylidene and isobutenyl end groups, since the latter also arise from vinylidenes. It is clear that the hindrance on the ligands influences the chain termination mechanism also for the C_1-symmetric catalysts of this study, since each catalyst has a pattern of relative intensities of chain end groups at all the three temperatures.

A first observation is that 2- and 4-butenyl chain end groups are quite low with metallocenes **4** and **3**, which indicate that these catalysts are highly regioselective, while metallocene **1** is less regioselective because of structural modifications induced by the diphenyl on the bridge.

A comparison between metallocenes **3** and **4** reveals that for **4** allyl chain end groups are relevant, thus the presence of only one *t*-butyl substituent makes the transfer of the larger methyl group possible. Also for catalyst **1,** with one *t*-butyl substituent the β-methyl abstraction is a competitive chain end mechanism.

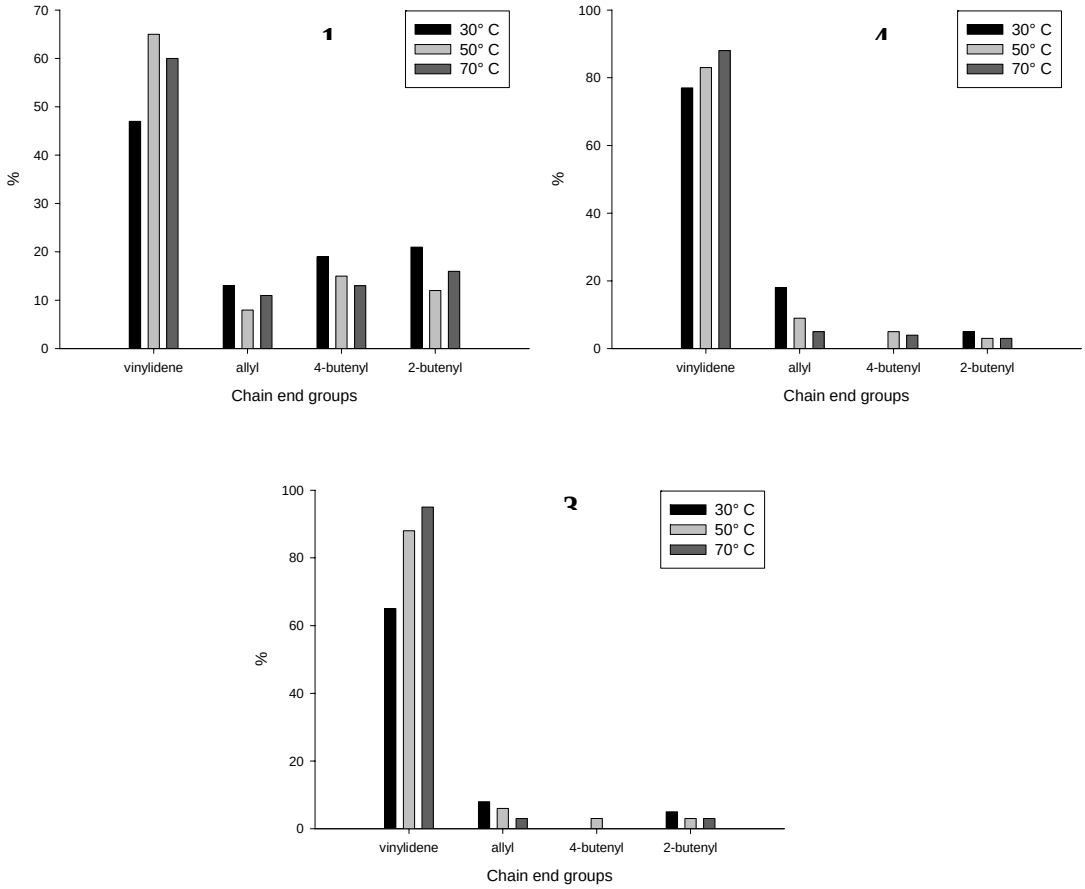

Figure 3.10 Chain end analysis for catalysts **1**, **3** and **4** at the three different temperatures. vinylidenes is the sum of vinylidenes, internal vinylidene and isobutenyl end groups

Such analysis now allows us to observe that there is a correlation between the relative vinilydene end groups of each catalyst and the polypropene molar masses found. If we compare the average results of molar masses for each catalyst in Table 3.7 with the average vinylidene end groups found in Figure 3.8 it is evident that the lower the relative vinylidene end groups, the higher the molar masses.

Finally, we point out that from Figure 3.8 it is clear that the relative intensity between external and internal vinylidenes is **3** > **1**> **4**, the same order of the pentads arising from epimerization. A mechanism involving dihydrogen/η^3-allyl complex intermediates was put forward from Resconi to explain epimerization events in C_2-symmetric catalysts. Even though mechanistic studies using a doubly labeled propylene by Bercaw gave evidence that an allyl/dihydrogen complex does not mediate chain epimerization, our results indicate that dihydrogen/η^3-allyl complex

intermediates may contribute to chain epimerization.

3.1.4 Propene homopolymerization by using supported catalysts

The industrial synthesis of polypropene is based on high temperature polymerization in liquid monomer, mediated by heterogeneous catalysts, in order to have a better control of the morphological properties of the polymer that results easier to process to reach the final use.

Thus, our attention moved on to the study the propene homo-polymerization by using supported metallocenes provided us by Total under experimental conditions as close as possible to industrial conditions, that is, in liquid propene and temperature of 70 °C.

Series of propene homopolymerization have been performed in order to get the right polymerization conditions, by using three supported metallocenes, named A, B and C:

Catalyst A: concentration in mineral oil: 20% wt; Zr content: 0.15% wt;

Catalyst B: concentration in mineral oil: 20% wt; Zr content: 0.15% wt;

Catalyst C: concentration in mineral oil: 10.6% wt; Zr content: 0.4% wt.

In particular we have verified, for each catalytic system, the right amount of catalyst and hydrogen, the type of aluminium cocatalyst and the Al/Zr ratio, suitable for obtaining good and reproducible activity in propene homopolymerization.

Catalyst C

First of all a set of homopolymerization by using catalyst **C** was carried out; initially under the experimental conditions listed in the following table:

Table 3.11 Autoclave experimental conditions

Catalyst	**mg**	37.5
Co Catalyst	**mmol**	0.48
H_2	**mmol**	1,7
Al/Zr	**m.r.**	300
Polym t	**min**	60
Polym T	**°C**	70

We obtained quite high activities but modest reproducibility. The particularly high activity obtained in run **MC171**, where the highest amount of C_3 was loaded into the reactor, suggests that, surprisingly, the activity is strongly influenced by C_3 amount.

Table 3.12 Experimental data of propene polymerizations with catalyst **C** under autoclave conditions listed in Table 3.10

	C_3	TEAL/C3	Activity	Conversion
	mg	g/kg	g/g/h	wt%
MC170	55.4	1.0	976	66.1
MC171	69.4	0.8	1493	80.7
MC172	45.6	1.2	944	77.6

Catalyst: 37.5 mg; co-catalyst: 0.48 mmol; H_2: 1.7 mmol; Al/Zr: 300 m.r.; time: 60'; temperature: 70°C;

Because the monomer conversion is quite high, we decided to reduce the amount of catalyst loaded in order to increase the activity. In the following table, the results obtained by using the half of the catalyst has been reported.

Table 3.13 Experimental data of propene polymerizations with catalyst **C** under autoclave conditions with half catalyst loading

	C_3	TEAL/C3	Activity	Conversion
	g	g/kg	g/g/h	wt %
MC173	49.6	0.6	711	26.8
MC174	48.8	0.6	176	6.8
MC175	52.8	0.6	144	5.1

Catalyst: 18.7 mg; co-catalyst: 0.24 mmol; H_2: 1.7 mmol; Al/Zr: 300 m.r.; time: 60'; temperature: 70°C;

Reducing the amount of catalyst loaded, in order to keep constant the molar ratio between Al and Zr, the amount of scavenger has to be reduced; but reducing the amount of scavenger affects both the activity and the reproducibility, as can be seen in Table 3.13,.

To assess this hypothesis, we have verified the effect of Al concentration by performing two experiments at higher TEAL/C3: one run using 37.5 mg of catalyst and one run using 18.7 mg of catalyst but double amount of co-catalyst.

Table 3.14 Effect of Al concentration on the homopolymerization activity

	Catalyst	C_3	Al/Zr	Activity	Conversion
	mg	g	m.r.	g/g/h	wt%
MC176	37.5	52.6	300	757	54.0
MC184	18.7	58.5	600	711	22.7

Co-catalyst: 0.48 mmol; H_2: 1.7 mmol; TEAL/C_3: 1.0 g/kg; time: 60'; temperature: 70°C;

Due to the high and constant TEAL/C3 weight ratio we can observe a good reproducibility.

Some of the homopolymers obtained were analyzed by ^{13}C-NMR at least at pentad level to determine the microstructure and by size exclusion chromatography to determine the molar masses and molar mass distribution; in the following table a mean value of the ^{13}C-NMR results is shown:

Table 3.15 ^{13}C-NMR pentad mean value percentage

mmmm **(%)**	***mmrr*** **(%)**	***mmmr*** **(%)**	***mrrm*** **(%)**
87.8	4.9	5.2	2.2

M_ws and molar mass distributions are strongly dependent on monomer conversion: the higher the conversion the higher the M_ws and the broader the molar mass distributions. This could be due to the fact that molecular weight is strongly dependent by the pressure; when the propene is consumed fast, that is high monomer conversion, the pressure goes down quickly during the polymerization and the length of the growing chains changes rapidly. Because of that the most significant results are those obtained when the conversion is below 30 wt %, and the mean value results to be:

***M_w*: 316.0 +/- 41.3 Kg/mol;** **D: 2.32 +/- 0.09**

Catalyst B:

Initially, a set of homopolymerization was performed under the following experimental conditions:

Table 3.16 Autoclave experimental conditions

Catalyst	**mg**	30
Co Catalyst	**mmol**	1,5
H_2	**mmol**	1,7
Al/Zr	**m.r.**	1500
Polym *t*	**min**	60
Polym T	**°C**	70

The results presented in the following table indicate a quite good reproducibility.

Table 3.17 Experimental data of propene polymerizations with catalyst **B** under autoclave conditions listed in Tab. 3.16

	C_3	**TEAL/C_3**	**Activity**	**Conversion**
	g	**g/kg**	**g/g/h**	**wt %**
MC180	55.4	1.6	1333	72.2
MC181	69.7	1.3	1960	42.2
MC182	63.7	1.4	1350	63.6
MC183	61.5	1.4	1340	65.4

Catalyst: 30mg; co-catalyst: 0.75 mmol; H_2: 1.7 mmol; Al/Zr: 15000 m.r.; time: 60' (MC181 t = 30'); temperature: 70°C;

Therefore with catalyst **B**, the amount of C_3 loaded into the reactor and the slight differences in Al/C_3 wt % ratio do not seem to have significant influence on the activities

Then we went on exploring the effect of the amount of H_2 loaded into the reactor (Tab 3.18); in fact, the hydrogen molecule is smaller than propene molecule and it could insert in a dormant sites after a regioerror, leading to an increase in activity.

It seems that the change in H_2 level does not substantially influence the average activity that is similar to the results reported in Table 3.17, but it is more variable.

It seems that the change in H_2 level does not substantially influence the average activity that is similar to the results reported in Table 3.17, but it is more variable.

Table 3.18 Experimental data of propene polymerizations with catalyst **B** under autoclave conditions listed in Table 3.15, reducing the amount of hydrogen

	C_3	Activity	Conversion
	g	g/g/h	wt %
MC210	65.4	1847	42.4
MC211	65.6	2093	47.9
MC212	66.2	1113	25.2
MC213	69.7	1507	32.4

Catalyst: 30 mg; co-catalyst: 0.75 mmol; H_2: 1 mmol; TEAL/C_3: 1.3 g/kg; Al/Zr: 1500 m.r.; time: 30'; temperature: 70°C;

Then we tested the influence of co-catalyst type on the homopolymerization activity. We chose to use triisobutylaluminum (**TIBAL)** instead of **TEAL** as co-catalyst, on the basis of previous experiments conducted in bench reactor at Total.

Table 3.19 Effect of different cocatalyst with **B**

	C_3	TIBAL/C_3	Activity	Conversion
	g	g/kg	g/g/h	wt %
MC263	67.1	1.9	5920	44.4

Catalyst: 15 mg; co-catalyst: 0.65 mmol; H_2: 2,2 mmol; Al/Zr: 2500 m.r.; time: 30'; temperature: 70°C;

We note a high increase in activity. Even if it is a single run test, we could conclude that under our experimental conditions the use of TIBAL instead of TEAL as co-catalyst lead to the best activity.

This is probably due to the fact that isobutyl groups react with the MAO adsorbed on the silica support of the catalyst, leading to modified MAO (MMAO); the MMAO, due to the bulkier hindrance, stabilizes the ionic couple responsible for the polymerization.

Some of the homopolymers obtained were analyzed by ^{13}C-NMR at least at pentad level to determine the microstructure and by SEC to determine the molar masses and molar mass distributions. the following table a mean value of the ^{13}C-NMR and SEC results are shown

mmmm (%)	*mmrr* (%)	*mmmr* (%)	*mrrm* (%)
97.9	1.1	1.0	n/a

H_2 level (mmol)	M_w (kg/mol)	D (M_w/M_n)
1	349.9	3.68
1.7	328.1	5.68

Also with **B** catalyst the M_w and the molar mass distributions strongly depend on monomer conversion; moreover the homopolymers obtained by using the lower hydrogen content (1 mmol) do not show a significant variation in molar masses and molar mass distribution. Therefore, we consider the polymers obtained by using 1.7 mmol of hydrogen and with monomer conversion closer to 40% to give significant results on molar masses.

The average M_w and D are:

M_w: 429.7 +/- 67.1 kg/mol **D: 3.36 +/- 1.20**

In the following graphs the relationship between M_w and monomer conversion has been reported:

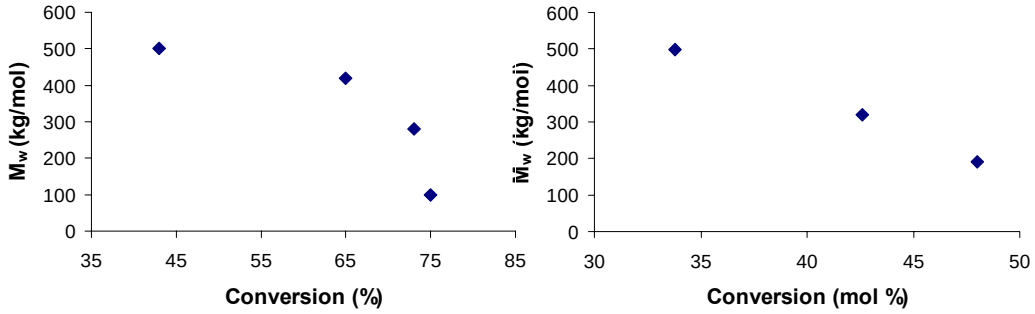

Figure 3.11 Molecular weights dependence on monomer conversion. H_2 level: 1.7 mmol (right), H_2 level 1 mmol (left)

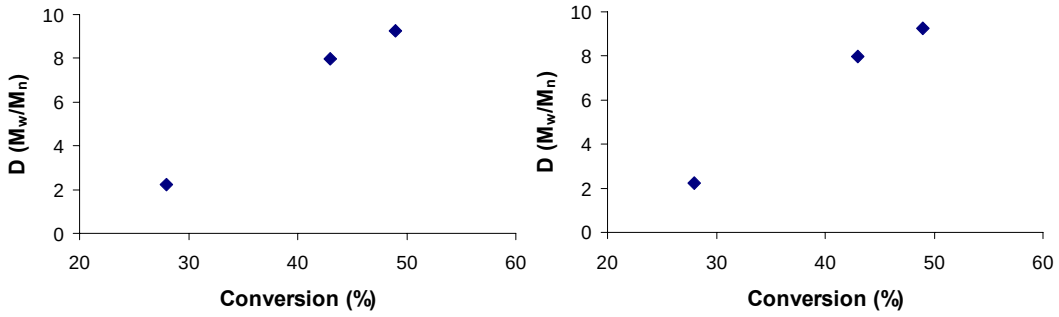

Figure 3.12 Molecular weight distributions dependence by monomer conversion. H_2 level 1.7 mmol (left), H_2 level 1 mmol (right)

We note that there is a quite linear relationship between M_w and monomer conversion; higher the monomer conversion lower the M_w.

A similar but opposite relationship could be observed also with molar mass distribution (see Figure 3.12).

Polydispersities increase linearly with the conversion: higher the monomer conversion higher the molar mass distribution.

Catalyst A:

First of all we tested the catalyst under the following experimental conditions.

Table 3.20 Autoclave experimental conditions

Co Catalyst	**mmol**	0,75
H_2	**mmol**	1,7
TEAL/C_3	**g/kg**	1,3
H2/C_3	**Nl/l_{C3}**	0,4
Al/Zr	**m.r.**	1500
Polym t	**min**	60
Polym T	**°C**	70

The main results have been reported in the following table:

Table 3.22 Experimental data of propene polymerizations with Catalyst **A** under autoclave conditions listed in Table 3.20

	C_3	TEAL/C_3	Activity	Conversion
	g	g/kg	g/g/h	wt %
MC198	50.3	1.7	2333	69.6
MC199	60.2	1.5	2973	74.1
MC200	55.9	1.6	813	21.8
MC201	65.8	1.3	1806	41.2
MC202	65.3	1.3	3593	82.5
MC203	68.6	1.3	1980	43.3
MC204	55.9	1.3	2033	54.6

Catalyst: 30 mg; co-catalyst: 0.75 mmol; H_2: 1.7 mmol; Al/Zr: 1500 m.r.; time: 30'; temperature: 70°C.

The results indicate good activity but quite poor reproducibility. This is likely due to the high sensitivity of this catalyst; the poisoning level of our system is probably too high, and this sensibly affect the reproducibility.

Then we explored the effect of the amount of H_2 loaded into the reactor. In the following tables the results reported regard two series of experiments with lower (1 mmol) and higher (4.3 mmol) amounts of H_2, respectively.

The main results are reported in the following tables:

Table 3.22 Experimental data at lowest hydrogen level with Catalyst **A**

	C_3	TEAL/C_3	Activity	Conversion
	g	g/kg	g/g/h	wt %
MC206	55.4	1.6	1580	42.8
MC207	69.7	1.3	2987	64.3
MC208	62.4	1.4	2367	56.9
MC209	50.5	1.7	1180	35.0

Catalyst: 30 mg; co-catalyst: 0.75 mmol; H_2: 1 mmol; Al/Zr: 1500 m.r.; time: 30'; temperature: 70°C.

No noticeable effect of hydrogen concentration has been detected (Tab. 3.23); the maximum in activity has been obtained by using 1.7 mmol of hydrogen but it is slightly higher than the activity obtained by adding greater amount of hydrogen; probably, it was not been possible to appreciate the effect of hydrogen level because the lack of reproducibility; the activity mean value seems to be slightly higher with lower hydrogen level but the reproducibility is really poor and nothing can be assured.

Table 3.23 Experimental data at highest hydrogen level with Catalyst **A**

	C_3	TEAL/C_3	Activity	Conversion
	g	g/kg	g/g/h	wt %
MC210	72.4	1.2	1593	33.0
MC211/a	75.8	1.2	1447	28.6
MC217	76.4	1.1	1013	19.9
MC239	66.7	1.3	2480	55.8

Catalyst: 30 mg; co-catalyst: 0.75 mmol; H_2: 4.3 mmol; Al/Zr: 1500 m.r.; time: 30'; temperature: 70°C.

Finally, we tested the influence of different co-catalyst on the activities. We used **TIBAL** instead of **TEAL**, and in the following table the results obtained are shown.

Table 3.24 Effect of different co-catalyst type with Catalyst **A**

	C_3	TIBAL/C_3	Activity	Conversion
	g	g/kg	g/g/h	wt %
MC214	**72.4**	1.1	8067	83.6
MC215	**63.5**	1.2	4893	57.8
MC216	**65.2**	1.2	5520	63.5

Catalyst: 15 mg; co-catalyst: 0.65 mmol; H_2: 4.3 mmol; Al/Zr: 1500 m.r.; time: 30'; temperature: 70°C

A noticeable increase in activity has been observed; as observed with catalyst **B**, TIBAL is a better co-catalyst in our experimental conditions.

A selection of the homopolymers obtained were analyzed by ^{13}C-NMR at pentad level to determine the microstructure and by SEC to determine the molar masses and molar mass distributions. In the following table a mean value of the ^{13}C-NMR results is shown:

mmmm **(%)**	***mmrr*** **(%)**	***mmmr*** **(%)**	***mrrm*** **(%)**
96.5	1.8	1.7	n/a

Regarding the M_w, also with **A** catalyst, the M_w and the molar mass distributions strongly depend on monomer conversion; because of that the most significant results are chosen from polymers with the lowest conversion and the lowest molar mass distributions.

The average M_w and D are:

H_2 level: 1 mmol: M_w 346.4 +/- 110.0 kg/mol;
D: 3.76 +/- 0.35;
H_2 level: 1.7 mmol: M_w 402.9 +/- 79.0 kg/mol;
D: 4.48 +/- 0.33;
H_2 level: 4.3 mmol: M_w 301.4 +/- 25.2 kg/mol;
D: 3.73 +/- 0.29;

Probably, the lower M_w value at H_2 level of 1 mmol is not significant because of the lower reproducibility of those experiments.

In the following figures, the relationship between M_w and monomer conversion has been reported:

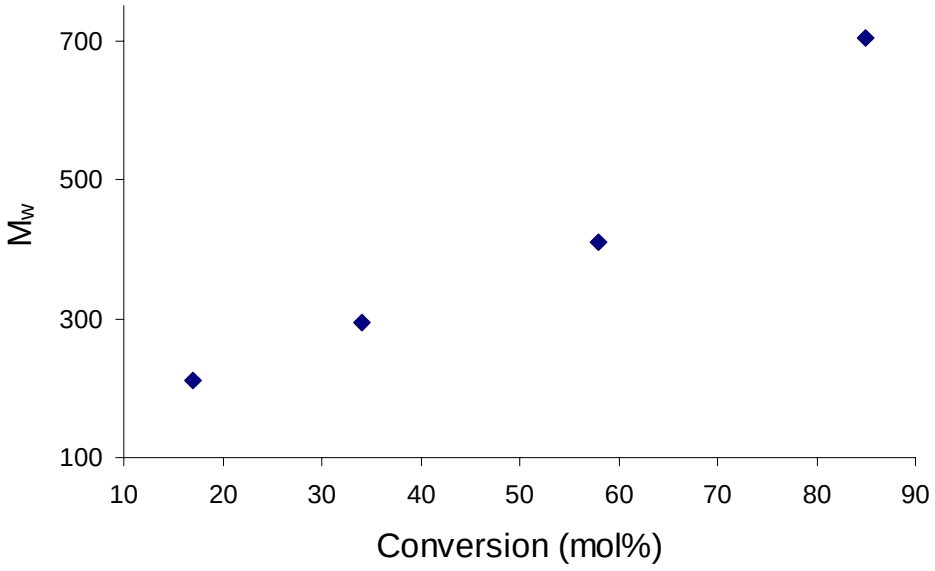

Figure 3.13 Molecular weights dependence by monomer conversion. H_2 level: 1 mmol

Also with catalyst a linear relationship between the M_ws and the monomer conversion is observed, with this catalyst we denote an opposite relationship with respect to catalyst **B**: the higher the conversion, the higher the M_ws. This phenomenon could be related to the high activity of the system and to the consequent hydrogen consumption.

An analogous relationship can be observed also with molar mass distributions:

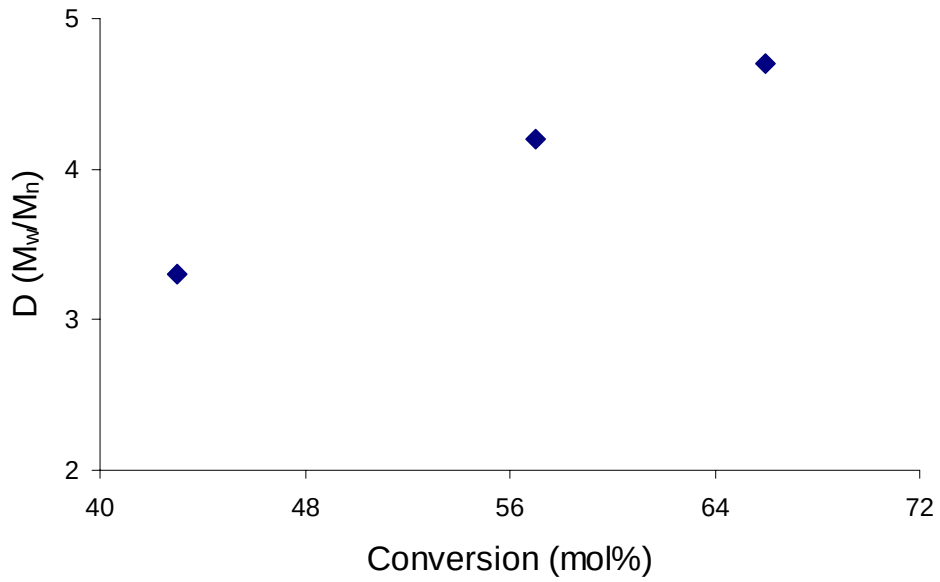

Figure 3.14 Molecular weight distributions dependence by monomer conversion: H_2 level: 1 mmol.

In conclusion, taking a carefully look at the activities we note that the catalyst **A** is the most active, especially with 1.7 mmol of hydrogen, followed by the catalyst **B** (higher activity with 1 mmol H_2 level but a slightly less reproducible). The lowest activities have been obtained with catalyst **C**. Such results are summarized in the following graphs.

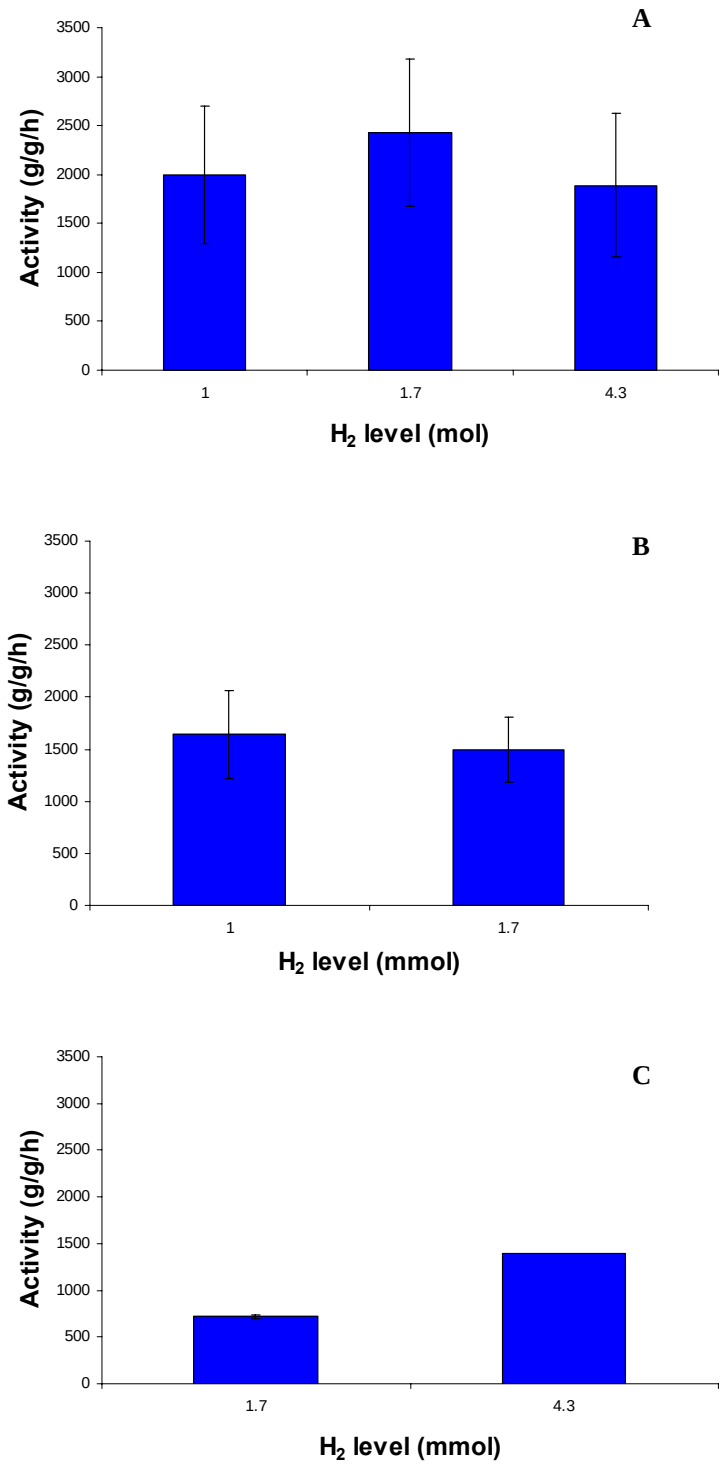

Figure 3.15 Activities dependence by the H_2 level for the three supported metallocenes named **A**, **B** and **C.**

As to results from ^{13}C-NMR characterization, we note that catalyst **A** and **B** give a most isotactic polypropene (slightly high mmmm percentage with catalyst **B**). The catalyst **C** gives the lowest percentage of isotactic pentad and the highest percentage of the stereoerrors (*mmrr, mmmr* and *mrrm*).

Regarding the molecular weight, **B** catalyst gives polypropene with the highest M_w but a quite broad molar mass distribution (***M*$_w$ = 430 Kg/mol, D = 3.36**), catalyst **A** also gives quite high molecular weight (**403 Kg/mol**) but very broad molar mass distribution (**4.48**), finally catalyst **C** gives the lowest molecular weight (**316 kg/mol**) and the narrowest molar mass distribution (**2.32**)

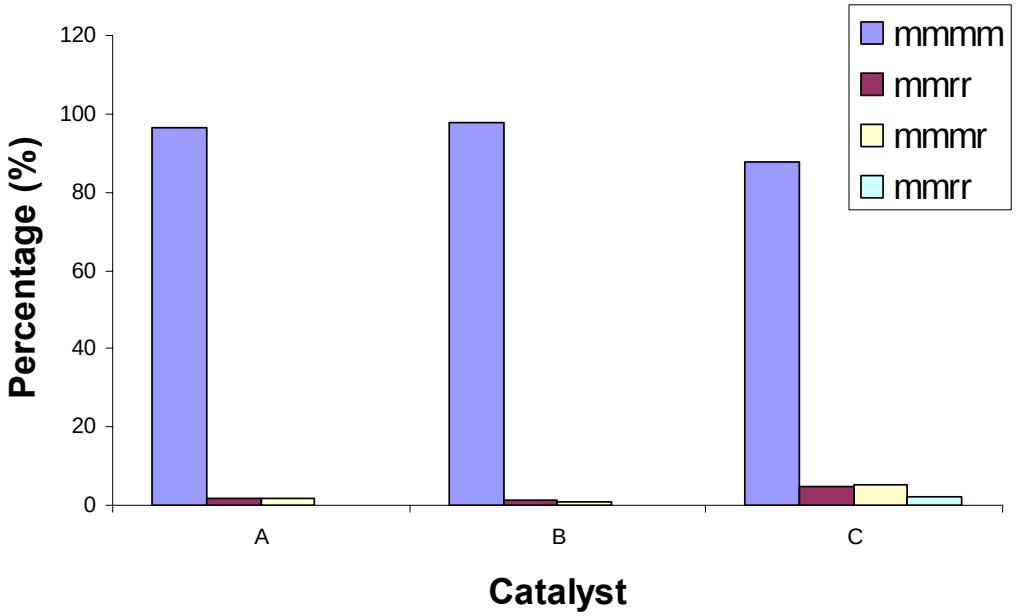

Figure 3.16 Mean pentad distribution for polypropylenes obtained with the three supported metallocenes, named **A**, **B** and **C**, calculated by ^{13}C-NMR.

3.2 Propene-Ethene copolymerization

The development of well-defined homogeneous metallocene catalysts for olefin polymerization has created new opportunities for the synthesis of olefin copolymers with uniform compositions and random sequence distributions and with tailored microstructures and properties. The copolymerization of propene with ethene is a

common way of tailoring the density and crystallinity of ethene polymers. It is known that by adding low amount, ranging between 1 and 5 mol %, of ethene it is possible to obtain a material that is more elastic than sPP homopolymer, and simultaneously allows the control of the crystallization process. These copolymers form a new class of thermoplastic elastomers with lower melting points, lower glass transition temperatures and higher impact strength than sPP homopolymers.

One of the most important characteristics of these copolymers is the molecular weight. Thus, much emphasis has been given to molecular weight control, which is influenced by the catalyst structure, for accessing the practical production of polymeric materials. Indeed, both for C_s-symmetric and C_2-symmetric catalysts it was found that the M_w of ethene-propene copolymers are in general lower than those of propene homopolymers. Brintzinger and Spaleck[17] reported some exceptions in the case of the C_2-symmetric catalysts, by introducing 2-methyl and benzo substituents on silylene bridged bis(indenyl) zirconocenes which give isotactic PP have developed a catalyst which gives rise to a substantial increase in molecular weight of copolymers compared to that of homopolymers.

C_1-symmetric catalysts also afford only low molecular weight copolymers although they lead to high molecular weight homopolymers. This is a serious drawback for the use of single-site catalysts in olefin polymerization.

C_1-symmetric catalysts with a relatively small group allows one to obtain hemi-isotactic PP. These systems are amenable to study fine details of the polymerization mechanism. However, if the group used to introduce C_1 symmetry is large enough isotactic PP is obtained, which is of great interest from a practical point of view since the isotactic polymers synthesized by C_2-symmetric indenyl based catalysts often produce small undesirable fractions of atactic polymers[18]. In the presence of ethene as comonomer, the C_1-symmetric catalysts can produce an alternating isotactic P-E copolymer, according to Waymouth[19] an alternating site mechanism that is the ethene monomer inserts at less stereoselective site and the propene monomer inserts at more stereoselective site.

The objective of this work was to identify among the C_1 symmetric catalysts (Figure 3.11) those most promising for obtaining copolymers with high molar masses, as well as to give a rationale to such possibility.

Finally, the industrial synthesis of homo- and copolymers by homogeneous catalysts has to be achieved by supported systems in liquid propene because homogeneous processes present serious drawbacks such as the fouling as well as morphological issues. Thus, we have made efforts to study the variables that need to controlled in order to produce in the laboratory reproducible copolymers with highly active supported catalysts.

3.2.1 Propene-Ethene copolymerization by homogenous metallocene based catalysts

The six metallocene precursors shown in Figure 3.17 were activated with MAO and tested in homogeneous copolymerisation reactions of propene with low amount of ethene (in autoclave about 30 g of propene, Al/Zr molar ratio of 3000 in a total 150 mL of toluene, at temperature of 50 °C); the experimental conditions and the catalyst activities are reported in Table 3.24.

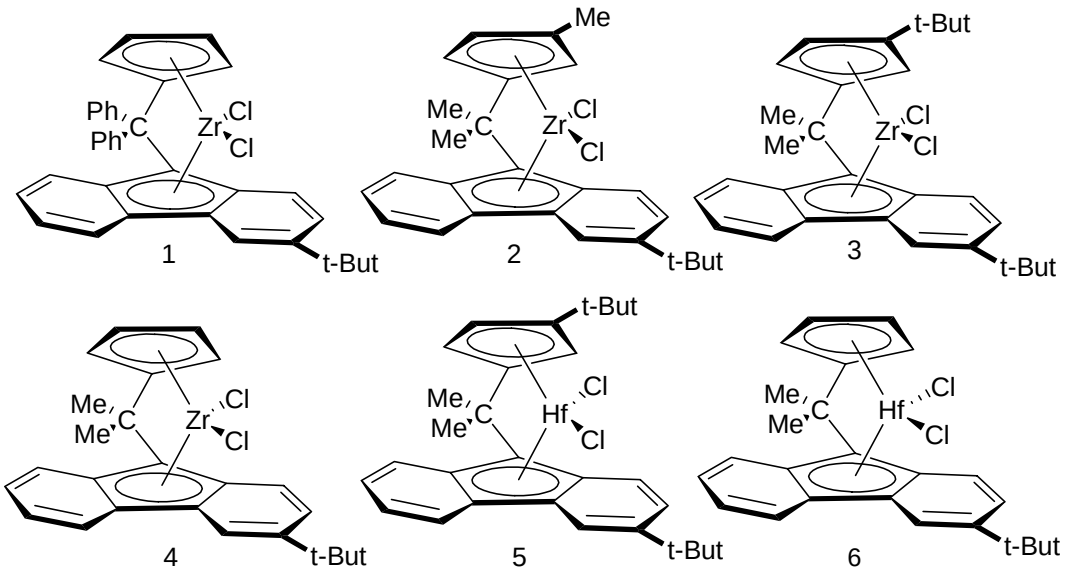

Figure 3.17 Metallocene precursors used in propene-ethene copolymerizations

The catalysts activities in the copolymerisation reactions are much higher than the activities in the homopolymerization reactions (see Table 3.3); this phenomenon so called comonomer effect has been often observed and has been object of numerous studies. One of the most plausible explanations is the possibility that ethene molecule being smaller than propene one, inserts more easily in a dormant site, after a regioerror.

Table 3.25 Copolymerization activity for the six catalysts used under autoclave conditions

Catalyst Type	Activity ç $Kg_{P\text{-}E}/mol_M*h*P$	E content mol %
1	1308	8.23
2	440	16.76
3	709	15.95
4	1146	5.98
5	n/a	n/a
6	95	2.60

Temperature = 50°C; Solvent = 150 ml Toluene; Al/Zr= 3000 m.r.; Catalyst = 10μmol; Propene ~ 30g; 5 bar < P < 7 bar (depending on propene loaded in the reactor); 1% < Ethene < 2% (mol % in feed)

By comparing the results of Table 3.25 to those of Table 3.3 referring to homopolymerization, we can realize a great increase in activity mainly for the **2** and **3** catalysts. In addition, it is worth noting the great amount of ethene content in copolymer; this fact seems to confirm the assumption that ethene molecule could insert faster in a dormant site, reactivating the polymerization.

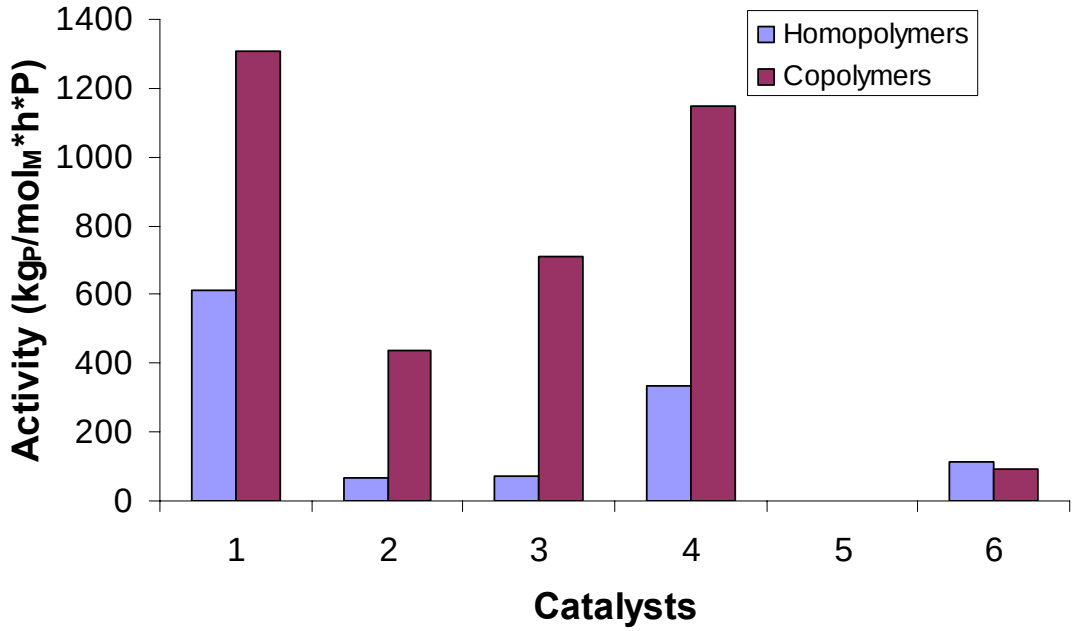

Figure 3.18 Comparison among the activities in homo and **c**opolymerization reactions for the six catalysts used under autoclave conditions

All the copolymers have been characterized by size exclusion chromatography to determine the molar masses and molar mass distributions. The SEC results are reported in the table below.

Table 3.26 Molecular masses and molecular mass distributions of the propene-ethene copolymers obtained by using the six C_1-symmetric catalysts

Catalyst	M_w	D
Type	Kg/mol	M_w/M_n
1	282	2.23
2	147	3.77
3	119	2.54
4	152	2.00
5	n/a	n/a
6	585	2.37

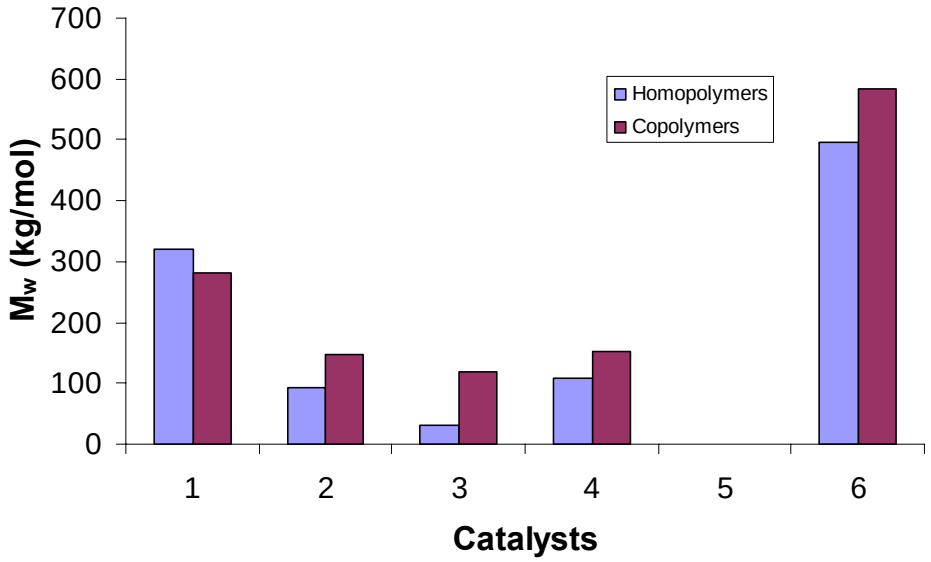

Figure 3.19 Comparison among the molecular weight of homo and copolymers obtained by using the six C_1-symmetric catalysts

The trend in molecular weight results to be the same of the homopolymerization reactions: in fact, the Hf-based metallocene leads to the highest M_w, the diphenyl bridged catalyst **1** confirms to be the metallocene with the best performance characteristics. Among the isopropyl-bridged metallocenes no significant differences in molecular weight have been revealed, except for the t-butyl Cp substituted catalyst **3** that leads to a strong increase of molar mass with respect to the corresponding homopolymer.

After this preliminary screening in copolymerization reaction, we focused our attention to investigate deeply the catalytic performance of the three most promising catalysts in various experimental conditions. So propene-ethene copolymerizations were conducted under slurry experimental conditions at three different temperatures (30, 50, and 70°C) by using the zirconocenes **1**, **3** and **4**.

The experimental conditions and the activity results are shown in Table 3.27.

The catalyst activities in the copolymerisation reactions are much higher than the activities in the homopolymerization reactions. The increase in activity could be explained by the small size of ethene which could coordinate easily to the metal centre and could reactivate the dormant sites.

Table 3.27 Copolymerization activities and ethene content for the copolymers obtained under autoclave conditions.

Catalsts	T	Pressure	E content in feed	Copolymer E content	Activity
Type	**°C**	**bar**	**mol %**	**mol %**	**$kg_{P\text{-}E}/mol_{Zr}$*h*P**
1	30	9.0	1.0	13.1	2253
1	50	12.6	1.0	8.8	2619
1	70	17.2	1.0	4,3	1426
3	30	8.1	0.5	11.4	969
3	30	9.0	1.0	12.0	1070
3	50	12.2	0.5	20.5	685
3	50	12.5	1.0	33.4	880
3	70	16.2	0.5	31.0	391
3	70	18.3	1.0	27.6	335
3	70	18.7	2.0	33.9	368
4	30	8.9	1.0	16.4	1321
4	50	12.6	1.0	18.6	955
4	70	17.6	1.0	27.7	850

The trend of the activities (Figure 3.20) in copolymerization reactions is the same of the homopolymerizations: catalyst **1** is the most active and catalyst **3** the least active one; due to the presence of phenyl groups on the bridge of **1** and to bulky *t*-butyl group on Cp side in **3**. Moreover, the activities still are dependent on temperature, that is, decrease with increasing in temperature.

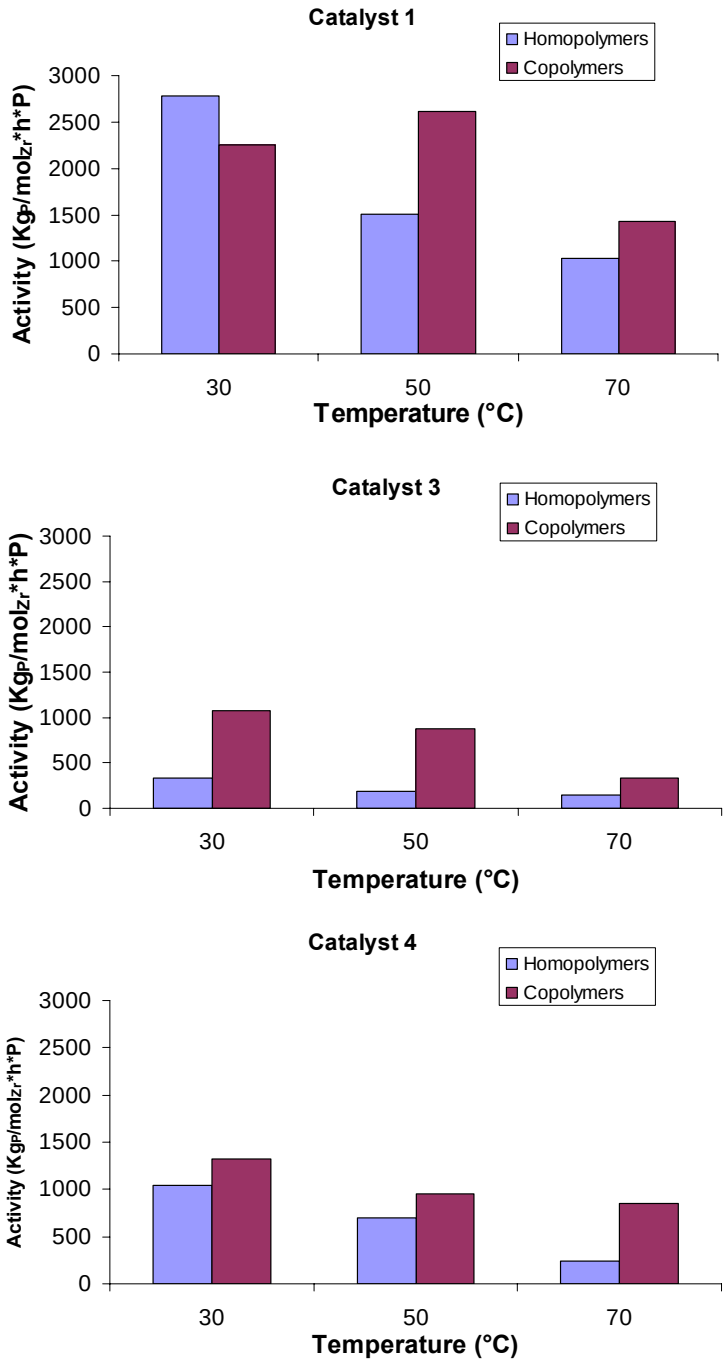

Figure 3.20 Comparison among the homo and copolymerization activities by using the three most promising catalysts.

The influence of ethene on the activity is confirmed for catalyst **3** (see Figure. 3.21): higher is the amount of ethene in feed higher is the activity.

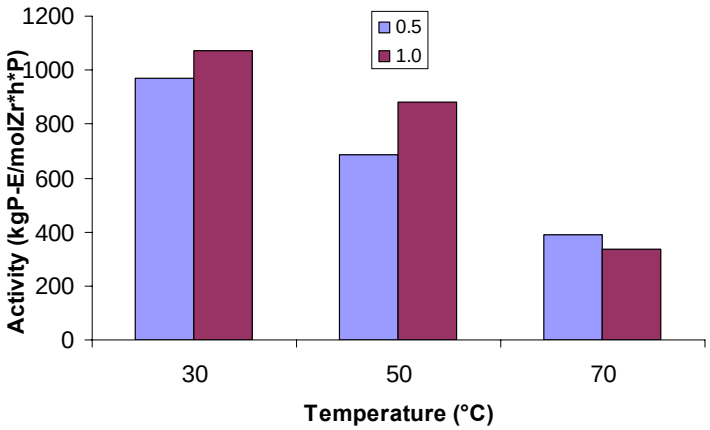

Figure. 3.21 Dependence of activity on ethene concentration in feed for the copolymers obtained by using catalyst **3**.

3.2.2 Propene-Ethene composition

The copolymers have been characterized by ^{13}C-NMR to determine the ethene content. The reactivity of the three catalysts versus the ethene monomer is very different; the monomer conversion, the ethene content in the copolymers, and the triad analysis are reported in Table 3.28

The syndiospecific catalyst **1** shows a quite low preference for the comonomer and the ethene percentage in the copolymers does not seem to be dependent on the polymerization temperature. It seems that there is a correlation between the ethene percentage in the copolymer and activity (Table 3.28): the higher the ethene the higher the activity. This supports the interpretation that the positive effect of ethene on activity is related to the insertion after 2,1 inserted propene units (dormant species).

Table 3.28 ^{13}C-NMR analysis of the copolymers obtained by using the most promising catalysts: **1**, **3** and **4**

Catalyst	T	Ethene in feed	Monomer conversion	Ethene Copolymer	PPP	PPE	EPE	PEP	PEE	EEE
Type	°C	mol %	$g_{polymer}/g_{C3}$	mol %	mol %	mol %	mol %	mol %	mol %	mol %
1	30	1.0	23.3	7,4	86.6	2.4	3.6	6.4	0.7	0.2
1	50	1.0	72.3	8,9	81.2	2.3	3.4	11.0	1.8	0.3
1	70	1.0	64.4	4,5	94.8	n/a	1.0	3.1	0.9	0.2
3	30	0.5	17.4	10.6	75.4	11.1	2.1	8.3	2.6	0.6
3	30	1.0	21.9	14.0	54.2	2.6	31.2	8.3	3.1	0.6
3	50	0.5	24.9	17.9	65.7	9.8	4.1	12.4	6.7	1.3
3	50	1.0	30.9	31.6	37.4	21.1	8.1	13.2	14.4	5.8
3	70	0.5	35.9	24.7	41.4	20.1	7.5	11.8	13.5	5.7
3	70	1.0	29.1	27.6	42.7	23.6	6.1	11.4	11.9	4.3
3	70	2.0	33.4	33.3	31.5	26.4	8.1	11.1	15.6	7.3
4	30	1.0	20.7	17.4	59.1	18.7	5.8	13.3	2.7	0.4
4	50	1.0	27.6	18.6	55.4	19.1	6.8	14.3	3.5	0.9
4	70	1.0	33.3	27.7	41.5	22.0	8.8	14.7	8.7	4.3

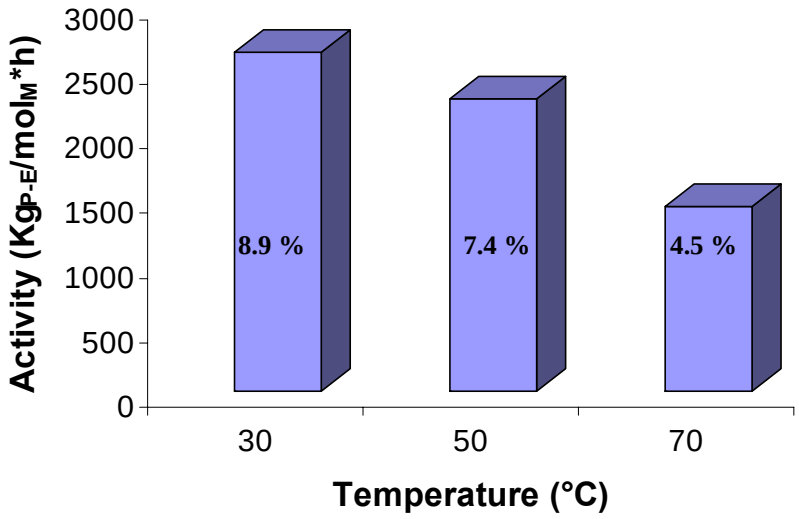

Figure 3.22 Activity versus temperature and ethene percentage for catalyst **1**

Catalyst **4** shows a preference for ethene monomer higher than the analogous syndiospecific catalyst **1**. The ethene percentage in the copolymers is strongly dependent on the polymerization temperature, that is the higher the temperature the higher the ethene percentage.

The isospecific catalyst **3** shows a very high preference for ethene monomer, in fact the ethene incorporation is much higher than the initial feed molar ratio. Moreover a relation between ethene content in copolymers and temperature has been observed (Figure 3.23): the higher the temperature the higher the ethene incorporation

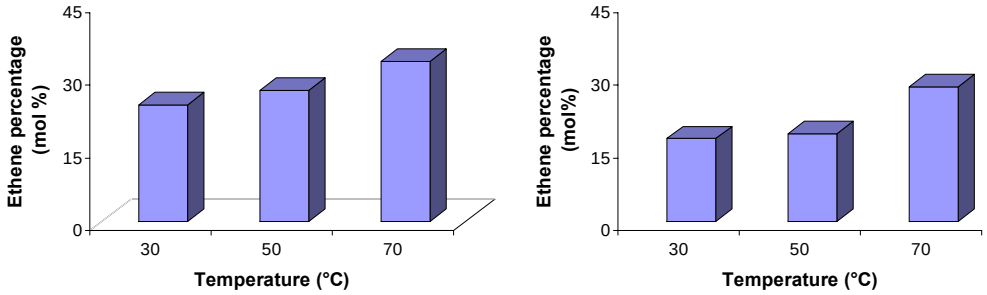

Figure 3.23. Ethene content versus temperature for catalyst **3** (left) and **4** (right)

3.2.3 Propene-Ethene copolymerization by supported metallocenes

The industrial synthesis of propene-based copolymers has to be achieved by supported systems in liquid monomer, because homogeneous catalysis presents drastic drawbacks such as morphological properties of the materials obtained that results difficult to process to reach the final use. Consequently, after the preliminary screening of the three supported metallocenes in homopolymerization reactions, they have been tested in propene-ethene copolymerization reactions.

Catalyst A: concentration in mineral oil: 20% wt; Zr content: 0.15% wt;

Catalyst B: concentration in mineral oil: 20% wt; Zr content: 0.15% wt;

Catalyst C: concentration in mineral oil: 10.6% wt; Zr content: 0.4% wt.

The copolymerizations were conducted in liquid propene under the same operative conditions used in homopolymerization reactions; the ethene comonomer was added in gaseous phase, as overpressure by using a mass flow to supply the consumption of monomer and a pressure controller to keep the overall pressure

constant during the polymerization time. The catalyst is added after equilibration of comonomer mixture.

Catalyst C:

We started with **C** catalyst following the best experimental conditions used in homopolymerization reactions listed in the following table:

Table 3.29 Copolymerization conditions

Catalyst C	**microL**	200
Catalyst	**mg**	18,7
Co-Catalyst	**mmol**	0,48
H_2	**mmol**	4,3
Temperature	**°C**	70

We performed 2 runs by using an ethene overpressure of 1 and 0.5 bar, respectively, but no yield was obtained in both the tests.

We decided to perform a few ethene homopolymerization tests, in order to evaluate the purity of ethene, and the goodness of our purification system. Results are shown in Table 3.30.

Table 3.30 Ethene homopolymerization results with catalyst **C**

	Co-Catalyst	**C_2 Pressure**	**Activity**
	mmol	**bar**	**g/g/h**
MC219	0.24	20	2310
MC220	0.24	40	1369
MC225	0.24	35	2888

Catalyst: 18.7 mg; solvent: toluene: 100 ml; Al/Zr: 300 m.r.; H_2: 4.3mmol; time: 30' (MC225; *t*: 10'); temperature: 70°C

We went on with propene-ethene copolymerization tests in liquid propene; in the following runs at low ethene concentration in feed, in order to avoid the occlusion of injection system, the catalyst was injected at 40 °C since the catalytic system is quite inactive at low temperature.

Table 3.31 Propene-ethene copolymerization results with catalyst **C**

	C_3	**TEAL/C_3**	**C_2 in feed**	**Activity**
	g	**g/kg**	**Nl/L_{C3}**	**g/g/h**
MC223	61.5	0.9	1.0	no
MC224	72.2	0.8	0.8	no

Catalyst: 18.7 mg; co-catalyst: 0.48 mmol; Al/Zr: 300 m.r.; H_2: 4.3mmol; time: 30'; temperature: 70°C

Because no yield was obtained even in this case, we decided to test the system by using a homogeneous metallocene as a reference catalyst.

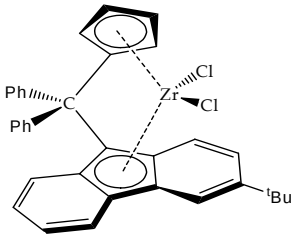

Conditions:

Solvent: 100 ml of toluene; Cat: 10μmol; Co-cat: MAO; Al/Zr: 3000 m.r.

Propene: 30 g; Ethene: 0.5 % in feed.

Previous result: Activity: 965 $Kg_{P\text{-}E}/mol_{Zr}$•h•P

Current result: Activity: 969 $Kg_{P\text{-}E}/mol_{Zr}$•h•P

Under the same experimental conditions we obtained yields very comparable with our previous results.

Because no problem concerning the ethene purity was revealed, we turn on again with **C** supported catalyst, repeating the runs MC225 and MC224 of Table 3.30 and 3.31.

Table 3.32 Copolymerization results with catalyst **C**

	C_3	TEAL/C_3	C_2 in feed	Activity
	g	g/kg	Nl/l_{C3}	g/g/h
MC226	67.1	0.8	0.9	96
MC227	62.6	0.9	1.0	21

Catalyst: 18.7 mg; co-catalyst: 0.48 mmol; Al/Zr: 300 m.r.; H_2: 4.3mmol; time: 30'; temperature: 70°C

Also in this case we obtained very low yield.

After that we tried a single run without adding H_2 and a set of copolymerization reactions reducing the amount of ethene in feed:

Table 3.33 Copolymerization results with catalyst **C**: effect of H_2 concentration and ethene concentration in feed.

	C_3	C_2 in feed	Activity
	g	Nl/l_{C3}	g/g/h
MC228	**63.7**	0.9	588
MC229	**73.5**	0.4	86
MC230	**61.0**	0.5	91
MC231	**62.5**	0.5	128

Catalyst: 18.7 mg; co-catalyst: 0.48 mmol; Al/Zr: 300 m.r.; TEAL/C_3: 0.9 g/kg; H_2: 4.3mmol (MC228: no H_2); time: 30'; temperature: 70°C

Reducing the amount of H_2 in feed slightly increases the yield; this could probably due to the insertion of hydrogen molecule in a dormant site, reactivating the polymerization. Indeed, changing the amount of ethene does not really influences the activities.

At last we tried a single run using **TIBAL** instead of **TEAL** as co-catalyst, because in homopolymerization reactions better results in terms of activity were obtained.

Table 3.34 Effect of TIBAL on copolymerization activity with catalyst **C**

	C_3	TIBAL/C_3	C_2 in feed	Activity
	g	g/kg	Nl/l_{C3}	g/g/h
MC266	66.3	2.0	0.7	182

Catalyst: 18.7 mg; co-catalyst: 0.67 mmol; Al/Zr: 830 m.r.; H_2: 2.2 mmol; time: 30'; temperature: 70°C

However, as visible in Table 3.34, this change does not give the expected results; in the copolymerization reaction the effect of TIBAL on activities was not revealed and the yield obtained was not much higher than the previous runs.

Catalyst A:

Initially, the copolymerization reactions with catalyst **A** were performed following the experimental conditions used in homopolymerization tests.

Table 3.35 Copolymerization experimental conditions

Catalyst A	**mg**	30
Co-Catalyst	**mmol**	0,75
H_2	**mmol**	1,7
TEAL/C_3	**g/kg**	1,3
C_2 in feed	**Nl/l_{C3}**	1.9
Al/Zr	**m.r.**	1500
Polym t	**min**	60
Polym T	**°C**	70

By using the H_2 level of 1.7 mmol a very low activity was obtained, so the effect of H_2 on copolymerization activities was evaluated:

Table 3.36 Effect of H_2 concentration on P-E copolymerization activities with catalyst **A**

	C_3	H_2	H_2/C_3	C_2 in feed	Activity
	g	mmol	Nl/l_{C3}	Nl/l_{C3}	g/g/h
MC233	67.6	0	0	0.4	727
MC238	65.2	1.1	0.2	0.5	117
MC240	67.5	1.1	0.2	0.5	117
MC232	65.6	2.2	0.4	0.5	367
MC237	64.0	2.2	0.4	0.5	807
MC234	65.2	4.3	0.8	0.5	90
MC235	61.2	4.3	0.8	0.4	187
MC236	64.9	4.3	0.8	0.5	173

Catalyst: 30 mg; co-catalyst: 0.75 mmol; Al/Zr: 1500 m.r.;TEAL/C_3: 1.4 Nl/L_{C3}; time: 30'; temperature: 70°C

Apparently the best activity was observed with hydrogen amount of 2.2 mmol. Indeed, best yields were obtained either with no hydrogen or at 2.2 mmol. The differences in the yields could be probably due to the low reproducibility of the polymerization system.

Anyway, we decided to focus our attention on the hydrogen amount of 2.2 mmol, and we evaluated the effect of ethene concentration in feed on activities.

Table 3.37 Effect of ethene percentage in feed on copolymerization activities with catalyst **A**

	C_3	TEAL/C_3	C_2 in feed	Activity
	g	g/kg	Nl/l_{C3}	g/g/h
MC241	**63.2**	1.4	0.6	53
MC242	**63.7**	1.4	0.5	243
MC245	**67.3**	1.3	0.3	353
MC243	**74.1**	1.2	0.2	637
MC244	**74.2**	1.2	0.2	840

Catalyst: 30 mg; co-catalyst: 0.75 mmol; Al/Zr: 1500 m.r.;H_2: 2.2 mmol; time: 30'; temperature: 70°C

With this catalyst, it seems that the activity is dependent on comonomer concentration; that is the higher the concentration the lower the activity. (see Figure 3.24).

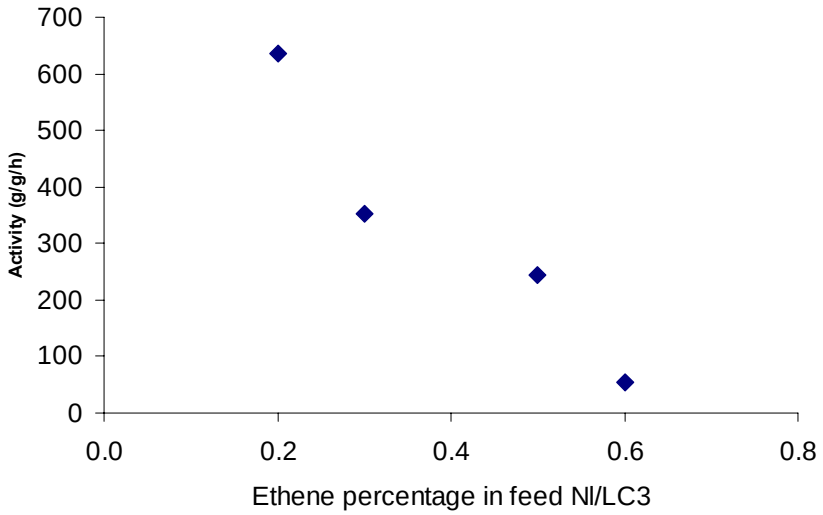

Figure 3.24 Linear dependence of activities by ethene level

Although a linear relationship between the C_2 level and the activities has been observed, the copolymerization activities result to be quite low. So we decided to evaluate the influence of different Al/Zr molar ratios on the copolymerization activities in order to find conditions suitable for obtaining more reproducible results.

Table 3.38 Effect of Al/Zr m.r. on P-E copolymerization activities

	C_3	Co-Catalyst	TEAL/C_3	Al/Zr	Polym time	Activity
	g	mmol	g/kg	m.r.	min	g/g/h
MC247	68.0	0.58	1.0	1000	60	920
MC248	71.2	0.58	1.0	1000	30	373
MC249	69.2	1.3	2.2	2500	60	1043
MC250	69.4	1.3	2.2	2500	30	760

Catalyst: 30 mg; H_2: 2.2 mmol; C_2 in feed: 0.3 Nl/L_{C3}; temperature: 70°C

It seems that by increasing the Al/Zr ratio there is an increase in activity. This could be due to the presence of poisoning agents in our polymerization system; by increasing the concentration of co-catalyst, acting as scavenger, as well as alkylating agent, the amount of poisoning molecules is reduced. Moreover, even if slightly better results have been obtained, we surprising found that the activities increase by increasing the polymerization time (***t***).

After that, we evaluated the effect of a different co-catalyst on activities; we used **TIBAL** instead of **TEAL**, because we obtained better results in homopolymerization reactions.

Table 3.39 Effect of different Al/Zr m.r. and ethene percentage in feed on copolymerization activities with catalyst **A**

	Catalyst	Co-Catalyst	C_3	TIBAL/C_3	C_2 in feed	Al/Zr	Activity	Yield
	mg	mmol	g	g/kg	Nl/l_{C3}	m.r.	g/g/h	g
MC251	30	1.3	69.9	3.7	0.3	2500	2950	88.8
MC252	30	1.3	71.4	3.6	0.2	2500	4440	66.6
MC253	15	0.65	69.1	1.9	0.3	2500	9053	67.9
MC258	15	0.65	66.7	1.9	0.8	2500	2640	19.8
MC256	15	0.65	64.1	2.0	1.3	2500	2000	15.0
MC257	15	0.65	70.5	1.8	1.6	2500	1107	8.3
MC259	15	0.65	71.3	1.8	1.5	2500	1107	8.3
MC255	15	0.51	70.3	1.4	1.2	2000	1107	8.3
MC254	15	0.38	64.5	1.2	0.2	1500	853	6.4

H_2: 2.2 mmol; time: 30' (MC251: *t*: 60') temperature: 70°C

We performed several runs changing the Al(**TIBAL**)/Zr m.r. and the amount of comonomer in feed; as it is inferred from Table 3.34, the best activities have been obtained using Al/Zr = 2500 m.r., but as observed also in the previous results, the activities decrease by increasing the amount of ethene. This may be due either to an effect of the comonomer or to some impurity in C_2, not scavenged by the TIBAL.

It has to be noted, that, due to the extremely high yields obtained, the propene concentration in the system, at the end of the reaction, was close to zero, so the MC251 and MC253 run activities are not comparable.

Activity of run MC253 was very high, thus it was decided to replicate it in order to confirm the activity by using a lower amount of catalyst (Table 3.40):

Table 3.40 Evaluation of copolymerization activity reproducibility with catalyst **A**

	C_3	C_2 in feed	Activity
	g	Nl/l_{C3}	g/g/h
MC268	56.0	1.7	7820
MC269	57.8	0.4	11300
MC270	61.0	0.4	8180

Catalyst: 10 mg; co-catalyst: 0.43 mmol; TIBAL/C_3: 1.4g/kg; Al/Zr:2500 m.r.; H_2: 2.2 mmol; time: 30';temperature: 70°C

The activities are confirmed to be very high, the lower reproducibility probably depends on the lower amount of catalyst, which becomes close to our level of poisoning components in our system.

Some of the copolymers synthesized were analyzed by ^{13}C-NMR and by size exclusion chromatography to determine the ethene percentage and the molar masses and molar mass distribution, respectively (Table 3.41).

Looking at ethene percentage in copolymers we could see that the amount of comonomer incorporated into the copolymers increase with the conversion: higher the conversion higher the amount of ethene; this seems due to the increasing in the C_2/C_3 ratio during the reaction; higher the consumption of propene higher the C_2/C_3 ratio.

An exception is the **MC268** run: high conversion low C_2 percentage in copolymer; but this is probably due to the different procedure of copolymerization; in fact in **MC268** the ethene was injected in one shot, and not continuously added, and probably the amount of comonomer injected was too low.

Table 3.41 SEC and ^{13}C-NMR analysis of some of the copolymers synthesized

	Cat	Co-Cat	C_2^*	C_2^{**}	M_w	D	Conversion	C_3
	mg	mmol	Nl/L_{C3}	mol %	kg/mol	(M_w/M_n)	mol %	g
MC251	30	1.3	0.3	n/d	185	17.15	126.6	69.9
MC252	30	1.3	0.2	n/d	125	6.23	93.3	71.4
MC253	15	0.65	0.3	19.9	311	6.82	98.3	69.1
MC254	15	0.38	0.2	2.2	346	4.83	9.9	64.5
MC256	15	0.65	1.3	1.3	340	3.46	23.4	64.1
MC257	15	0.65	1.6	1.8	321	5.28	11.8	70.5
MC258	15	0.65	0.9	1.4	376	3.31	29.7	66.7
MC259	15	0.65	1.5	2.0	453	3.59	11.6	71.3
MC260	15	0.65	0.9	n/d	421	4.03	18.8	69.6
MC261	15	0.65	0.2	n/d	405	3.44	17.1	71.9
MC267	15	0.65	0.3	30.4	230	8.76	60.1	70.4
MC268	10	0.43	1.7	1.3	350	3.44	69.8	56.0
MC269	10	0.43	0.4	27.2	327	5.97	97.8	57.8
MC270	10	0.43	0.4	2.3	348	3.87	67.0	61.0
MC275	15	0.65	1.0	5.0	331	3.63	59.4	59.3
MC276	10	0.43	0.9	1.9	368	3.21	28.5	60.0
MC277	10	0.43	0.9	1.3	453	3.13	46.3	58.3
MC278	10	0.43	1.9	2.9	409	3.66	6.4	59.1
MC279	10	0.43	1.9	1.9	550	3.06	19.9	57.7
MC280	10	0.43	1.7	3.3	605	3.76	6.0	50.4
MC283	15	0.65	1.7	4.7			2.3	66.0
MC284	15	0.65	1.7	n/d			6.4	64.0
MC286	15	0.65	1.8	n/d			2.5	60.0

*C_2 molar percentage in feed; **C_2 amount in copolymer;

Regarding the molecular masses and the molecular mass distribution (**D**); as we can see, the D seems to be somehow related to the conversion: higher the conversion higher the D. However some exceptions are observed: i.e. **MC254**, **MC257** (low conversion high **D**); or **MC268**, **MC270** (high conversion low **D**).

Taking off the best results (low conversion, low **D**), the M_w seems to be:

$$M_w = 379{,}0 \pm 43{,}7 \text{ kg/mol}$$

$$D = 3{,}52 \pm 0{,}19$$

The molecular weight seems to be related to the amount of propene loaded into the reactor; in fact, the M_ws increase with the increasing of amount of propene loaded into the reactor. (Figure 3.25)

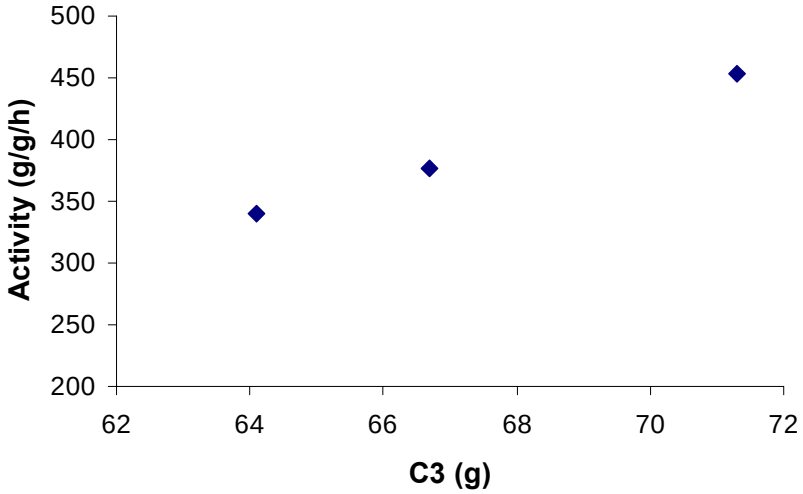

Figure 3.25 Linear dependence of M_w by propene loaded into the reactor

Summarizing, as we could see in Figure 3.26, the activity in copolymerization reactions under our homopolymerization best conditions are lower than the activity obtained in homopolymerization reactions. The best and highest activity in copolymerization reactions was obtained by using **TIBAL** as co-catalyst.

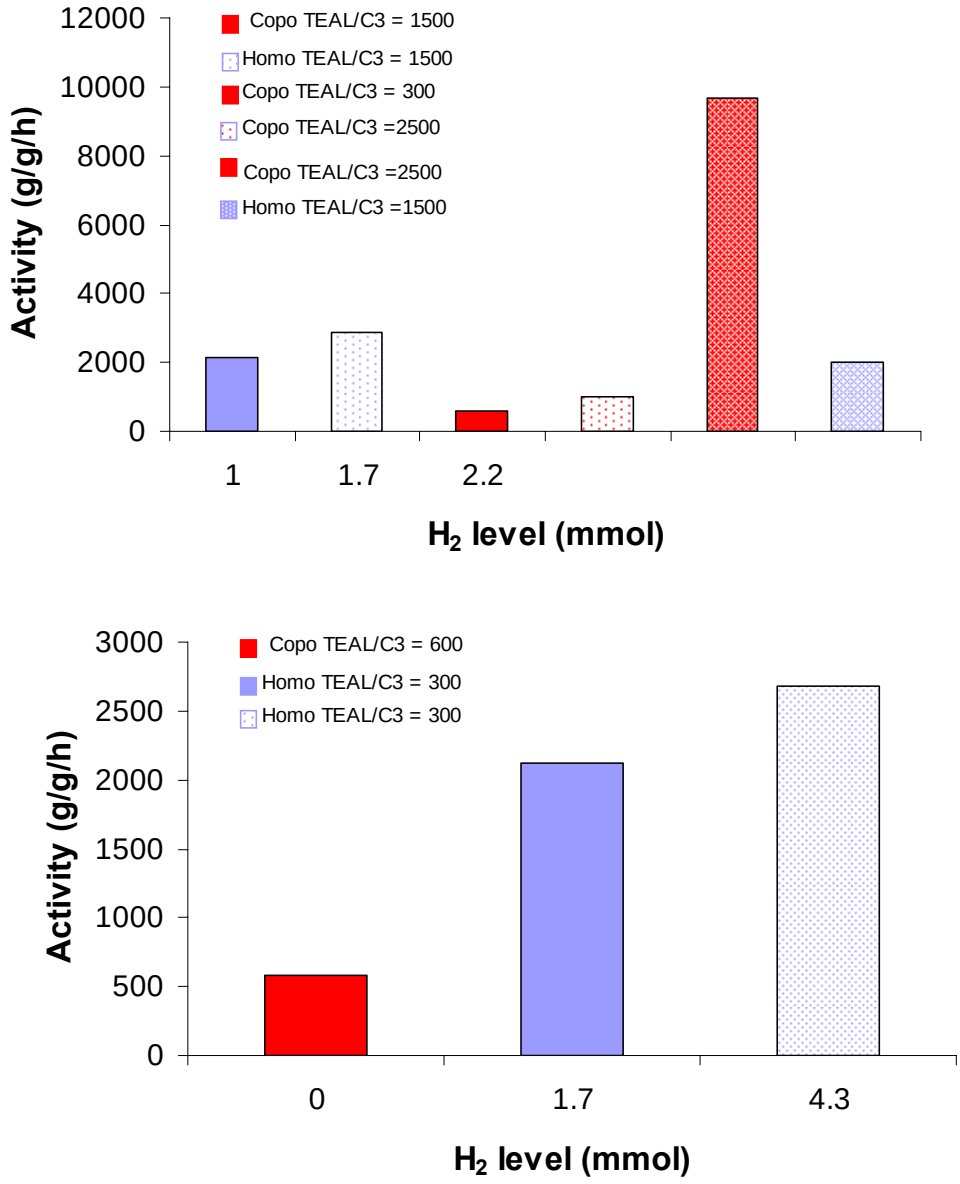

Figure 3.26 Comparison among homo and copolymerization reaction for the catalyst A (up) and C (down)

Regarding the exploration of these supported catalysts in propene-ethene copolymerization, we should conclude:

1. Under the best conditions found in homopolymerization reactions in the presence of TEAL, the copolymerization activities are lower and somehow depending on comonomer concentration (the higher the comonomer amount the lower the activity);

2. A strong effect of the aluminium alkyl has been observed: TIBAL gives much higher activity than TEAL (these studies were mainly performed with catalyst A).

These two factors, namely, the differences in activity due to the influence of E amount and of the type of aluminium alkyl, seem to suggest that the Mt-Et or the Mt-E bonds of these catalysts may be less stable than the Mt-*iso*-Bu or Mt-P bonds. We cannot exclude a further possible cause of the lower activity in propene/ethene copolymerization, that is, that these catalysts are much more sensitive to the impurities present in ethene than the other catalysts used so far.

Moreover, it appears that the control of the C_2/C_3 ratio during the copolymerization and of the conversion is quite important. Indeed, the amount of ethene incorporated in the copolymers has been shown to be dependent on conversion. Thus, to achieve the target E content of 1-5 mol %, we must control the yield in order to keep the monomer conversion not higher than 10-15%, otherwise, due to the high consumption of propene, the C_2/C_3 ratio increases during the reaction and consequently the amount of ethene in the final copolymer exceeds the desired value. High conversion in the copolymers synthesized using A catalyst and TIBAL as co-catalyst led to broad D.

In conclusion we believe that the use of TIBAL is fruitful for comparing the potential activities of different catalysts in homopolymerization. However, we have observed that such a high activity prevents the proper control of ethene incorporation and of molecular masses in propene-ethene copolymerizations. When the work is aimed to evaluating the potentialities of novel catalysts in propene-ethene copolymerization, less favourable polymerization conditions are advisable, that is, conditions under which the yields are lower (namely: lower amount of catalyst, less active co-catalyst, shorter polymerization time).

References

1 A. Razavi, J. L Atwood*; J. Organometallic Chem.,* **1993,** *459* 117.

2. (a) Angermund, K.; Fink, G.; Jensen, V. R.; Kleinschmidt, R. *Macromol. Rapid Commun*. **2000**, *21*, 91. (b)Farina, M.; Di Silvestro, G.; Sozzani, P. *Macromolecules* **1993,** *26*, 946

3 E. Kirillov, T. Roisnel, A. Razavi, J. F. Carpentier, *Organometallics*, **2009**, 28, 5036.

4 Miller, S. A.; Bercaw, J. E.. *Organometallics*, **2006**, *25*, 3576-3592.

5 K. J. Ivin, J. J. Rooney, Cecil D. Stewart, M. L. H. Green, R. Mahtab *J. Chem. Sot., Chem. Commun.,* **1978**, *14*, 604.

6. M. Brookhart, M. L. H. Green, L. L. Wong; *Prog. Inorg. Chem*., **1988,** *36,*

7. (a) P. L. Watson; *J. Am. Chem. Soc.,* **1982,** *104 337; (b)* L. Clawson, J. Soto, S. L. Buchwald, M. L. Steigerwald, R. H. Grubbs *J. Am. Chem. Soc.;* **1985,** *107* 3377.

8. W. E. Piers, J. E. Bercaw ; *J. Am. Chem. Soc.;* **1990,** *112,* 9406.

9. W. Röll, H. H. Brintzinger, B. Rieger, R. Zolk; *Angew. Chem., Int. Ed.,***1990,** *29*, 279.

10. W. Kaminsky*; Metalorganic Catalysts for Synthesis and Polymerization*, Springer Press, Heidelberg **1999,** 1-674..

11. J. A. Bercaw, S. A. Miller; *Organometallics*, **2006,** *25*, 3576.

12. S. Tomasi, A. Razavi, T.; Ziegler *Organometallics* **2009**, *28*, 2609–2618.

13. (a) A. Carvill, I .Tritto, P. Locatelli, M. C. Sacchi, *Macromolecules*, **1997,** *30*, 7056; (b) A. Carvill, L. Zetta, G. Zannoni, M. C. Sacchi; *Macromolecules*, **1998,** *31*, 3783.

14. L. Resconi J. Mol. Catal A: Chem. **1999**, *146*, 167.

15. N. Kawahara, S. Kojoh, Y. Toda, A. Mizuno, N Kashiwa; *Polymer*; **2004**, *45*, 355.

16. L. Resconi, I. Camerati, O. Sudmeijer *Topics in Catalysis***1999**, *7*, 145.

17. (a) W. Spalech, F. Kuber, A. Winter, J. Rohrmann, B. Bachmann, M. Antberg, V. Dolle, E. F. Paulus, *Organometallics*, **1994**, *13*, 954; (b) W. Spaleck, M. Antberg, J. Rohrmann, A. Winter, B. Bachmann, B. Krprof, J. Behm, A. W. Herrmann; *Angew. Chem*., **1992**, *104*, 1373; (c) W. Spaleck, M. Antberg, V. Dolle, R. Klein, J. Rohrmann, A. Winter, *New J. Chem.*, **1990**, *13*, 499; (d)U. Stehling, J. Diebold, R. Kirsten, W. Roll, H. H. Britzinger, S. Jungling, R. Mulhaupt, F. Langahuster, *Organometallics*, **1993**, *13*, 965.

18. E. Kirillov, T. Roisnel, A. Razavi, J. F. Carpentier, *Organometallics*, **2009**, 28, 5036.

19. W. Fan, R. M. Waymouth, *Macromolecules*, **2003**, *36*, 3010.

4. Results and Discussion of Norbornene-based Co- and Terpolymers

4.1 Norbornene-based copolymers

The discovery of metallocene catalysts has opened the possibility to synthesize cyclic olefin copolymers via addition polymerization without ring-opening methatesis (ROMP) in contrast with the behaviour of conventional heterogenous Ziegler-Natta catalysts. In ROMP polymerizations the opening of the unsaturated cycles of the monomers and the release of the ring strain constitute the driving force of the reaction. In the addition polymerization catalysis, the ring strain as well as the non-planarity of the reacting double bond strongly influences the reactivity. Cycloolefin homopolymers have high decomposition temperatures, small optical birefringence, good transparency for short wavelength radiation and high plasma etch resistance, and are suitable for application in microelettronic industry[1]. Such polymers can be obtained for example by metallocene catalysis, but are not processable due to their low solubility in the most common organic solvents.

Copolymerization with linear α-olefins allows to synthesize processable cyclic olefin copolymers (COC); in particular (E-*co*-N) copolymers were firstly synthesized by Kaminsky[2] with *ansa*-zirconocenes. Since then, both academic and industrial researchers have moved their research interests on COCs; TICONA and MITSUI have developed this copolymers to commercial products TOPAS[3] and APEL[4].

Within the family of COCs, ethene-norbornene (E-*co*-N) copolymers are the most studied ones; (E-*co*-N)s are amorphous materials with a wide range of glass transition temperatures, ranging from r.t. to 220 °C, depending on polymer composition, the higher the norbornene content, the higher is the percentage of norbornene diads and triads[5-7], and the higher is the T_g; they show excellent transparency and high refractive index because of their rigid bicyclic monomer units and high chemical resistance and are suitable for many applications such as coatings for high-capacity CDs and DVDs, for lenses, medical equipments, blisters, toner binder, and packaging.

In the last few decades development of single-site catalysts has brought several catalytic systems that allows to synthesize (E-*co*-N)s with different microstructures and with considerable activities. For examples *ansa*-zirconocenes allow to obtain copolymers with an N content well above 50 mol % in isolated, alternating, NN diad or NNN triads and T_g up to 200 °C. [*i*-Pr(3-RCp)Flu-$ZrCl_2$] (R = Me, *t*-Bu) allows to obtain a perfect alternating E-*co*-N copolymer[8]; Ti complexes with pyrrolidimine ligand produce living alternating (E-*co*-N)s[9]. Nomura et al. reported that the non bridged aryloxo or ketimide cyclopentadienyltitanium(IV) complexes produced random E-co-N copolymers where the highest norbornene content was 49 mol %[10].

A promising approach to further expand the properties of COCs is the introduction of a third monomer like a linear α–olefin such as 1-octene or the substitution of the bicyclic norbornane unit with a cyclopentane unit by 1-5 hexadiene cyclopolymerization.

4.1.1. State of the Art of Tailored COCs by α–ω diene terpolymerization

One of the most important goal in polymer chemistry in recent years is to investigate the chemical and physical properties of polyolefins from Ziegler-Natta catalysis by introducing chemical modifications. Among the possible functionalization, the introduction of an α–ω diene into the polyolefin backbones

can bring a variety of structures and represents an emerging area in the metallocenes-mediated polymerizations.

1,5-hexadiene is one of the most used monomer in chemical functionalization of polyolefins; Scheme 4.1 shows three types of propagating reactions[11-15] that are possible for 1,5-hexadiene copolymerization. The first type of reaction is a repeated 1,2-addition of hexadiene, that leaves pendant vinyl groups on the chain backbone of the resulting polymers; the free double bonds can be easily converted in different functional groups through simple organic reactions, obtaining post-polymerization functionalization.

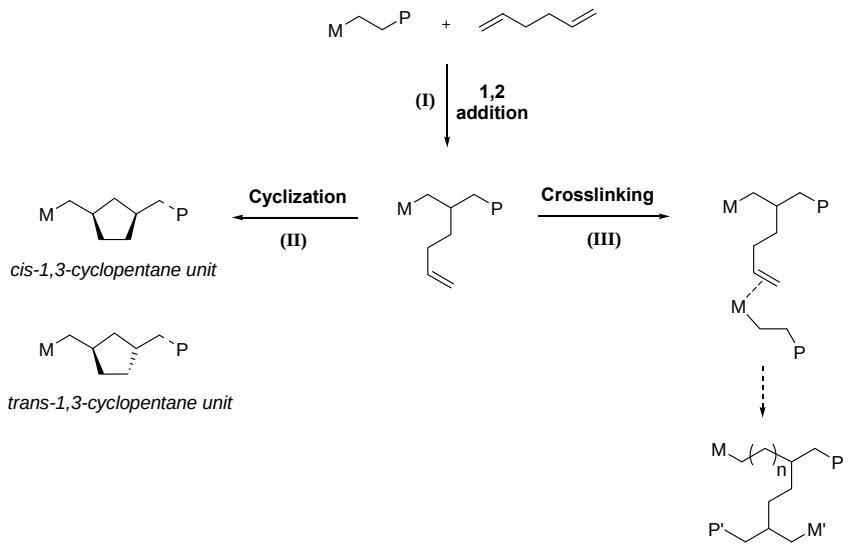

Scheme 4.1 Propagation modes of 1,5-hexadiene (HED) in the copolymerization with ethene (M = metal, P = polymer chain).

The second possible route involves a 1,2-addition of one double bond of the diene, followed by intramolecular cyclization to form cyclopentane structures in *cis* and *trans* conformations. The possibility of 1,5-hexadiene to cyclize is an interesting feature which can lead to polymers with interesting properties; in fact, due to steric reasons, the polymerization of five-membered ring cycloolefins is poorly active. In this sense, due to the higher polymerization activity of non-conjugated dienes, metallocene-mediated cyclopolymerization of 1,5-hexadiene may represent an alternative synthetic route to cycloolefin copolymers.

The last polymerization route involves the reaction of a pendant double bond with another propagating chain, resulting in long-chain branching and chemically crosslinked polymer networks. The branching, which increases melt viscosity and elasticity, is one of the most common and useful approach to improve and facilitate the processing of the material[16]; on the other hand, the introduction of crosslinking is an unwanted process, because, in most of the cases, the presence of crosslinking makes the analysis of the resultant polymer difficult, since solubility of the sample is always required and, by the point of view of processing, the material is useful only if the crosslinking degree is lower than 2 mol%.

The first example of 1,5-hexadiene homopolymerization was reported by Marvel and Stille[17]; the most relevant topic of the paper was that non-conjugated dienes do not always produce crosslinked polymers; in presence of heterogeneous aluminium triisobutyl-titanium tetrachloride catalytic system described by Ziegler[18], the authors found that, although with very low activity, cycloaddition was favoured on 1,2 addition. Two decades later, Cheng[19] reported an example of complete cyclopolymerization of 1,5-hexadiene, using catalyst derived from $TiCl_3$ and $TiCl_4$ in presence of aluminium compounds such as $AlEt_2Cl$. ^{13}C-NMR spectroscopy analysis of the resulting polymer afforded detailed information on the structure and the mechanism, revealing, for the first time, the presence of both the *cis* and *trans* conformation in 1:1 molar ratio.

These reports represent milestones in 1,5-hexadiene cyclopolymerization, that was extensively studied by homogeneous catalysis using metallocenes activated by MAO. It was found that the nature and type of ligands in the metallocene complexes had strong effects on the diasteroselectivity of ring formation, leading to the first example of atactic, *cis* and *trans* poly(methylene-1,3-cyclopentane)[20-21].

Many examples of 1,5-hexadiene/ethene copolymerizations mediated by metallocene/MAO systems are present in literature[22-25], showing that the diene inserts preferentially into the backbone as cyclopentane unit; Pietikäinen[26] was the only one that performed a microstructural analysis of these copolymers,

synthesized by Cp_2ZrCl_2 and *rac*-$Et(Ind)_2ZrCl_2$ activated with MAO, as function of diene content and temperature.

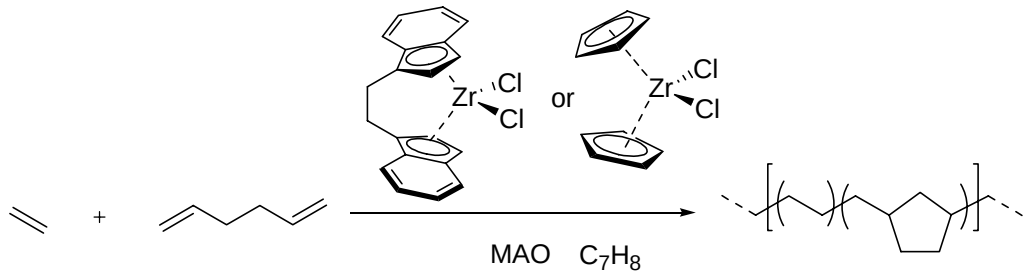

Scheme 4.2 Ethene/1,5-Hexadiene copolymerization performed by $Et(Ind)_2ZrCl_2$/MAO catalytic system or by Cp_2ZrCl_2/MAO system.

A ^{13}C-NMR study showed that at high temperature crosslinking was avoided and the diene incorporates into the polymer backbone exclusively as cyclopentane ring. Moreover, the amount of vinyl bond and the formation of crosslinking, induced by 1,5-hexadiene addition is dependent on $[diene]_{feed}$: the higher is the concentration the higher is the degree of crosslinking. Temperature also plays a crucial role in the control of the molecular structure of the polymer; when the polymerization was conducted at 20° C the degree of crosslinking was nearly 100 %, but it was less than 100 % when the temperature was increased up to 80° C.

As far as the terpolymerization is concerned, the unique example of 1,5-hexadiene terpolymerization, with ethene and styrene, was carried out with the half sandwich catalyst [$Ti(\eta^5:\eta^1$-$Me_4CpSiMe_2NCMe_3)Cl_2$] activated by MAO, as shown in Scheme 4.3.[27]

The ^{13}C-NMR analysis revealed that the cyclopolymerization of the diene afforded randomly distributed *cis* and *trans* cyclopentane rings in the terpolymer backbone; it was worth noting that the cyclopolymerization was in competition with the 1,2 linear addition, producing unsaturated vinyl side chains. The ratio of vinyl groups and cyclopentane rings was controlled by 1,5-hexadiene in feed concentration.

Scheme 4.3 Ethene/Styrene/1,5-Hexadiene terpolymerization performed by CGC complex [Ti(η^5:η^1-$Me_4CpSiMe_2NCMe_3$)Cl_2] activated by MAO.

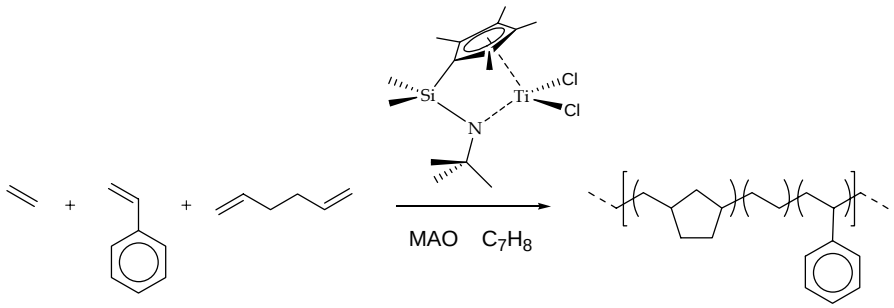

Recently, a PhD study has been performed by Roberto Marconi on ethene, norbornene, 1,5-hexadiene (HED) terpolymerizations by two different representative group IV metal-based catalysts [Zr(η^5:η^5-$C_5H_4CPh_2C_{13}H_8$)Cl_2] (**I**) and [Ti(η^3:η^1-$C_{13}H_8SiMe_2NCMe_3$)Cl_2] (**II**), and by the family of catalysts [M(L_1L_2AB)] bearing different. substituents on the ancillary ligand, activated by methylaluminoxane (MAO)

The latter family of catalysts showed a remarkably high selectivity towards cyclopolymerization, affording terpolymers with a cyclopentane content ranging from 1 to 4 mol % and very low amount of vinylic pendant groups.

Catalyst **I** was not able to discriminate the incorporation modality of HED units, affording terpolymers with the same content of cyclopentane and vinylic units (1-2 mol %).

Catalyst **II** behaved differently from the other two catalysts investigated; it was observed high incorporation of cyclopentane units (up to 9 mol %), high amount of vinylic units (up to 4 mol %), and also a high degree of crosslinking, increasing from 9 to 43 wt % with the increasing of HED in feed concentration.

The main drawback of the catalytic systems used was the difficulty to obtain high molecular weight terpolymers with high cyclopentane units content and with vinylic and crosslinking degree as low as possible.

Design and synthesis of efficient transition metal complexes capable to promote a precise and controlled olefin polymerization has attracted considerable attention, and nonbridged half-metallocene-type group IV transition metal complexes of the type Cp'M(L)X_2 (Cp' = cyclopentadienyl group; M = Ti, Zr, Hf;

L = anionic ligand such as OAr, NR_2, $N=CR_2$, etc.; X = halogen or alkyl) have been considered one of the most promising candidates for new efficient catalysts. This is because these complexes are simple to be synthesized and steric and electronic ligand modifications are easier than in case of the half-metallocene complexes. recently reported to display unique features, especially for synthesis of new polymers[28-30]. These precatalysts in combination with appropriate activators such as MAO are efficient catalysts for copolymerization of ethylene with α-olefins containing bulky substituents such as vinylcyclohexane and 3-methyl-1-pentene, and with cyclic olefins, yielding polymers with high molecular weight and in high activities[28-30]. In particular, the Cp-ketimide $[Ti(\eta^5\text{-}C_5Me_5)(N=C^tBu_2)Cl_2]$ exhibits both remarkable catalytic activity and efficient N incorporation in copolymerization with E. In principle, this coordinatively open catalyst structure offers the opportunity to readily accommodate 1,5-hexadiene or 1-octene monomers and to lead to terpolymers with novel properties.

4.1.2. Tailored COCs by α–ω diene terpolymerization by nonbridged half titanocenes

In the present work we have investigated the catalytic performances of nonbridged half titanocenes, sketched in Figure 4.1, provided us by Prof Nomura of Tokyo Metropolitan University, Japan

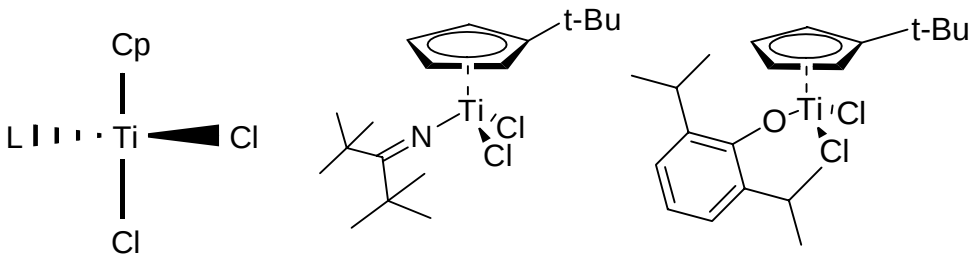

A **B** **C**

Figure 4.1 The three nonbridged titanocene precursors used in ethene-norbornene copolymerizations. Structure of nonbridged half-titanocene **A** will not be disclosed for patent applications.

Initially, a set of ethene-norbornene copolymerization has been performed with three different non bridged titanocenes; a study of catalyst activity in dependence of molecular structure and E/N feed molar ratio has been performed, in order to evaluate the catalytic performance in terms of activities, microstructure and molecular weight.

First of all a preliminary screening with titanocene **A** in ethene-norbornene copolymerizations has been done, in order to get the right polymerization conditions. On the basis of results reported in literature by Nomura et al[31]. we have chosen the following experimental conditions.

Table 4.1 Autoclave experimental conditions

	IN AUTOCLAVE
Total volume	250 ml
Temperature	60° C
N/E	2 m.r.
Solvent	50 ml of Toluene
Pressure	4 bar

The most relevant results are shown in Table 4.2.

The activity of the catalyst by using an Al/Ti molar ratio of 500 was evaluated by varying the catalyst loading from 10 μmol to 5 μmol in order to keep the monomer conversion low.

Table 4.2 Copolymerization activities for half titanocene **A** under autoclave conditions listed in Table 4.1

Run	**Cat. μmol**	**Al/Ti m.r.**	**Time min.**	**Yield g**	**Activity kg/mol $_{Ti}$ h**
03	10	500	15	11.7	4680
04	5	500	15	0.3	240
05	5	500	15	0.9	720
06	7	500	15	2.4	1371
07	10	1000	2.5	4.2	10080
09	7	1000	2.5	5.1	17486
11	5	1000	10	5.1	6120

MAO content was doubled to increase the reproducibility and to reduce the polymerization time in order to control the monomer conversion. However,

the catalyst was too active and it was difficult to keep the conversion of norbornene below 40 %.

The best activity results have been obtained with the Al/Ti m.r. of 1000, and a good compromise between activity and conversion has been obtained by using a catalyst loading of 5 μmol, so we decided to use these conditions to evaluate the catalytic performances at different E/N m.r. (Table 4.3)

Table 4.3 Copolymerization activities for half titanocene **A** under autoclave conditions listed in Table 4.1 at different E/N m.r.

Run	N/E ratio m.r.	Cat mol	Co-Cat mmol	Al/M m.r.	time min	Yield g	Activity Kg/mol_{Ti}•h
12	4	5	5	1000	15	4.7	3760
13	4	5	5	1000	10	7	8400
14	6	5	5	1000	15	4.6	3680
15	8	5	5	1000	15	0	n.d.

The activities result to be dependent on the ethene-norbornene molar ratio, as reported in Figure 4.2, that is, the higher is the $[N]_{feed}$, the lower is the activity. **A** negative comonomer effect is in line with the data reported in literature for poly(E-co-N) copolymers.

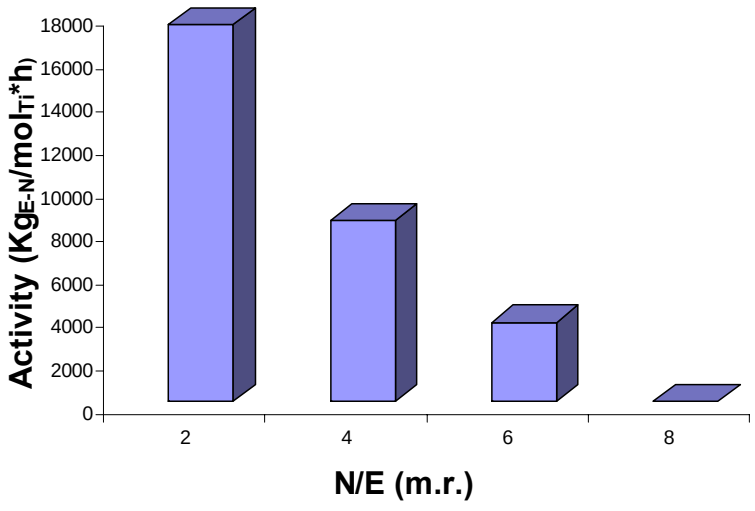

Figure 4.2 Activity versus N/E m.r. for (E-co-N) obtained by using catalyst **A**

Then, the catalytic performance of the catalyst **B** and **C** was tested in ethene-norbornene copolymerizations by using our best experimental conditions, that is: Al/Ti: 1000 m.r., catalyst loading: 5 μmol.

In Table 4.4 the main results are reported.

All half-titanocene precursors are remarkably or moderate active in E/N copolymerization; the activity is dependent on the substituent on Cp ligand and on the ancillary donor ligand. The half-titanocene **A**, having an unsubstituted cyclopentadienyl ligand**,** results to be two times more active than the *t*-Bu substituted one, while the aryloxo substituted one, although highly active, presents the lowest activity.

Table 4.4 Copolymerization activities for half-titanocene **A, B, C** under autoclave conditions.

Run	N/E ratio m.r.	Cat type	Cat mol	Co-Cat mmol	Al/M m.r.	time min	Yield g	Activity $Kg/mol_{Ti}•h$
13	4	**A**	5	5	1000	10	7	8400
21	4	**B**	5	5	1000	10	3.6	4320
34	4	**B**	5	5	1000	10	3.9	4680
24	4	**C**	5	5	1000	30	2.6	1560
15	4	**C**	5	5	1000	30	2.7	1620

Copolymers have been characterized by SEC to determine the molar mass and molar mass distributions; principal results are reported in Table 4.5. The catalysts produce very high M_w copolymers with unimodal molar mass distributions with polydispersity (M_w/M_n) values of nearly two, which are consistent with a single-site polymerization process.

Table 4.5 Molar Masses and molar mass distribution for E/N copolymers obtained with half-titanocenes **A**, **B,** and **C**.

Run	N/E ratio m.r.	Cat type	M_w kg/mol	D M_w/M_n
03	2	**A**	1165	2.46
07	2	**A**	1685	2.81
09	2	**A**	1046	1.96
11	2	**A**	965	2.66
12	4	**A**	1089	1.95
13	4	**A**	1424	3.31
21	4	**B**	633	2.10
24	4	**C**	1921	1.61

The more hindered *t*-Bu substituted half-titanocene **B** produces copolymers with lower M_w than the unsubstituted analogous and three times lower than the aryloxo substituted titanocene as reported by Nomura et al.[32] for ethylene-styrene and ethylene-vinylcyclohexane copolymerization.

Copolymers have been characterized by ^{13}C-NMR to determine the microstructure and the norbornene content. Some of the results are reported in Table 4.6. A general structure of an E/N copolymer with the relative labelling of carbon atoms is shown in Figure 4.3.

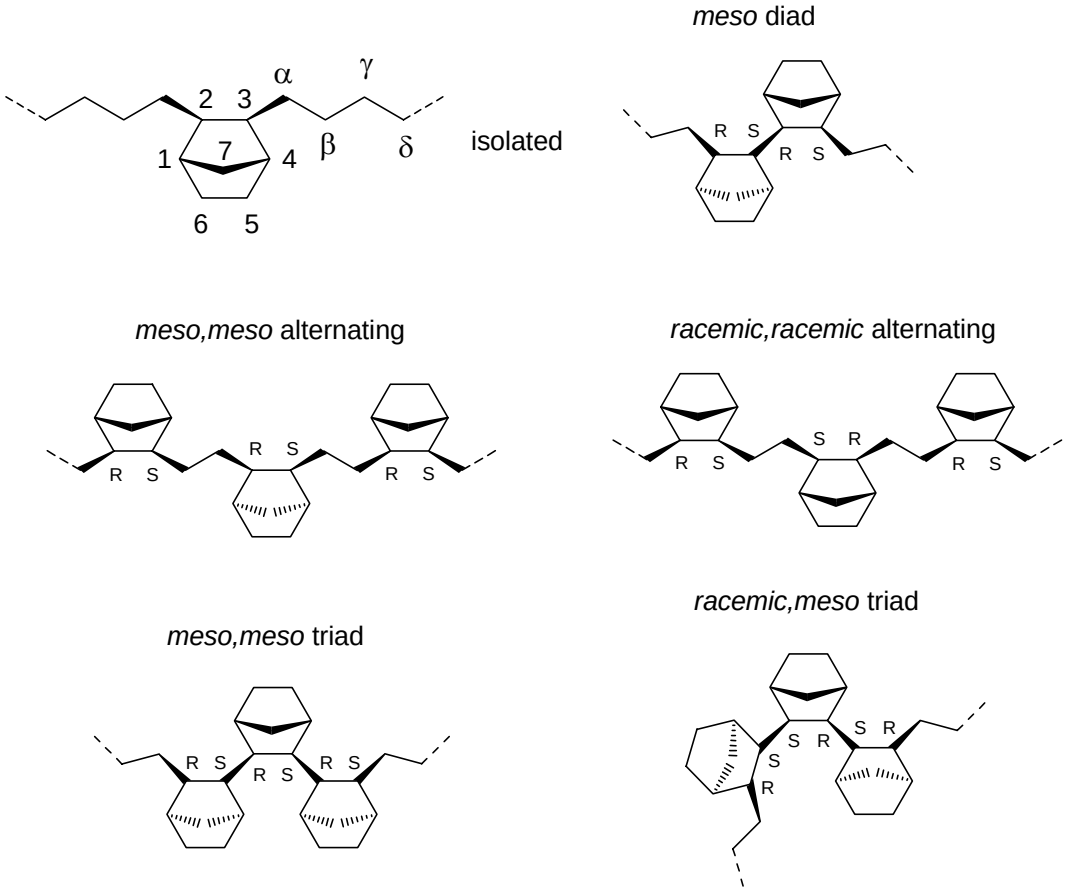

Figure 4.3 General structure of poly(E-co-N) and relative carbon atom labelling

The copolymer microstructure and composition were calculated on the basis of NMR assignment (Figure 4.4) as reported in literature[33].

Table 4.5 Norbornene content and monomer conversion calculated by ^{13}C-NMR for E/N copolymers obtained with catalyst **A, B** and **C.**

Run	N/E ratio m.r.	Cat type	N mol %	Conversion mol %
11	2	**A**	33	44
12	4	**A**	45	20
21	4	**B**	33	31
24	4	**C**	27	22

The behaviour of the catalysts toward norbornene molecules is different: the most active titanocene **A** shows the highest preference for norbornene, yielding copolymers with the highest N percentage; worth to note is that the copolymer N content increases with the increasing of the norbornene concentration in feed.

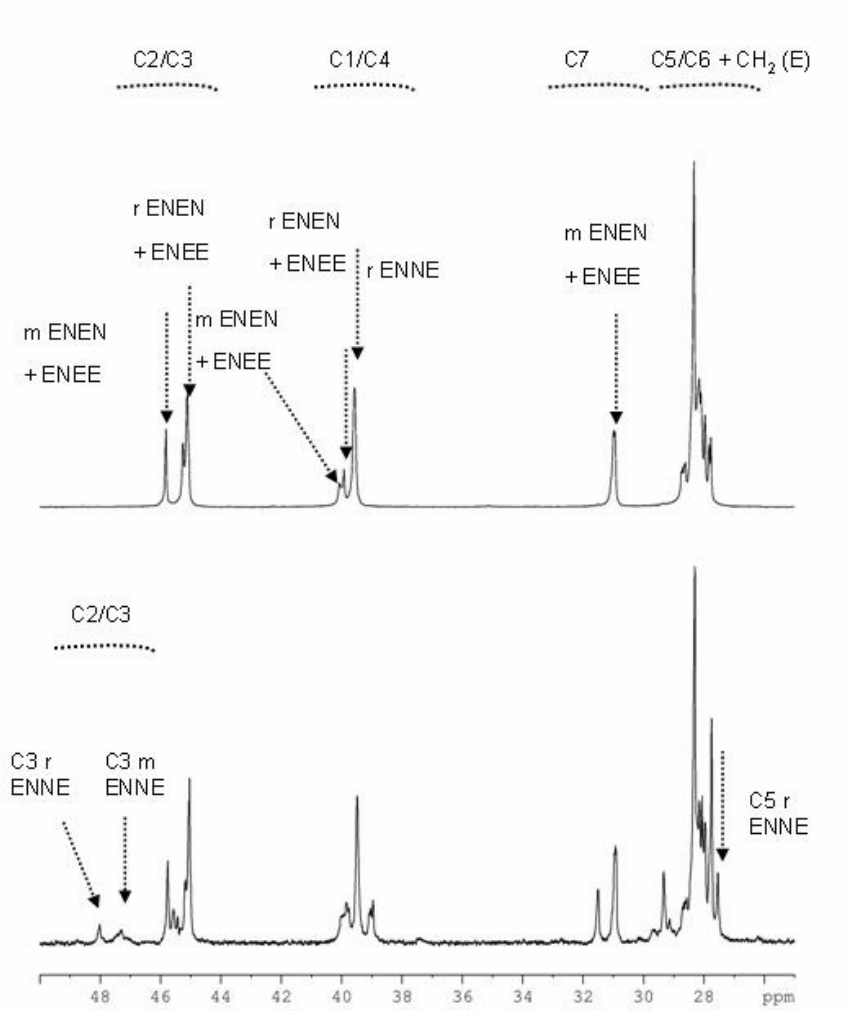

Figure 4.4 ^{13}C-NMR spectrum (108.58 MHz, $C_2D_2Cl_4$, 103 °C) of poly(E-co-N) samples prepared by **A**/MAO catalyst (bottom) and **B**/MAO (top) system (Table 4.5, run 11 and 21).

Among the *t*-Bu substitituted Cp half-titanocenes, the aryloxo structured one presents the lowest affinity towards norbornene molecules, yielding copolymers with the lowest cycloolefin content.

The copolymer microstructure is also different: as evident in Figure 4.4, catalyst **A** gives mainly atactic copolymers with both *racemic* and *meso* NN diads and NNN triads, catalyst **B** gives quite alternating ENEN copolymers.

The thermal properties of the copolymers have been determined by DSC; the thermal analysis of poly(E-*co*-N) obtained by the three non-bridged half-titanocenes showed well-defined glass transition temperatures (T_g) and no endothermic peak corresponding to the melting of any crystalline phase was

observed. This observation implies that all the copolymers are homogeneous with an amorphous morphology. Most relevant analytical data are reported in Table 4.6.

Table 4.6 Thermal analysis of some of the poly(E-*co*-N) synthesized using half-titanocenes **A**, **B** and **C**

Run	N/E ratio m.r.	Cat type	T_g °C	N mol %
07	2	**A**	90	30
12	4	**A**	115	45
13	4	**A**	119	46
21	4	**B**	67	33
24	4	**C**	27	21

The T_g values, at least for catalyst **A**, are linearly dependent on the content of norbornene incorporated, which has been varied by changing the N/E feed molar ratio. In Figure 4.5, the glass transition temperature of some of the copolymers prepared with the **A**/MAO system are plotted as a function of norbornene incorporated evaluated by ^{13}C-NMR.

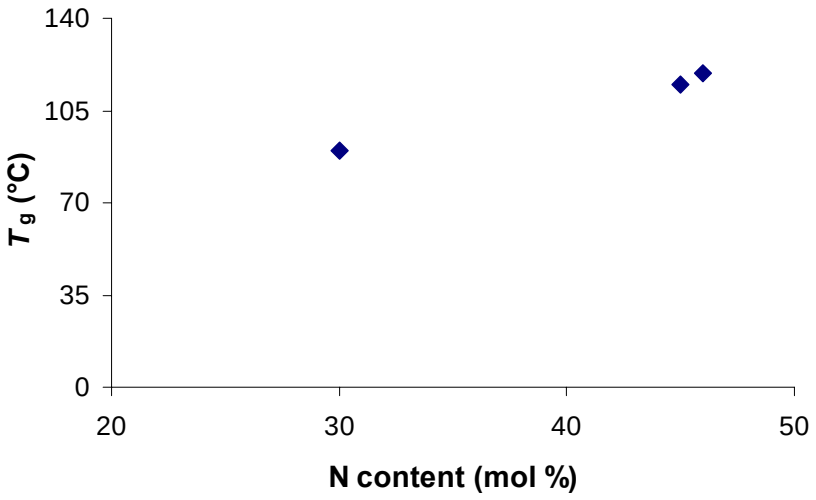

Figure 4.5. Plot of glass transition temperature (*T*g) values versus norbornene content in some poly(E-*co*-N) obtained with catalysts **A**.

As evident in Figure 4.5 T_g values are a linear function of the N content and rapidly increases with the increasing of molar percentage of norbornene as expected from data reported in literature.

On the basis of results on E/N coplymerization, the terpolymerization of 1,5-hexadiene (HED) with ethene and norbornene (Scheme 4.4) was studied using the three nonbridged half-titanocene compounds shown in Figure 4.2.

Scheme 4.4 Ethene/Norbornene/1,5-Hexadiene terpolymerization performed by titanocene **A, B, C**/MAO systems.

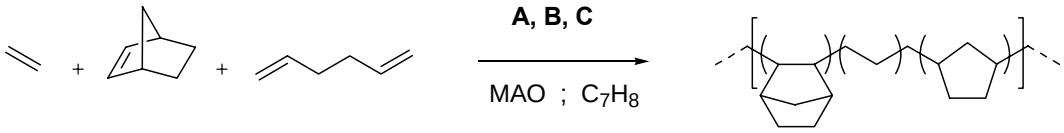

Priority was to synthesize terpolymers that meet industrial requirements; therefore the synthesis has been conducted at conditions as close as possible to those used in industrial plants, that is temperature: 60° C and 4 bar ethene pressure. Two different [N]/[HED] molar ratios in feed have been investigated to evaluate the activity, the molar mass and molar mass distributions and the molecular structure of the terpolymers obtained.

In Table 4.6 the analytical data concerning the terpolymerization activity are reported; for comparison the results of E-N copolymerization conducted under identical or similar conditions, used here as reference, are also included in the table.

Table 4.6 poly(E-ter-N-ter-HED) activity by using half-titanocene **A**, **B**, **C**/MAO systems

Run	N/E/HED m.r.	Cat type	Activity kg/mol
03	2/1	**A**	4680
16	2/1/4	**A**	2480
27	1/1/4	**A**	333
21	4/1	**B**	4320
09	2/1/4	**B**	815
11	1/1/4	**B**	2760
24	4/1	**C**	1560
12	2/1/4	**C**	258
13	1/1/4	**C**	400

For all the three half-titanocenes, the addition of 1,5-hexadiene seems to negatively affect the activity, that results to be much lower with respect the activity in E/N copolymerizations. Moreover, the behaviour of the catalysts towards the termonomer results to be quite different. Half-titanocene **A** seems to be negatively affected by the concentration of HED; in fact, the lower the N/HED

m.r. the lower is the activity. Opposite behaviour is observed for the other two half-titanocenes.

The behaviour of the most active half-titanocene **A** has been more deeply investigated at different ethene pressure and different polymerization temperature, to evaluate the dependence of polymer properties and catalytic performances by these factors. The analytical data are summarized in Table 4.7.

Both the temperature and the ethene pressure have a drastic effect on catalyst productivity, that results to be up to 10 times lower (run 16 and 17) when the ethene concentration was lowered to 1 bar and the temperature was lowered to 30 °C.

Table 4.7 poly(E-ter-N-ter-HED) activity dependence by ethene pressure and polymerization temperature for **A**/MAO system.

Run	N/E/HED m.r.	T °C	E Pressure Bar	Activity kg/mol
16	2/1/4	**60**	4	2480
18	2/1/4	**30**	1	420
27	2/1/4	**60**	4	333
17	1/1/4	**30**	1	276

The terpolymers have been characterized by ^{13}C-NMR spectroscopy; the main objective was to determine the polymer composition in terms of norbornene and 1,5-hexadiene content.

The ^{13}C-NMR study of the terpolymers obtained in the present research has been conducted on the basis of previous study performed by Marconi[34] to clarify if cyclopentane units can be effectively introduced into ethylene/norbornene based copolymers, by definitely introducing interesting features to the material. He synthesized poly(E-*ter*-N-*ter*-HED) at low norbornene content *ad hoc* to assign the complex ^{13}C-NMR spectra. The ^{13}C-NMR microstructural analysis of the poly(1,5-hexadiene) sample proved clearly that HED was mainly incorporated as 1,3-cyclopentane (CP) units; this was unambiguously an evidence that intramolecular cyclization of 1,2-inserted HED occurred before next monomer insertion.

Of interest was a new group of signals, indicated with symbol αβγ, seen in the range between 34.81 and 35.4 ppm related to carbons from the main chain, immediately adjacent to cyclopentane and in proximity to norbornene unit.

The analysis of the spectra of poly(N-*co*-HED) clearly demonstrated that the ^{13}C-NMR resonance positions of signals ascribed to 1,3-cyclopentane units of HED were highly sensitive to compositional and stereochemical effects, which depend on the terpolymer microstructure and to catalyst structure.

Thus, starting by the previous experimental evidences, a ^{13}C-NMR study of the terpolymers synthesized by half-titanocene **A**, **B**, **C**/MAO systems has been performed. Indeed, especially at high norbornene content, the terpolymers obtained give rise to particularly complicated spectra and the peak assignment is very difficult; the chemical shifts of norbornene cyclic units results to be fairly similar to those ascribed to cyclopentane units. When the N content in the terpolymers is high, an overlapping between E/N backbone resonances and the major part of signals attributed to cyclopentane units, as well as the shifting of some other peaks, is reasonable to happen.

As a consequence, to give unambiguous assignment of the CP structure peaks, a preliminary study of ^{13}C-NMR spectra of N/HED and E/HED copolymers as function of feed composition has been performed (Table 4.7).

Table 4.8 Polymerizations carried out using **A**/MAO system.

Run	N/E/HED m.r.	T °C	Yield g	Activity kg/mol
50	0/0/1	**60**	0.4	176
51	0/1/2	**60**	5.7	2264
52	0/1/4	**60**	1.0	416
53	1/0/2	**60**	2.3	628
54	1/0/4	**60**	1.4	560

The polyHED ^{13}C-NMR spectra showed in Figure 4.6 is quite simple, no evidence of linear structure or olefinic moieties is detected and clearly proved that 1,5-hexadiene inserts preferentially as 1,3 cyclopentane units. This means that intramolecular cyclization of 1,2-inserted HED happens before every monomer insertion, so only a small fraction of inserted monomer formed vinyl (Vy) terminated branches. The peak assignment has been based on a comparison to literature data[19]. The cyclopentane structures has been assigned as follows: *cis*

rings: 30.21 ppm (4',5'-*c*), 37.45 ppm (1',3'-*c*), 39.60 ppm (2'-*c*); *trans* rings: 31.44 ppm (4',5'-*t*), 36.04 ppm (1',3'-*t*), 37.64 ppm (2'-*t*); methylene bridge carbon, 42.05 ppm (αα).

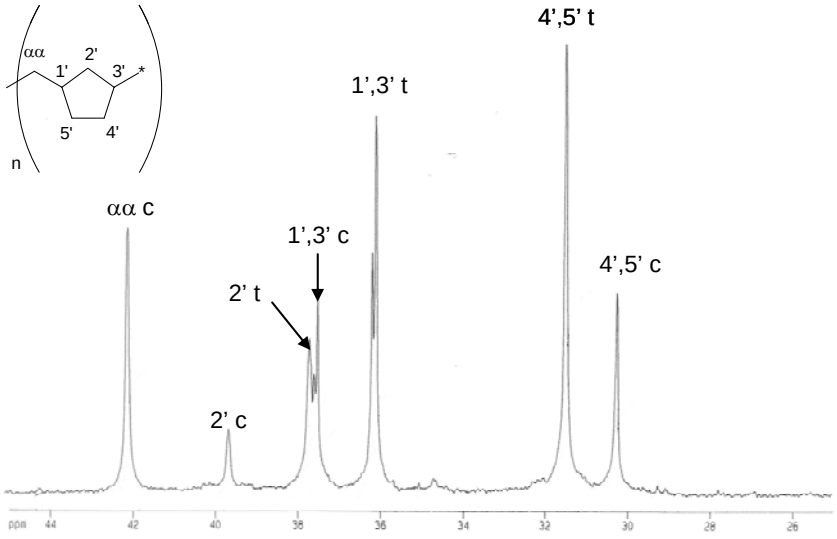

Figure 4.6. ^{13}C-NMR spectrum (108.58 MHz, $C_2D_2Cl_4$, 103 °C) of poly(HED) sample prepared by **A**/MAO catalytic system (Table 4.7, run 50).

In Figure 4.7 the ^{13}C-NMR spectrum of poly(HED) (**c)** is compared to that of a copolymer of HED with norbornene (**a**), and with the copolymer of HED with E (**b**) prepared under similar polymerization conditions (Table 4.8, entries 50, 52, 54).

The analysis of the spectra clearly demonstrates that the ^{13}C-NMR resonance positions of signals ascribed to 1,3-cyclopentane units of HED are highly sensitive to compositional and stereochemical effects.

It appears from Figure 4.7 that the resonances of carbon atoms 1',3'-*cis* and 1',3'-*trans* of the two copolymers depicted in (**a** and **b)** are slightly shifted at lower chemical shift by c.a. 0.05 ppm compared to those of poly(HED) depicted in c. This effect is due to the placements of different substituents at position C_1 and C_3 of the cyclopentane ring, most likely ethene or norbornene units in the present situation. In this regard, signals appearing between 34.8 and 35 ppm indicated in Figure 4.7 c with αβγ, was ascribed to methylene carbons from the main chain immediately adjacent to cyclopentane units, and in proximity to

norbornene. Interestingly, in case of poly(N-*co*-HED) and poly(E-*co*-HED) depicted in Figure 4.7 a and b , the presence of several weak signals in the region between 36 and 39 ppm is most likely associated to the shifting of the resonance of cyclopentane units depending on the microstructure of the terpolymer.

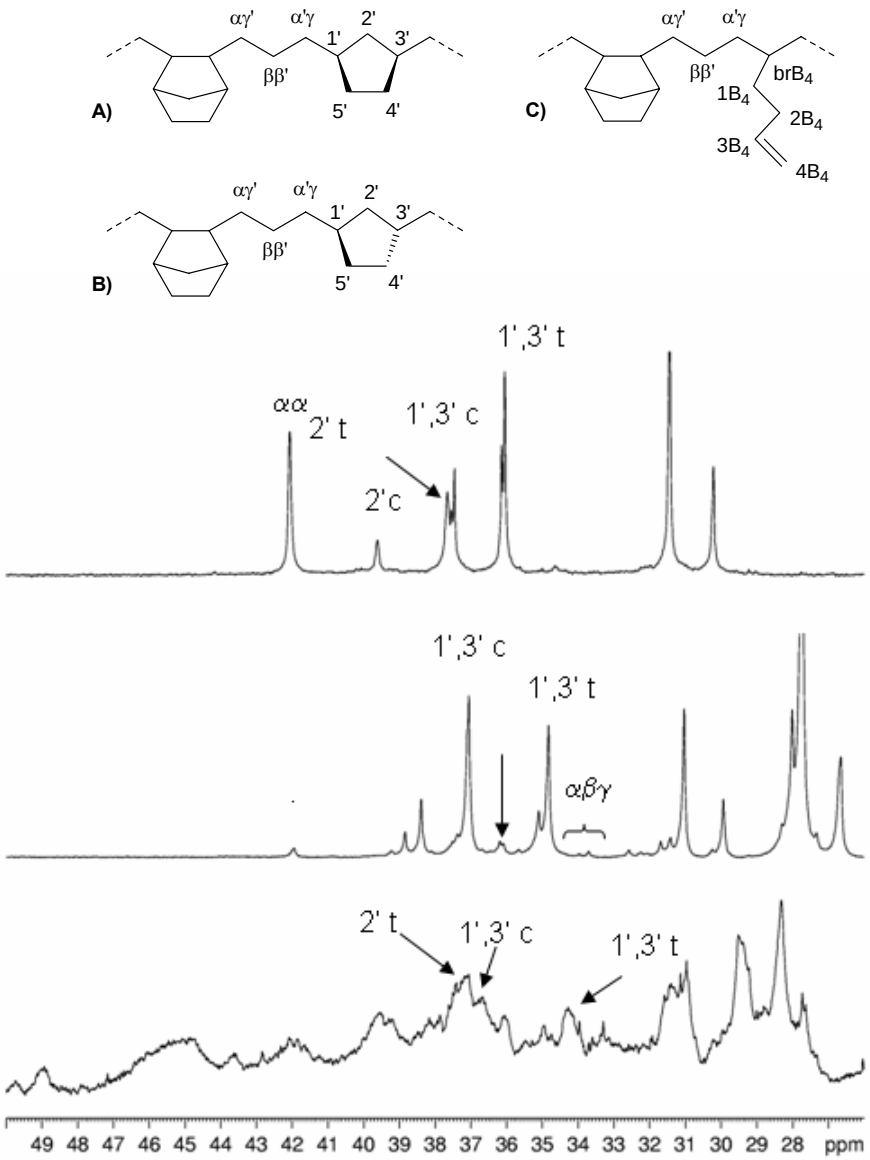

Figure 4.7 ^{13}C-NMR spectra (108.58 MHz, $C_2D_2Cl_4$, 103 °C) of a) poly(N-*co*-HED) (run 54 Table 4.8), b) poly(E-*co*-HED) (run 52 Table 4.8), c) polyHED (run 50 Table 4.8)sample prepared by **A**/MAO

Thus, the assignment of ^{13}C-NMR shift of cyclopentyl carbons resulted to be quite complicated, and could cause errors in calculating the CP content in poly(E-*ter*-N-*ter*-HED) prepared in this study.

On the basis of this preliminary study, a compositional analysis of poly(E-ter-N-ter-HED)s obtained with the three half-titanocenes **A**, **B**, and **C** by ^{13}C-NMR has been performed, and the analytical data are reported in the following table.

Table 4.9 ^{13}C-NMR data of poly(E-t*er*-N-*ter*-HED) obtained by using **A**, **B** and **C**/MAO systems

Run	E	Cat	E/N/HED	N content	CP	Vinyl
	bar	type	m.r.	mol %	mol %	mol %
16	4	**A**	2/1/4	26	16	2
18	1	**A**	2/1/4	33	15	1
17	1	**A**	1/1/4	31	18	1
22	4	**B**	2/1/4	27	15	0.2
28	4	**B**	1/1/4	20	15	0.9
25a	4	**C**	2/1/4	27	28	4
29	4	**C**	1/1/4	22	34	3

A deep insight into ^{13}C-NMR spectra of the terpolymers obtained with the three catalytic systems (Figure 4.8) reveals that the microstructure is sensibly affected by the catalyst structure. The aryloxo substituted half-titanocene **C** presents the highest preference toward the 1,5-hexadiene monomers (Table 4.9, run 25a and 29), that insert into the polymer backbone preferentially as 1,3 cyclopentane units, even though an appreciable amount of unsaturated vinyl side chain group is detected. The 1,5-hexadiene percentage incorporated by titanocenes **A** and **B** results to be similar and the half with respect the half-titanocene **C**, that clearly indicates that **A** and **B** present lower reactivity towards the diene molecules. Even though for both the half-titanocenes intramolecular cyclization preferentially happens before every 1,2 diene addition, for **A**/MAO system it seems that the vinyl pendant group percentage increases with the decrease of $[1,5\text{-hexadiene}]_{feed}$ (Table 4.8, entry16 and 18).

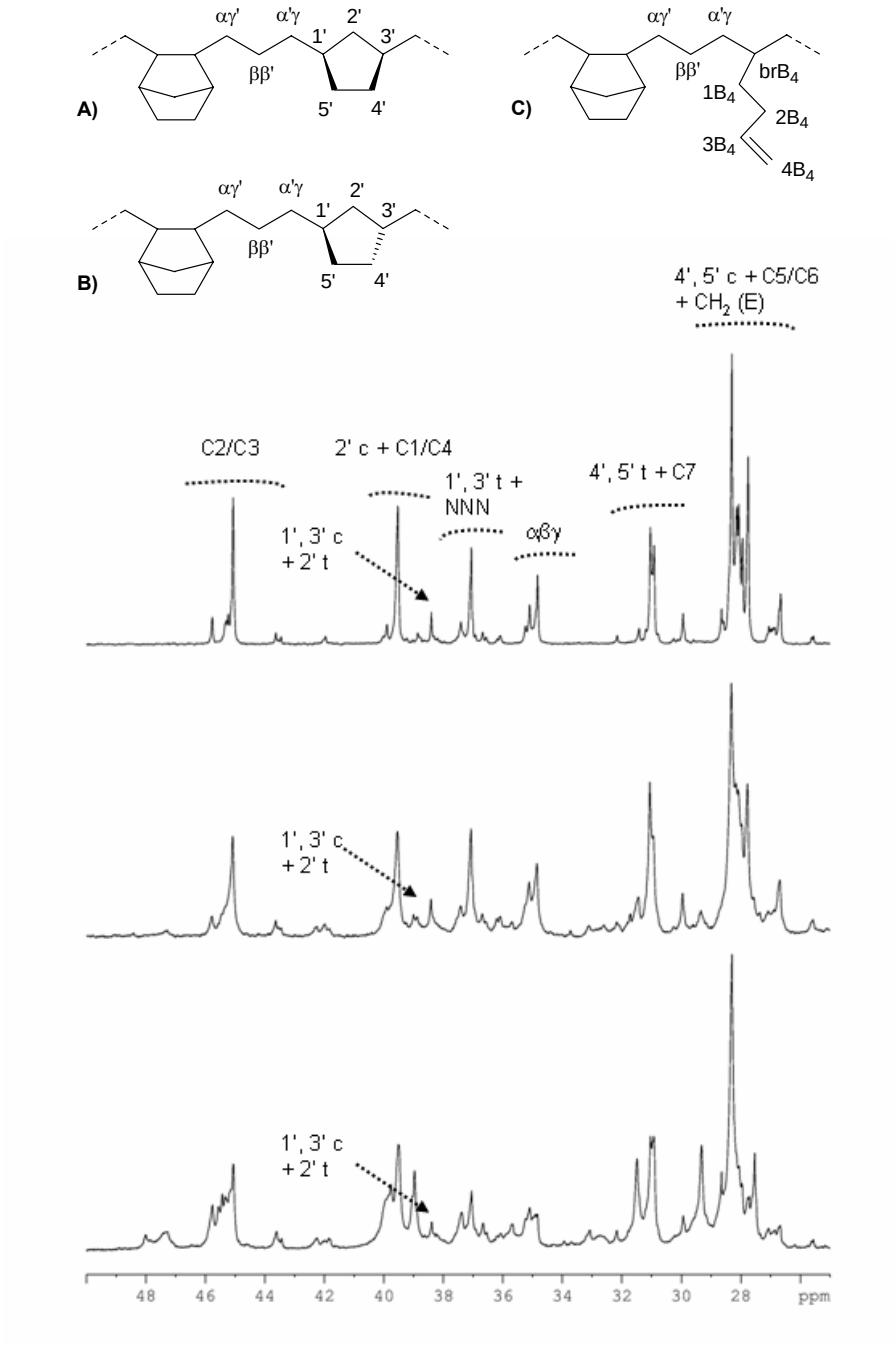

Figure 4.8 Expansion of the region between 26-50 ppm of ^{13}C-NMR spectra (108.58 MHz, $C_2D_2Cl_4$, 103 °C) of poly(E-ter-N-ter- HED) samples prepared by **A**/MAO (bottom), **B**/MAO (middle) and **C**/MAO (top) catalytic system (Table 4.7, run 18, 28, 29 respectively).

The terpolymers have been characterized by SEC to determine the molar mass and molar mass distribution; in the following table the principal results are shown.

Table 4.10 Molar masses and molar mass distribution of poly(E-*ter*-N-*ter*-HED)s obtained with **A**, **B** and **C**/MAO systems

Run	Cat type	E/N/HED m.r.	M_w kg/mol	D M_w/M_n	N content mol %	CP mol %	Vinyl mol %
16	**A**	2/1/4	n.s.	-	26	16	2
18	**A**	2/1/4	1565	3.04	33	15	1
17	**A**	1/1/4	n.s.	-	31	18	1
27	**A**	1/1/4	n.s.	-	n.d.	n.d.	n.d.
22	**B**	2/1/4	n.s.	-	27	15	0.2
28	**B**	1/1/4	n.s.	-	20	15	0.9
25	**C**	2/1/4	19	2.01	n.d.	n.d.	-
25a	**C**	2/1/4	n.s.	-	27	28	4
29	**C**	1/1/4	30	1.54	22	34	3

n.s.: not soluble in orthodichlorobenzene (ODCB) at high temperature

As clearly evident in Table 4.10, SEC characterization of the terpolymers was difficult, because most terpolymers were not soluble in ODCB even at high temperature. Runs 18, 25, and 29 produced terpolymers partially soluble, and the molar mass values calculated belong to the soluble part.

We reasonably attribute the reason of the low or zero solubility of the terpolymers to the presence of crosslinked chains into the polymers. The assumption seems confirmed by the fact that the percentage of the vinylic free double bond along the polymer chain is low. Another important validation of our assumption comes from taking in account the vinyl percentage of the terpolymers obtained with titanocene **C**; comparing the vinyl percentage of the terpolymers obtained with this catalyst, with the vinyl percentage of the terpolymers obtained with the catalyst **B**, there is an amount 20 times lower, and 2 or 3 times higher than those obtained with titanocene **A**. This seems to indicate that the degree of crosslinking is less than those obtained with catalysts **A** and **B** under the same conditions.

The investigation of the thermal behaviour of poly(E-*ter*-N-*ter*-HED) synthetized by these complexes exhibited difficulties as far as terpolymers with

extremely high molar masses were concerned. The detected T_g. values are reported in Table 4.11.

Table 4.11 Poly(E-ter-N-ter-HED) thermal analysis results

Run	E	Cat	E/N/HED	T_g	N content	CP	Vinyl
	bar	type	m.r.	(°C)	mol %	mol %	mol %
16	4	**A**	2/1/4	75	26	16	2
18	1	**A**	2/1/4	94	33	15	1
17	1	**A**	1/1/4	76	31	18	1
22	4	**B**	2/1/4	46	27	2.3	0.2
28	4	**B**	1/1/4	27	20	15	0.9
25a	4	**C**	2/1/4	56	27	28	4
29	4	**C**	1/1/4	29	22	34	3

The T_g values of the terpolymers obtained were noticeably dependent on the content of norbornene incorporated and on the amount of cyclopentane units present in the polymer backbone.

As it could be evinced by Figure 4.9 there is a linear relationship between the norbornene and cyclopentane content and the T_g; it seems that the T_g linearly increases with the increasing of norbornene content in copolymers and linearly decreases with the increasing of CP content, that is, the positive contribution to the T_gs due to the norbornene units is in contrast with the negative contribution of hexadiene units.

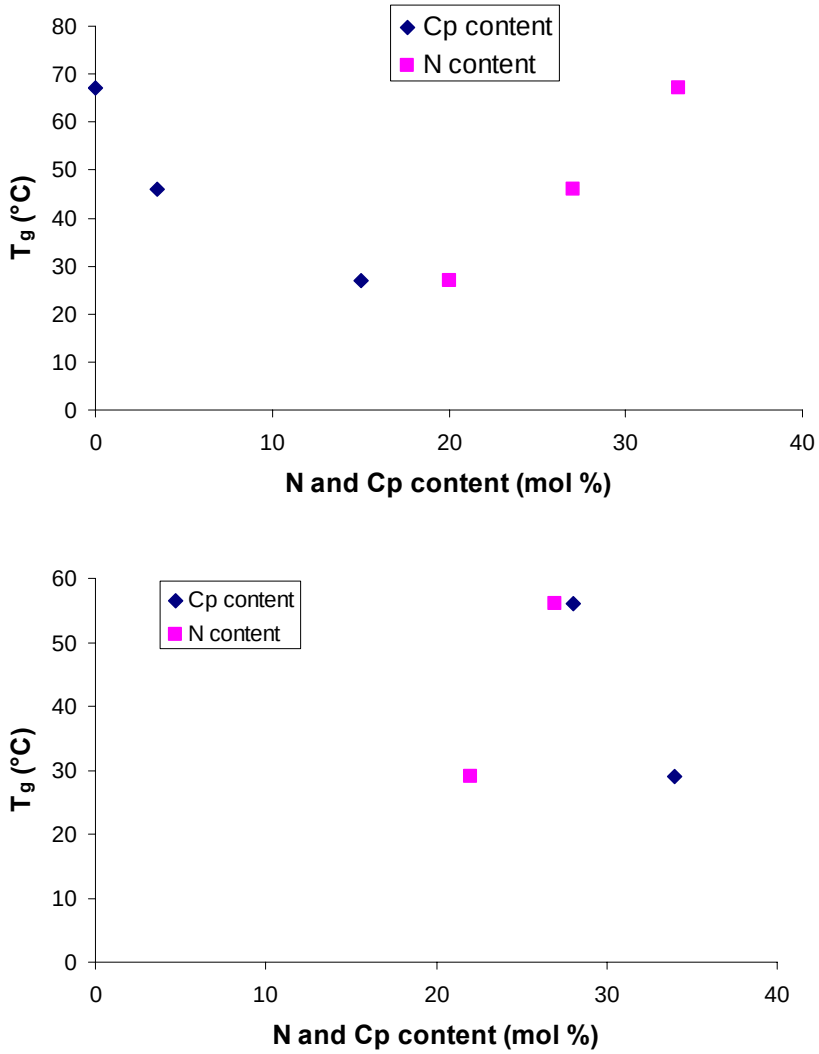

Figure 4.9 T_g dependence on N and Cp content for poly(E-*ter*-N-*ter*-HED) obtained with titanocene **B** (top) and **C** (bottom)

4.1.3 Ethene-Norbornene-1-Octene terpolymers by nonbridged half titanocenes

Another important route to improve the properties of E/N-based materials is the terpolymerization including other linear olefins. The introduction of a linear termonomer, such 1-octene, is a promising approach to expand the material performance of commercial COCs. The presence of a long linear α-olefin into E-N copolymer backbone could increase the flexibility of the copolymer chain and

improve the commercial applicability of the material, while maintaining a high transparency and the other characteristic properties of E-N copolymers.

1-octene is one of the monomer most employed worldwide in polyolefin field, principally as comonomer in the synthesis of Linear Low Density PolyEthene (LLDPE); LLDPE represents one of the most important class of commercialized plastics, with many applications in packaging, in shrink films with a low steam permeation, in elastic films when containing a high comonomer concentration, in cable coatings, in the medical field because of the low part of extractables, etc. The performances of this material are mainly influenced by the type and by the amount of comonomer used, and by the distribution of the short chain branches (SCB) introduced by the comonomer into the linear polymer chain[35]. It is well known that the presence of high amount of SCB disturbs the crystallization kinetic; generally, these side groups are concentrated in amorphous regions, and only a small portion of the alkyl groups are located inside the crystallites[36, 37]. Crystallinity and melting temperature are linearly correlated to the content of comonomer, decreasing with increasing comonomer content, and making films formed from these materials more flexile and processable[38].

The first example of modification of polyethene with linear α-olefins reported the use of traditional heterogeneous Z-N catalysts, that gave copolymers with broad molecular weight distribution and relatively broad short chain branching distribution.

The use of *single-site* metallocene catalysts opened the possibility to tailor the properties and the structures of these copolymers, and opened the possibility to obtain a novel LLDPE resin class. Metallocene-based catalysts permits to incorporate high amount of comonomer with a resulting polymer with narrow molecular weight and composition distributions.

Ethene-1-octene copolymers obtained with metallocene catalysis were deeply investigated in industrial laboratories[39, 40], but most of the results are not available, due to patent reasons, and, by academic research point of view, these field results to be still open.

The first example concerning 1-octene-based terpolymers was reported by Mülhaupt[40] (Scheme 4.5).

Scheme 4.5. Ethylene/Styrene/1-octene terpolymerization performed by $Me_2Si(Me_4Cp)TiCl_2$/MAO catalytic system.

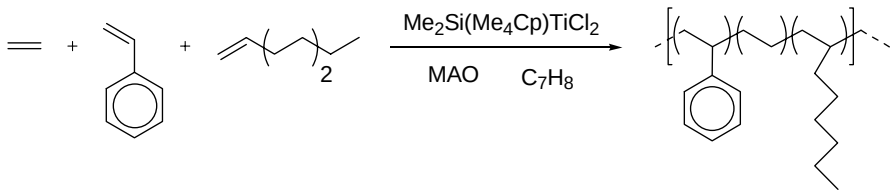

The synthesis of mLLDPE containing alkyl and phenyl side chains by metallocene catalyzed terpolymerization of ethene, vinyl benzene (ST) and 1-octene (O), conducted using MAO activated $Me_2Si(Me_4Cp)TiCl_2$ catalytic system was reported.

Terpolymerizations resulted in poly(E-*ter*-O-*ter*-ST) with 1-octene incorporation in the range of 8 to 21 mol-% and styrene content up to 25 mol %. The influence of comonomers concentration on polymerization behavior and on thermal properties of the resulting terpolymers were investigated.

In the present work, terpolymerizations of ethene with norbornene and 1-octene has been investigated using three different nonbridged half-titanocene precursors depicted in Figure 4.10, using dMAO as cocatalyst.

Current research started on the basis of previous studies conducted in our laboratory on the synthesis of ethene, norbornene, 1-octene terpolymerizations by using different class IV metallocenes bearing various substituents on the ancillary ligand, activated by methylaluminoxane (MAO).

In his PhD thesis, Marconi[34] performed a series of terpolymerization of ethylene with norbornene and 1-octene to evaluate the influence of termonomer concentration on polymerization behavior. A set of different experimental conditions (e.g. ethene pressure and temperature) was investigated to discover whether altering polymerization parameters would have an impact on molar masses and termonomer incorporation. High [N]/[E] molar ratios in feed were considered to achieve synthesis of terpolymers having more than 30 mol-% of norbornene content, and thus materials with glass transition temperatures (T_g)

higher than 80 °C. The [N]/[E] molar feed ratio was kept constant at 4/1, 8/1 and 12/1 and the termonomer concentration was varied, trying to attain terpolymers with termonomer content as high as possible and molar masses (M_w) possibly higher than 60000 g mol^{-1}.

The addition of termonomer remarkably decreased the activity for all the catalytic systems investigated, compared to E/N copolymerizations, and the activity seemed to be related to 1-octene concentration and ethene pressure, that is the higher the concentration and the pressure, the lower is the activity.

On the basis of these previous data the behaviour of three half-titanocene **A**, **B**, **C**/MAO (Figure 4.10) systems has been investigated in E/N/O terpolymerizations.

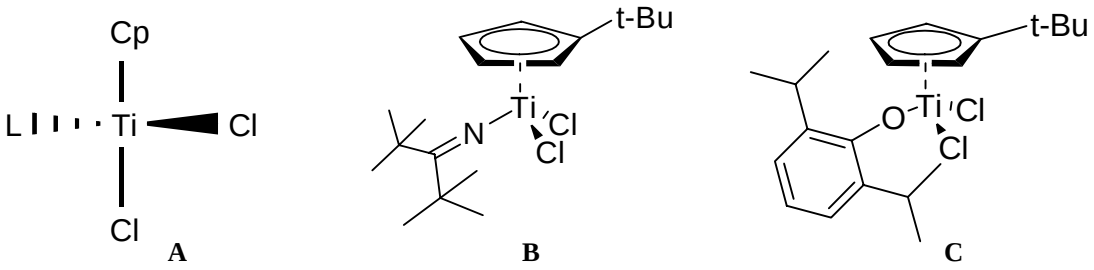

Figure 4.10 The three nonbridged titanocene precursors used in ethene-norbornene -1-octne terpolymerizations. Structure of nonbridged half-titanocene **A** will not be disclosed for patent applications.

The synthesis of poly(E-*ter*-N-*ter*-O) have been carried out in a lab-scale autoclave (see Paragraph 2.3.1) under conditions as close as possible to those used in industrial plants, that is at high ethene pressure (P_E = 4 bar) and high polymerization temperature (T = 60 °C). The terpolymers obtained (Scheme 4.6) were characterized by ^{13}C-NMR to determine the polymer compositions, by SEC to determine the molar masses and molar mass distributions and by DSC to determine the glass transition temperatures. It is worth pointing out that, the data reported in this thesis are just preliminary data; a deeper investigation is needed in order to fully understand the catalytic performances and the properties of the material obtained.

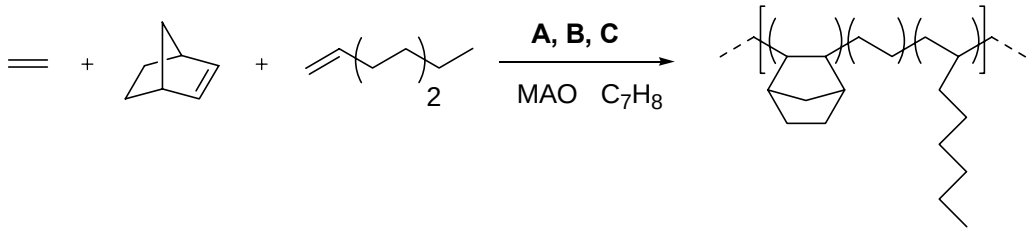

Scheme 4.6. Synthesis of poly(E-*ter*-N-*ter*-O) performed using different group IV precatalysts.

In this preliminary study the terpolymers have been synthesized at quite high N content to achieve synthesis of terpolymers with at least 30 N mol %, and thus T_g higher than 70 °C. [N]/[E] was fixed to 4/1 and just one 1-octene composition has been investigated.

Very low amount of poly(E-*ter*-N-*ter*-O) has been obtained with all the catalytic systems; the data are reported in Table 4.12 and E/N copolymerization results have been reported as reference.

Table 4.12 Terpolymerization activities for half-titanocene **A, B, C** under autoclave conditions.

Run	E bar	Cat type	N/E/O m.r.	Yield g	Activity $Kg_{polymer}/mol_{Ti}*h$
13	4	**A**	4/1	7.00	8400
20	4	**A**	4/1/1	0.30	131
35	-	**A**	4/0/1	1.14	1368
21	4	**B**	4/1	3.60	4320
26	4	**B**	4/1/1	0.13	77
24	4	**C**	4/1	2.60	1950
30	4	**C**	4/1/1	0.76	459
31	4	**C**	4/1/1	0.59	352

Under these experimental conditions the addition of 1-octene lowers notably the activity, showing depressed values for all the catalytic systems.

All the terpolymers prepared have been characterized by ^{13}C-NMR spectroscopy to determine the molar composition; the spectra exhibit the presence of signals characteristic of 1-octene units, even if, at high N content, an overlapping between E-N backbone resonances and 1-octene signals is revealed.

Figure 4.11 shows the ^{13}C-NMR spectra of poly(E-*ter*-N-*ter*-O) samples performed using the **3** active titanocenes; a general structure for terpolymers is also included in figure, with the relative common labelling of carbon atoms based on nomenclature present in literature.

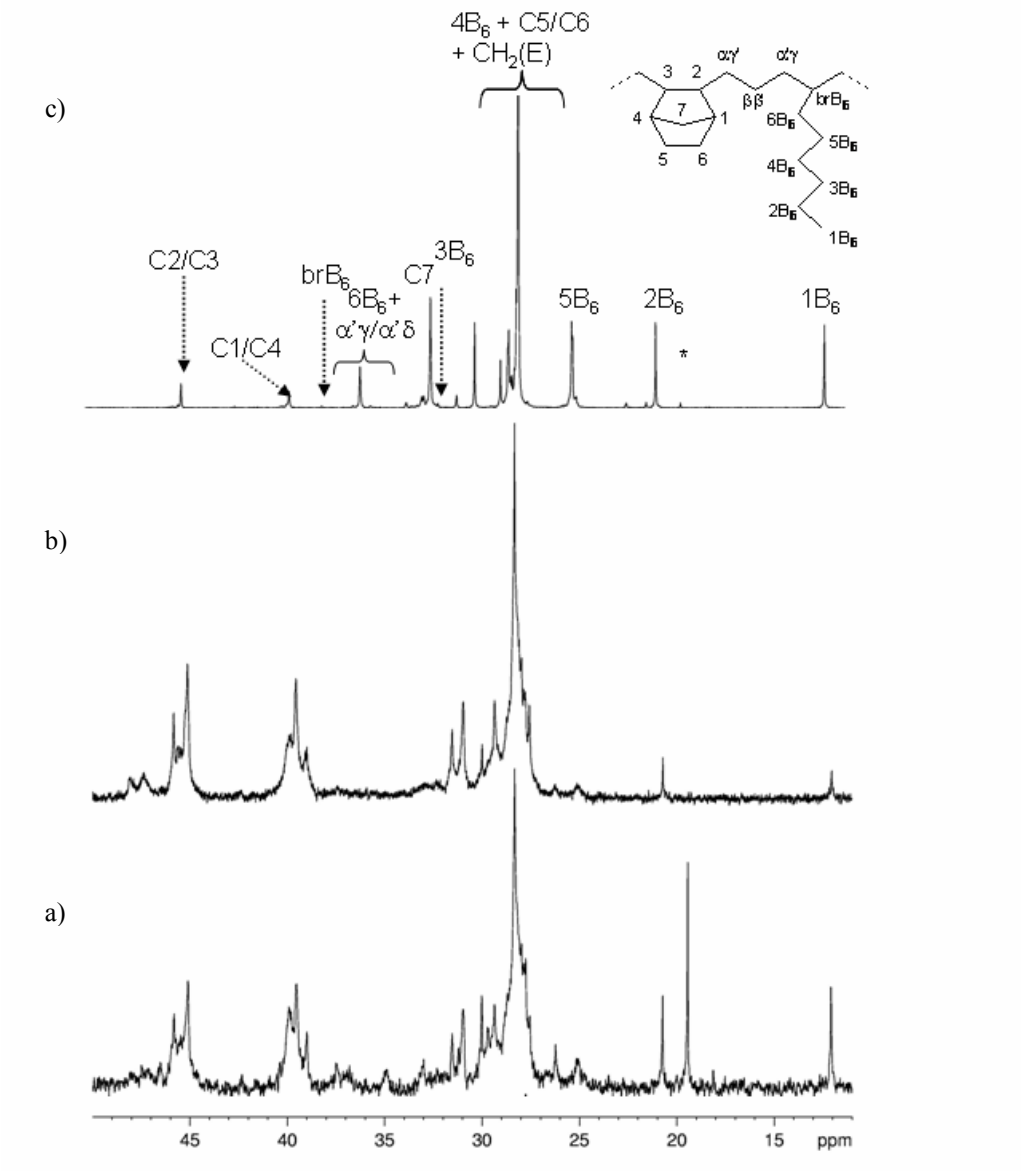

Figure 4.11 ^{13}C-NMR spectra (108.58 MHz, $C_2D_2Cl_4$, 103 °C) of poly(E-ter-N-ter-O)s obtained by using **A**, **B**, **C**/MAO systems (runs 26 (a), 20 (b), 31 (c) Table 4.11)

The peak assignments of terpolymers synthesized have been based on data reported in literature on poly(E-*co*-O) copolymers[41, 42]. Signals between 12.1 and 11.9 ppm have been attributed to the methyl carbon $1B_6$; peaks in the 20.9 to 20.5 ppm region have been attributed to methylene carbon $2B_6$. Peaks from 24.9 to 25.6 ppm have should be corresponding to the side chain CH_2 carbon $5B_6$ and secondary carbon atoms βδ. More complicated the assignment of the methylene

carbon 4B6 that is located in the complex cluster of peaks in the region between 29.7 and 27.5 ppm, in the same chemical shift interval of the E and C5/C6 resonances of N. The peak at 30.0 ppm was identified as the side chain methylene carbon $3B_6$. The cluster of peaks appearing in the 33.4-32.1 ppm region in spectra b), c) and d) (Figure 4.10) has been attributed to the $6B_6$ carbon of O units and to $\alpha\gamma$ and $\alpha\delta^+$ carbons of the main chain. The small area peak appearing at 36.3 ppm has been attributed to the branching methine carbons brB_6.

The content of ethylene, norbornene and 1-octene is quantitatively calculated on the basis of integration values of signals diagnostic for each monomer unit: the $1B_6$ methyl carbon of 1-octene, appearing in a region of the spectra free from other signals, allows to calculate O content (Eq 2.14 Chapter 2); the intensity of the C2/C3 carbon signals of norbornene units allows to evaluate N content (Eq 2.12 Chapter 2); the peak intensity of signals in the range from 30.6 to 24.3 ppm, in which an overlapping with 1-octene ($3B_6$, $4B_6$ and $5B_6$) and norbornene signals (C5/C6) is present, allows to calculated E content (Eq 2.13 Chapter 2). Main results from the compositional analysis are shown in Table 4.13.

Table 4.13 ^{13}C-NMR data of poly(E-t*er*-N-*ter*-O) obtained by using **A**, **B** and **C**/MAO systems

Run	E	Cat	E	N	O
	bar	type	mol %	mol %	mol %
20	4	**A**	57	43	3
26	4	**B**	41	48	11
30	4	**C**	84	3	13

Half titanocene **C** exhibits higher preference for 1-octene than norbornene monomer, as reported by Nomura et al.[43] for Cp^*TiCl_2(O-2,6-i-$Pr_2C_6H_3$ (Cp^* = Me_5C_5), incorporating up to 13 mol % of 1-octene, depressing the norbornene incorporation from 27 mol % in E/N copolymer, (run 24 Table 4.5) to 3 mol %. The two catalysts **A** and **B**, although they have similar reactivity towards norbornene monomer, behave differently towards 1-octene molecule; the *t*-butyl-substituted one incorporates high amount of termonomer, similar to titanocene **C**, while **A** incorporates very low amount of 1-octene, around 3 mol %.

The terpolymers have been characterized by SEC to determine the molar mass and molar mass distributions. The analytical data are reported in Table 4.14;

SEC data of poly(E-*co*-N) obtained in similar conditions have been reported therein for comparison.

Table 4.14 Molar mass and molar mass distribution of poly(E-*ter*-N-*ter*-O)s obtained with **A**, **B** and **C**/MAO systems

Run	N/E/O	Cat	O	T_g	M_w	D
	bar	type	mol %	°C	Kg/mol	M_w/M_n
12	4/1/0	**A**	-	115	1089	1.95
20*	4/1/1	**A**	3	-	319	16.08
21	4/1/0	**B**	-	67	633	2.10
26*	4/1/1	**B**	11	-	14	1.73
24	4/1/0	**C**	-	27	1921	1.61
30*	4/1/1	**C**	13	-	17	2.02

* Partially soluble in ODCB at high temperature.

Samples of terpolymers resulted to be partially soluble in ODCB at high temperatures and thus results of SEC analysis are related only to the soluble fraction.

Thus, all the half-titanocenes of Figure 4.1, as other metallocenes, afford terpolymers with molar masses significantly lower than those of corresponding E/N copolymers; in fact, 1-octene behaves as chain termination/transfer agent, that is it acts as reagent which both terminates and facilitates reinitiating of a growing polymer chain. Our findings are in agreement with the general observation that the introduction of α-olefins in copolymerization reaction leads to a decrease of molar masses[44].

Regarding the molar mass distributions, the titanocenes **B** and **C** afford partially soluble samples with unimodal distribution and values nearly equal to two, that is consistent with a single site catalysis. Titanocene **A** affords terpolymers with a bimodal distribution and high values of polydispersity; this clearly indicate that the sample is non homogenous.

Poly(E-*ter*-N-*ter*-O)s have been characterized by DSC to investigate thermal properties. Attempts of DSC thermal analysis of the samples synthesized with all the three titanocene precursors have given negative results. Probably the terpolymer obtained with **C** (run 30, Table 4.14) does not reveal any T_g due to the low norbornene content, the terpolymer obtained with **A** (run 20, Table 4.14) does not reveal a thermal event for the large mass distribution; it was not possible to

observe a thermal event also in sample 26 obtained with catalyst **B.** This seems to be in agreement with our assumption about the non homogeneity of all the samples of these preliminary (E-*ter*-N-*ter*-O) polymerizations.

References

1. C.G. Wilson, U. Okoroanyanwu, D. Medieros, US Patent, **2000**. *6, 103,* 445.

2. W. Kaminsky, A. Bark and M. Arndt *Makromol. Chem. Macromol. Symp.*, **1991**, *47*, 83.

3. M.-J. Brekner, F. Osan, J. Rohrmann, M. Antberg, *Process for the preparation of chemically homogeneous cycloolefin copolymers*, US Patent, **1994** *5, 324, 801*.

4. Modern Plastics **1995**, *72*, 137.

5. R. Wendt, G. Fink *J. Mol. Catal., Part A*, **2003**, *203*, 101.

6. (a) I. Tritto, C. Marestin, L. Boggioni, M.C. Sacchi, H. H. Brintzinger, D. R. Ferro, *Macromolecules*, **2001**, *34*, 5770; (b) J. Forsyth, J. M. Pereña, R. Benavente, E. Perez, I. Tritto, L. Boggioni, H. H. Brintzinger, *Macromol. Chem. Phys.,* **2001**, *202,* 614; (c) I. Tritto, C. Marestin, L. Boggioni, L. Zetta, A. Provasoli, D. R., Ferro *Macromolecules*, **2000**, *33*, 8931.

7. (a) A. R. Wendt, R. Mynott, G. Fink,. *Macromol. Chem. Phys.,* **2002**, *203*, 2531; (b) A. R. Wendt, G. Fink, *Macromol. Chem. Phys.,* **2001**, *202*, 3490; (c) A. R. Wendt, R. Mynott, K. Hauschild, D. Ruchatz, G. Fink, *Macromol. Chem. Phys.,* **1999**, *200*, 1340.

8. H. Cherdron, M.-J. Brekner, F. Osan, *Angew. Makromol. Chem*., **1994**, *323*, 121.

9. Y. Yoshida, J. Saito, M. Mitani, Y. Takagi, S. Matsui, S. Ishii, T. Nakano, N. Kashiwa, T. Fujita, *Chem. Commun.,* **2002**, 1298.

10. K. Nomura, M. Tsubota, M. Fujiki, *Macromolecules*, **2003**, *36*, 3797;

11. B.P. Etherton, J. J. McAlpin, T. Huff, H. N. Kresge, World patent 9117194, 7.5.1990.

12. R. C. Austin, H. C. Helborn, World patent 8804673, 18.12.1986.

13. Ch. Bergman, R. Cropp, G. Luft, *J. Mol. Catal. A: Chem*, **1997**, *116*, 317.

14. N. Naga, Y. Imanishi, *Macromol. Chem. Phys.* **2002**, *203*, 771.

15. I. Kim, Y. S. Shin, J-K. Lee, N. J. Cho, J-O. Lee, M-S. Won *Polymer* **2001**, *42*, 9393.

16. H. S. Makowski, K. C. Shim, Z. W. Wilshinsky, *J. Polym. Sci. Part A* **1964**, *2*, 1549;

17. (a) C.S Marvel, J. K. Stille, *J. Am. Chem .Soc*, **1958**, *80*, 1740; b)) C.S Marvel, W. E. Garrison, *J. Am. Chem .Soc*, **1959**, *81*, 4737.

18. K. Ziegler, H. Martin, *Makromol. Chem*., **1956**, *19*, 186. K. Ziegler, *Chem. Techn*., **1955**, *27*, 230.

19. H. N. Cheng, N. P. Khasat, *J. Appl*. *Polym. Sci.*, **1983**, *35*, 852.

20 G. Cavallo, P. Guerra, L. Corradini, L. Resconi, R. M. Waymouth, *Macromolecules* **1993**, *26*, 260-267.

21. a) L. Resconi, G. W. Coates, A. Mogstad, R. M. Waymouth, *J. Macromol. Sci. Chem.* **1991**, *A28*, 1225; b) G. W. Coates, R. M. Waymouth, *J. Mol. Catal.* **1992**, *76*, 189; c) C. J. Schaverien, *Organometallics* **1994**, *13*, 69; d) D. Jeremic, Q. Y. Wang, R. Quyoum, M. C. Baird, *J. Organomet. Chem.* **1995**, *497*, 143; e) M. Mitani, K. Oouchi, M. Hayakawa, T. Yamada, T. Mukaiyama, *Chem. Lett.* **1995**, *24*, 905; f) K. C. Jayaratne, R. J. Keaton, D. A. Henningsen, L. R. Sita, *J. Am. Chem. Soc.* **2000**, *122*, 10490; g) I. L. Kim, Y. S. Shin, J. K. Lee, M. S. Won, *J. Polym. Sci., Part A: Polym. Chem.* **2000**, *38*, 1520; h) P. D. Hustad, G. W. Coates, *J. Am. Chem. Soc.* **2002**, *124*, 11578; i) A. Yeori, I. Goldberg, M. Shuster, M. Kol, *J. Am. Chem. Soc.* **2006**, *128*, 13062; l) V. Volkis, C. Averbuj, M. S. Eisen, *J. Organomet. Chem.* **2007**, *692*, 1940; m) A. Yeori, I. Goldberg, M. Kol, *Macromolecules* **2007**, *40*, 8521.

22. H-J. Jin, C-H. Choi, E-S. Park, I-M. Lee, J-S Yoon, *J. Appl. Polym. Sci.* **2002**, *84*, 1048.

23. K. Nomura, A. Takemoto, Y. Hatanaka, H. Okumura, M. Fujiki, K. Hasegawa, *Macromolecules*, **2006**, *39*, 4009;

24. E. Kokko, P. Pietikäinen, J. Koivunen, J.V. Seppälä, *J. Polym. Sci. Part A: Polym. Chem.* **2001**, *39*, 3805;

25. P. Pietikäinen, T. Väänänen, J.V. Seppälä, *Eur. Polym. J.* **1998**, *35*, 1047.

26. P. Pietikäinen, P. Starck, J. V. Seppälä, *J. Polym. Sci., Part A: Polym. Chem.* **1999**, *37*, 2379;

27. F. G. Sernetz, R. Mülhaupt, R. M. Waymouth, *Polym. Bull*. **1997**, *38*, 141.

28 K. Nomura, *Dalton Trans.* **2009**, 8811, and references therein.

29 K. Nomura, W. Wang, M. Fujiki, J. Liu, *Chem. Commun.* **2006**, *25*, 2659.

30 K. Nomura, N. Naga, M. Miki, K. Yanagi and A. Imai *Organometallics* **1998**, *17*, 2152.

31. K. Nomura, J. Liu, *Adv. Synth Catal.*, **2007**, *349*, 2235.

32. K. Nomura, A. Tanaka, S. Katao, *J. Mol. Cat. A: Chemical,* **2006***, 254,* 197.

33. (a) I. Tritto, L. Boggioni, D. R. Ferro, *Coord. Chem. Rev.* **2006**, *250*, 212; (b) I. Tritto, L. Boggioni, C. Zampa, M. C. Sacchi, D. R. Ferro, *Topics in Catalysis*, **2006**, *40*, 151.

34 R. Marconi **PhD Thesis**: *Terpolymerization of α-Olefins and Non-Conjugated Dienes with Norbornene and Ethylene by Group IV Metal Based Catalysts* **2010** Pavia

34. W. Kaminsky, *Macromol. Chem. Phys.* **1996***, 197,* 3907.][K. B. Sinclair, R. B. Wilson, *Chem. Ind.* **1994***, 21,* 857.

35. E. Perez, D. L. VanderHart, B. Crist, P. R. Howard, *Macromolecules,* **1987**, *20*, 78;

36. C. McFaddin, K. E. Russell, E. C. Kelusky, *Polym. Commun.* **1988**, *29*, 258.

37. S. Al-Malaika, X. Peng, H. Watson, *Polym. Degrad. Stab.* **2006**, *91*, 3131.

38. J. M. Canich, U.S. Pat. 5,026,798 (**1991**).

39. S. Y. Lai, J. R. Wilson, G. W. Knight, J. C. Stevens, P.W. Chump, U.S. Pat. 5,272,236 (**1993**).

40. F. G. Sernets, R. Mülhaupt, *J.Polym. Sci. Part A: Polym. Chem.* **1997***, 35,* 2549.

41. X-H Qiu, D. Redwine, G. Gobbi, A. Nuamthanom, P. L. Rinaldi, *Macromolecules* **2007**, *40*, 6879.

42. W. Liu, P. L. Rinaldi, L. H. McIntosh, R.P. Quirk, *Macromolecules* **2001**, *34*, 4757.

43. K. Nomura, K. Itagaku, S. Hasumi, M. Fujiki; *J. Mol. Cat A: Chemical*; **2009**, *303*, 102.

44. V. Busico, R. Cipullo, N. Friederichs, H.Linssen, A. Segre, V. V. A. Castelli, G. Van Der Velden, *Macromolecules* **2005**, *38*, 6988, and references therein.